INL/EXT-21-61607
Revision 0

Management of the Three Mile Island, Unit 2, Accident Corium and Severely Damaged Fuel Debris

Contribution to International Atomic Energy Agency Coordinated Research Proposal T13015

Philip L. Winston

Changing the World's Energy Future

INL is a U.S. Department of Energy National Laboratory operated by Battelle Energy Alliance, LLC

INL/EXT-21-61607

Management of the Three Mile Island, Unit 2, Accident Corium and Severely Damaged Fuel Debris

Contribution to International Atomic Energy Agency Coordinated Research Proposal T13015

Philip L. Winston

February 2021

Idaho National Laboratory
Idaho Falls, Idaho 83415

Page intentionally left blank.

EXECUTIVE SUMMARY

The Three Mile Island, Unit Two (TMI-2) pressurized water reactor core melted down in 1979 due to an untimely combination of maintenance problems that led to a loss of feedwater, followed by a series of operational misunderstandings and errors. The melted core recovery process required development of a wide array of tools. After approximately three years of water management and other cleanup actions, the first views of the core revealed a much higher degree of damage than previously expected. Approximately 62 metric tons of the core had melted, leaving only 42 of the 177 fuel assemblies standing with a majority of rods intact. The core to be recovered was composed of loose debris and a solidified mass of formerly molten fuel. Robotic tools that had been designed for the task were of limited effectiveness due to the range of material types and phases.

Over a period of several years, the central melt was broken up, primarily by use of a core-boring drill originally designed to acquire samples through the depth of the debris field. The broken pieces were loaded into specially designed debris canisters by use of long-handled pick-and-place tools and suctioned into baffled knockout canisters using an airlift vacuum system. A remotely operable underwater plasma arc torch was developed for removal of the lower core-support structure to be able to retrieve the fuel pieces and secondary melt that had accumulated on the bottom reactor vessel head. Canister design played a central role in defining the initial retrieval process and later affected transportation, interim wet and its current interim dry storage.

Due to concerns about the potential for radiolysis of residual water in the debris and other canister material, the canisters were fitted with hydrogen-recombiner catalyst units to prevent a buildup of flammable gas and potential pressurization. To confirm the effectiveness of the recombiners during shipping, eight dewatered canisters were kept sealed for up to 205 days with periodic sampling of the headspace gas. The highest hydrogen value (9 vol%) was observed in a canister held for 147 days while the longest stored canister resulted in a 5% hydrogen concentration. The oxygen concentration never exceeded 0.5 %, and the primary backfill was >80% argon, meaning there was no flammability risk. Radiolytic hydrogen was also observed in wet pool storage, where the vented canisters discharged a portion of the water backfill as a result of gas production. The 344 canisters (268 fuel debris, 62 filter, and 12 knockout type) were dewatered, loaded in groups of seven into a double barrier shipping cask, and transported to the U.S. Department of Energy site in Idaho for 10 years of pool storage.

Decisions were made to move the debris to dry storage, and the canisters were dried by heated vacuum drying. Heated drying was required due to the low decay heat of the debris (maximum 60 W per canister, average 29 W/canister [SAR-II-8.4 Chapter 3]) and the presence of low-density concrete filler in the void space of the debris canisters. Drying was necessary to minimize radiolytic hydrogen production and to assure elimination of water moderator for prevention of recriticality. Groups of 12 dried canisters were loaded into welded, vented, selectively shielded carbon steel dry storage canisters that were moved from the pool area and placed into horizontally oriented concrete shield modules at a location approximately 18 miles from their wet storage facility. Monitoring of the

canisters for radiolytic hydrogen buildup has shown no significant hydrogen production and no release of radioactive material through the high-efficiency particulate sintered-metal filter vents. Various issues remain that need to be resolved prior to transfer of the material to what is assumed to be ultimate repository disposal.

A portion of this report discusses the process of debris recovery, which was, as part of the management action, approximately a decade of eventful investigation and development of solutions to problems that became progressively clearer as obstructions were cleared. Implicit within the design response were solutions that created later challenges. Although long-term interim storage has been uneventful, the debris were not treated to eliminate potential for production of radiolytic hydrogen, or to minimize the potential for water intrusion, which could have an effect during long-term disposal.

The current proposed approach for final disposal is to remove the individual debris canisters from the dry storage system canister and repackage them into standardized canister overpacks that would be incorporated into a final-storage system canister. The standard overpacks would probably be transported to the disposal site for the final disposal canister assembly.

Some management challenges exist due to institutional uncertainty regarding the ultimate disposition of the material. If the fissionable material had been recovered from the debris immediately following retrieval, a substantial amount of void and container volume necessary to store the debris would have been eliminated. Alternately, the loose debris could have been processed into a monolithic waste form suitable for disposal, eliminating voids and concerns of water intrusion and the attendant issues of radiolytic hydrogen generation and recriticality. Recovery by conventional dissolution and reprocessing would have been problematic due to inconsistent solubility of the ceramic phases of the melt. Reprocessing of commercial fuel in the United States has been prohibited by executive order since 1976. Treatment of the debris by conversion to a glass or glass-ceramic form could be achieved by use of cold-crucible melt technology.

At present, the debris-storage system is monitored according to an aging-management plan as part of its Nuclear Regulatory Commission license. This plan addresses structural concrete monitoring and inspection of the external surfaces of steel components such as the dry shielded canister (DSC).

Prior to the year 2035, the debris are mandated to be repackaged for incorporation into a final waste-disposal package for removal from Idaho according to a 1995 agreement between the state of Idaho and the U.S. Department of Energy. This is expected to require design and construction of a facility capable of opening the DSC and transferring the TMI-2 canisters into an alternate overpack.

CONTENTS

FIGURES

TABLES

ACRONYMS

ACES	Automatic cutting equipment system
ALARA	as low as reasonably achievable
ASME	American Society of Mechanical Engineers
CEA	Comissariat a l'energie atomique et aux energies alternatives (French Atomic Energy Commission)
DOE	Department of Energy
DSC	dry shielded canister
EPRI	Electric Power Research Institute
GEND	General Public Utilities, Electric Power Research Institute, Nuclear Regulatory Commission, U.S. Department of Energy
GPU	General Public Utilities
HEPA	high-efficiency particulate air
HSM	horizontal storage modules
HVDS	heated vacuum drying system
INEL	Idaho National Engineering Laboratory
INL	Idaho National Laboratory
INTEC	Idaho Nuclear Technology and Engineering Center
ISFSI	independent spent fuel storage installation
LCSA	lower core support assembly
LICON	light-weight concrete
NRC	Nuclear Regulatory Commission
NUHOMS	NUTECH horizontal modular storage system
NUTECH	Nuclear Technology, Inc.
OD	outer diameter
PORV	pilot-operated relief valve
ROSA	remotely operated service arm
RPV	reactor pressure vessel
SAR	safety analysis report
SDS	submerged demineralizer system
TAN	Test Area North
TMI	Three Mile Island
VECTRA	Formerly Pacific Nuclear Technologies, bankrupt in 1997, previously NUTECH. Assets acquired by Chem Nuclear, storage designs acquired by Transnuclear/Framatome, now ORANO

Management of the Three Mile Island, Unit 2, Accident Corium and Severely Damaged Fuel Debris

1. MANAGEMENT OF SEVERELY DAMAGED FUEL AND CORIUM

The best-documented and longest-managed example of severely damaged nuclear fuel and corium is the debris from the meltdown accident at Three Mile Island Nuclear Generating Station, Unit 2, (TMI-2) located in Dauphin County, Pennsylvania, USA, near Harrisburg. The process of system recovery and core removal was done forensically, with the purpose of understanding the effects of loss of coolant, the dynamics of the melt and the release of fission products. A consortium including General Public Utilities (GPU), Electric Power Research Institute (EPRI), the U.S. Nuclear Regulatory Commission (NRC), and the U.S. Department of Energy (DOE), collectively known as GEND, was responsible for determining the recovery process and directing the research into the cause and effects of the accident. A series of reports containing predictions and documenting design choices was produced; they are available for review. Report GEND-007 was one of the primary prediction reports that was used to estimate conditions in the core.

The accident recovery and debris management process following initial post meltdown stabilization included core status, melted core characterization, and design phases for core removal, packaging, and transportation. Following interim wet storage, a dry storage system design was identified and adapted for use with the debris and its unique canister designs.

1.1 Background

TMI-2 was a Babcock and Wilcox 177FA pressurized water reactor with dual coolant loops and a core composed of 177 fuel assemblies. The assembly design used a 15 × 15 rod array containing 208 fuel rods, 16 Zircaloy control-rod guide tubes, and one Zircaloy center-position instrument tube with eight Inconel spacer grids and upper and lower end fittings of Type 304L stainless-steel. The fuel was uranium dioxide (UO_2) pellets with enrichment ranging up to 2.98 wt%. Seventy-two of the assemblies contained Zircaloy rods with 1% boron carbide (B_4C) burnable poison, interspersed within 94% alumina (Al_2O_3) pellets. The total UO_2 fuel mass was 94,029 kg, with an average ^{235}U enrichment of 2.265 wt%. The Zircaloy-4 cladding mass was 23,177 kg, with zirconium being 97.9 wt% of the alloy.

Sixty-one control-rod assemblies, using 304L stainless-steel-clad rods that contained 3403 mm of silver-indium-cadmium alloy provided shutdown control in the core. At the time of the meltdown, the control rods were fully inserted. The fuel burnup at that point was 3175 MWD/MTU.

Eight stainless-steel-clad axial power-shaping rods, containing 914 mm sections of silver-indium-cadmium, were included in the core.

On the evening of March 28, 1979, thirteen months after initial criticality, problems in clearing blockages in the condensate polishing system led to an instrument air line being filled with water, resulting in a shutdown of the feedwater, condensate, and condensate booster pumps. Auxiliary feedwater pumps had been valved out for maintenance and were not available to provide water to the secondary cooling system. Without feedwater for heat removal, the reactor control system initiated an emergency shutdown, with insertion of control rods to end nuclear criticality. Because decay heat was not being removed from the core via the secondary cooling system, the primary circuit continued to heat, and pressure rose until the pilot-operated relief valve (PORV) on the primary system pressurizer opened, releasing water from the primary cooling loop. Although the electrical signal for the valve controller indicated that the valve had closed as the system required, the valve did not close due to a mechanical fault, meaning that it continued to release water from the primary cooling loop. Control-room instrumentation showed a high-water level in the pressurizer and decreasing pressure in the primary cooling loop. Concern that excessive water levels could eliminate the required void space in the

pressurizer led operators to turn off the emergency core-cooling pumps. Water was being released from the primary cooling loop to the extent that the core was becoming uncovered. The pressurizer relief tank overfilled due to the stuck-open PORV and discharged into the containment building sump. Then the water in the core and primary cooling loop boiled to an extent that water circulation was blocked due to a steam bubble. This resulted in temperatures that melted a substantial fraction of the fuel assemblies, starting with the Zircaloy cladding and eventually involving the UO_2 fuel pellets. As the fuel damage continued, the debris and molten material filled the central core zone, completely preventing any water circulation in that area. Temperatures were eventually shown to have reached 3100 K (i.e., the UO_2 melting point) The melting of the cladding exposed zirconium metal, which reacted with the steam and water to produce hydrogen.

Because the reactor had been shut down, cooling was the only control that could be applied to stop the progression of the core melt. The eventual addition of water is believed to have shattered some of the peripheral standing fuel assemblies, but probably prevented the melt from penetrating through the bottom of the reactor pressure vessel.

As a result of the accident, approximately 62 tons of the core assemblies melted, and an estimated 20 tons of core material flowed from the central core region and solidified on the lower vessel head. The upper plenum was largely intact, and analysis of the control-rod lead screws indicated that the temperature above the central core region reached 1250 K while the perimeter only reached 700 K, with the damage zones approximately 1.2 m in diameter and confined to the areas below the upper spacer grid. (Osetek 1990)

Core damage was defined in terms of four zones, as 1) a 9.3 m^3 void 1.5 to 2 m deep in center of the upper core, 2) a 0.6 to 1 m deep layer of loose fragmented debris that had reached 2200 K, 3) 32.7 metric tons of solidified metal and ceramic mixture, formerly molten core, primarily composed of uranium and zirconium oxide with metallic silver and iron inclusions, and 4) partial and full-length fuel assemblies around the periphery of the melt. The central melt was surrounded by a crust, with the 10 cm layer below the melt composed of zirconium, iron and silver metal, and the 1 to 3 cm upper crust containing iron and silver with indium and nickel.

The core support assembly was damaged in the east quadrant, where baffle plates partially melted, allowing molten material to flow into the lower core-support assembly and contact the wall of the reactor pressure vessel.

Low volatility fission products, ^{144}Ce, ^{154}Eu, and ^{155}Eu, and medium volatile fission products, ^{90}Sr, ^{125}Sb, and ^{106}Ru, were detected in melt samples while ^{85}Kr, ^{137}Cs and ^{129}I were largely released from the fuel. Approximately 3.5% of the medium volatility species were transported beyond the reactor vessel, with only 0.1% reaching the reactor coolant-bleed tanks in the auxiliary building. Isotopes ^{125}Sb and ^{106}Ru were found to have been selectively deposited in the metallic region below the core at concentrations six to 20 times that found in the fuel. Isotopes ^{85}Kr, ^{137}Cs and ^{129}I were transported by the cooling system and distributed throughout the reactor-building basement. Approximately 20% of the ^{137}Cs and ^{129}I was retained in the fuel debris, while 85% of the ^{85}Kr was released to the containment building atmosphere.

Given these data on release and retention and the low burnup of the fuel, the management challenge for long-term storage has less to do with extreme high dose rates and high transuranic content than other more recent examples such as Fukushima, which included high-burnup fuel and mixed-oxide fuel rods.

1.2 Timeline of Three Mile Island Unit Two Cleanup

- Milestones of the cleanup include:
- Mar 1979: TMI-2 nuclear power plant accident
- July 1980: First manned entry into reactor-building

- Mar. 1981: NRC directs core debris removal from site
- May 1982: Quick-look video inspection
- 1983: Ultrasonic mapping using core-topography system
- September–October 1983/March 1984: Loose debris grab sampling and analysis
- 1981–1984: Defueling equipment design
- 1984: Shipping cask design
- July 1984: Reactor vessel head removed
- December 1984: Upper plenum removed
- Oct. 1985: Defueling begun
- July 1986: Shipment of 125 tons of core debris to INL begun
- Apr 1990: Complete 22 rail shipments to INL; debris in wet storage
- May 1995: DOE/State of Idaho Settlement (Batt) Agreement mandates wet-to-dry conversion
- June 1997: Initiation of NRC license process for dry storage facility
- Mar 1999: TMI-2 independent spent fuel storage installation (ISFSI) NRC licensed for core material
- Mar 1999: First shipment of core debris from Test Area North (TAN) to Idaho Nuclear Technology and Engineering Center (INTEC) at INL using OS-197 cask transfer to NUTECH horizontal modular storage system (NUHOMS) storage modules
- Apr 2001: Last shipment (29 truck shipments) from TAN to dry storage
- Present: Core debris in vented dry storage at INL; Aging-Management Program monitoring hydrogen and structural conditions
- Future: Repackaging for final disposal to be completed prior to 2035.

2. WATER TREATMENT AND REACTOR AND AUXILIARY BUILDING CLEANUP

The initial response included cleanup of approximately ~2.12 million liters of water from the flooded reactor containment and auxiliary building.

This first involved the Cuno (brand) filter system, in which the filter vessels were specially constructed with lead weights in the bottom to assure that they did not float when submerged. The Cuno filters were a part of the submerged demineralizer system (SDS), which was installed in the TMI-2 fuel pool. This was followed by processing through a series of filters and ion-exchange media developed by Epicor, Inc. The EPICOR-II system used a three-stage system of prefilters and inorganic and organic resins to remove particulate and dissolved fission products.

2.1 Decontamination

Although it is common to focus on the mechanical and logistical heroics involved in removing the melted core material from the reactor vessel that occurred years after the accident, a major part of the initial post-accident recovery was decontamination of various parts of the reactor, auxiliary, and fuel-handling buildings. Contaminated water was released to the reactor-building sump in the early minutes of the accident when the primary coolant being dumped to the reactor coolant drain tank caused the overflow valve to open and then the rupture disc to burst. This sump water was transferred to the auxiliary building sump tank. Other systems, including the makeup and purification system, also received highly radioactive

core material. A relatively small quantity of core debris, estimated to be less than 10 kg, was spread through these systems following the opening of the PORV.

Reactor-building dose reduction started with processed water flushes of all surfaces of the accessible areas between the 305 and the 347-foot levels. This was followed by mechanical scabbling of painted and concrete surfaces to remove embedded activity. Cleaned areas were sealed with epoxy paint and other coatings to minimize recontamination potential.

Due to the material's porosity, some concrete-block wall surfaces were scarified using a remotely operated water lance. The internal voids of the block were flushed to remove sediment that had settled inside.

The water generated by the flushing, scabbling and scarification was processed through the submerged demineralizer and Epicor-2 filtration and ion-exchange systems, which are illustrated in Figure 1. The surface-cleaning operations generated an estimated 4900 kg of sludge. A remotely operated sludge-suction system was able to remove sludge from approximately 40% of the accessible reactor-building basement-floor area. An estimated 4 kg of fuel were contained in the sludge.

Fuel material and contamination in the reactor cooling system were removed using spray nozzles and submersible pumps during the first phase, followed by a remotely operated submersible that was used to pick up large discrete pieces that were present in the pressurizer vessel.

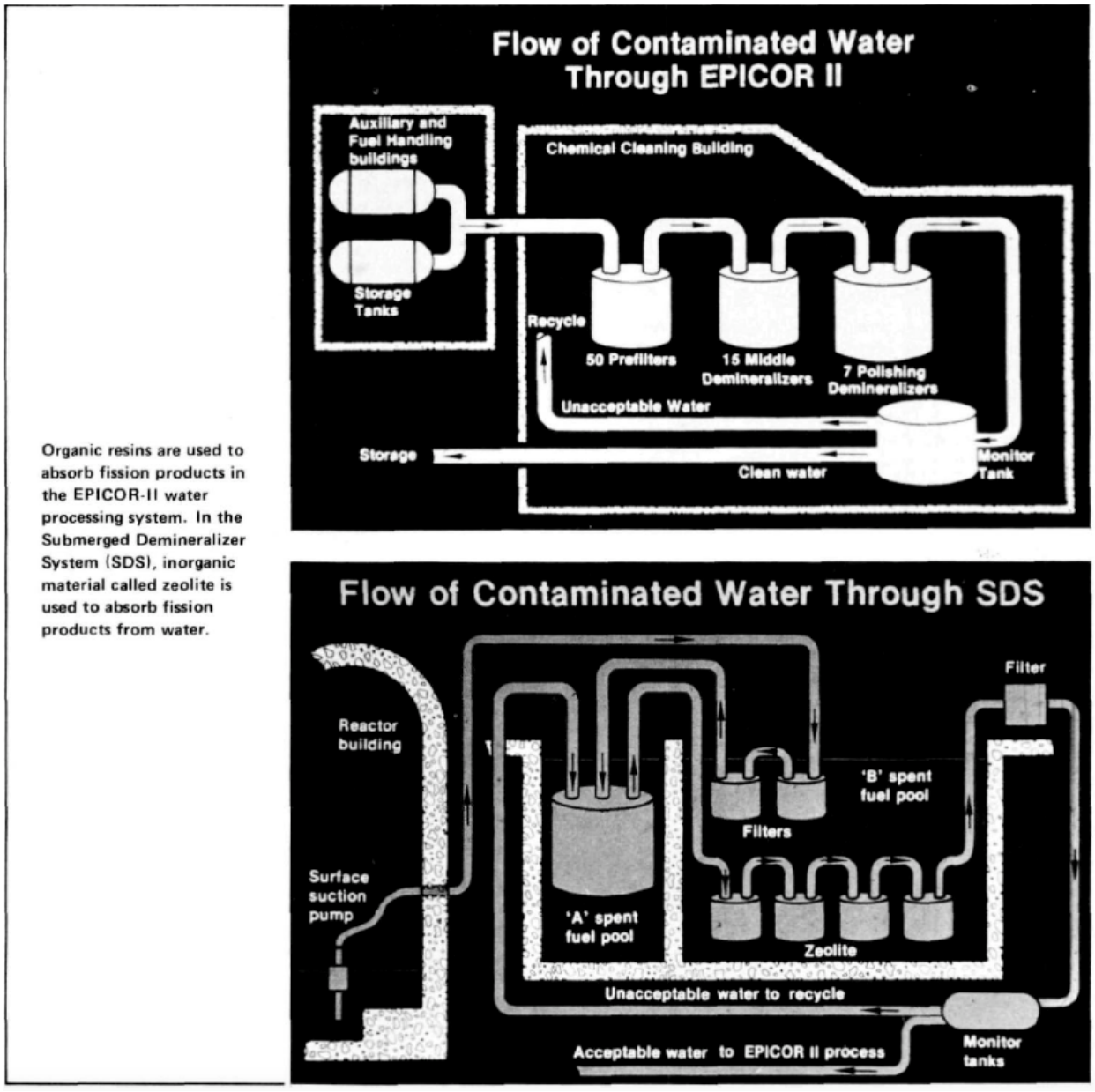

Figure 1. Water-cleanup schematic.

Following treatment, the water was contained onsite in two 1.9-million-liter epoxy-coated welded carbon steel tanks. In some instances, the water was recycled to be used for decontamination purposes.

In accordance with the supplement to the Environmental Impact Statement, 8.7 million liters of treated water was disposed by evaporation through the processed water disposal system. This unit was a closed-cycle evaporator that discharged the vapor through the facility's 30.5 m tall exhaust stack. Included in the vapor released to the environment was an estimated 1020 curies of tritium and 2.3 curies of other nuclides including Sr-90, C-14 and Cs-137. An estimated 136 tonnes of boric acid was included in the effluent. (GPU, 1993)

2.2 Core Recovery

The response to the TMI-2 meltdown followed a progression of investigation of the problem and design of tools and processes in the absence of clear information. During the cleanup of the buildings and management of the large quantity of water, analytical efforts attempted to reconstruct the accident and project the degree of damage that the core had undergone. Several scenarios were considered and integrated into a report identified as GEND-007. This document served as a design basis for the various proposals for core recovery. A primary assumption in this document was that the majority of the fuel assemblies was intact.

To proceed with core recovery, it was necessary to validate the predictions by means of visual examination. Video inspection was performed by inserting a camera into the reactor vessel through a control-rod penetration. After the confirmation that a significant amount of the fuel had been destroyed, the DOE funded investigation of the characteristics of the damaged fuel for the purpose of understanding the nature of the meltdown from the standpoint of material interactions.

Due to boiling and selective condensing, the primary coolant's boron concentration was found to be well below the operating condition of 1000 ppm, and due to uncertainty about the condition of the core, the boron concentration of the water filling the reactor vessel was raised to 3000 ppm and, ultimately≤ to 4350 ppm during defueling.

The technical issues addressed were:

- What part did reactor system thermal hydraulics play in the meltdown?
- What was the core damage progression?
- In what modes could the reactor pressure vessel have failed?
- What were the mechanisms of fission product release and transport?

To answer these questions, data on the core and system conditions were needed. A characterization campaign was undertaken as part of the overall cleanup activities.

2.2.1 Characterization

Characterization included:

1. In situ examination of the core and vessel by video camera and surface-contour mapping using ultrasonic sensors
2. Examination of cooling system artifacts, including debris from the plenum cover and filters from the makeup and letdown system and control-rod components such as leadscrews and support tubes
3. Chemical analysis (gamma and mass spectrometry to establish radiological retention and elemental composition) of rubble-bed grab samples, fuel-rod segments and other identifiable control-rod cluster and fuel assembly components, as well as the core stratification samples.

2.2.2 Vessel Internal Inspection

Several options were considered for doing a visual inspection of the reactor vessel, but logistics of crane availability and equipment movement limited the alternatives, which ultimately would have led to multiyear delays. Core characterization began in earnest in 1982 with the Quick-Look Program, which amounted to insertion of a modified commercial off-the-shelf video camera into the reactor vessel through one of the control-rod drive mechanism penetrations following the removal of the leadscrew (Sec 5.4.1 Cleanup TMI NP-6931). Figure 2 illustrates the video camera insertion approach, and Figure 3 shows an

example video image from that camera. The views indicated that there was a 1.2 m deep void in the center of the core. Probing with a with a steel rod showed that more than 30-cm of the material in the core center was loose debris, supported by a rigid layer that the probe could not penetrate (hard stop). Poor water quality limited visibility, meaning a great deal of uncertainty about the core conditions remained. In 1983 it was possible to acquire comprehensive video and insert sonar equipment to do a complete mapping of the core-melt surface. Grab samples were acquired using a narrow clamshell tool through the same penetration, as illustrated in Figure 2.

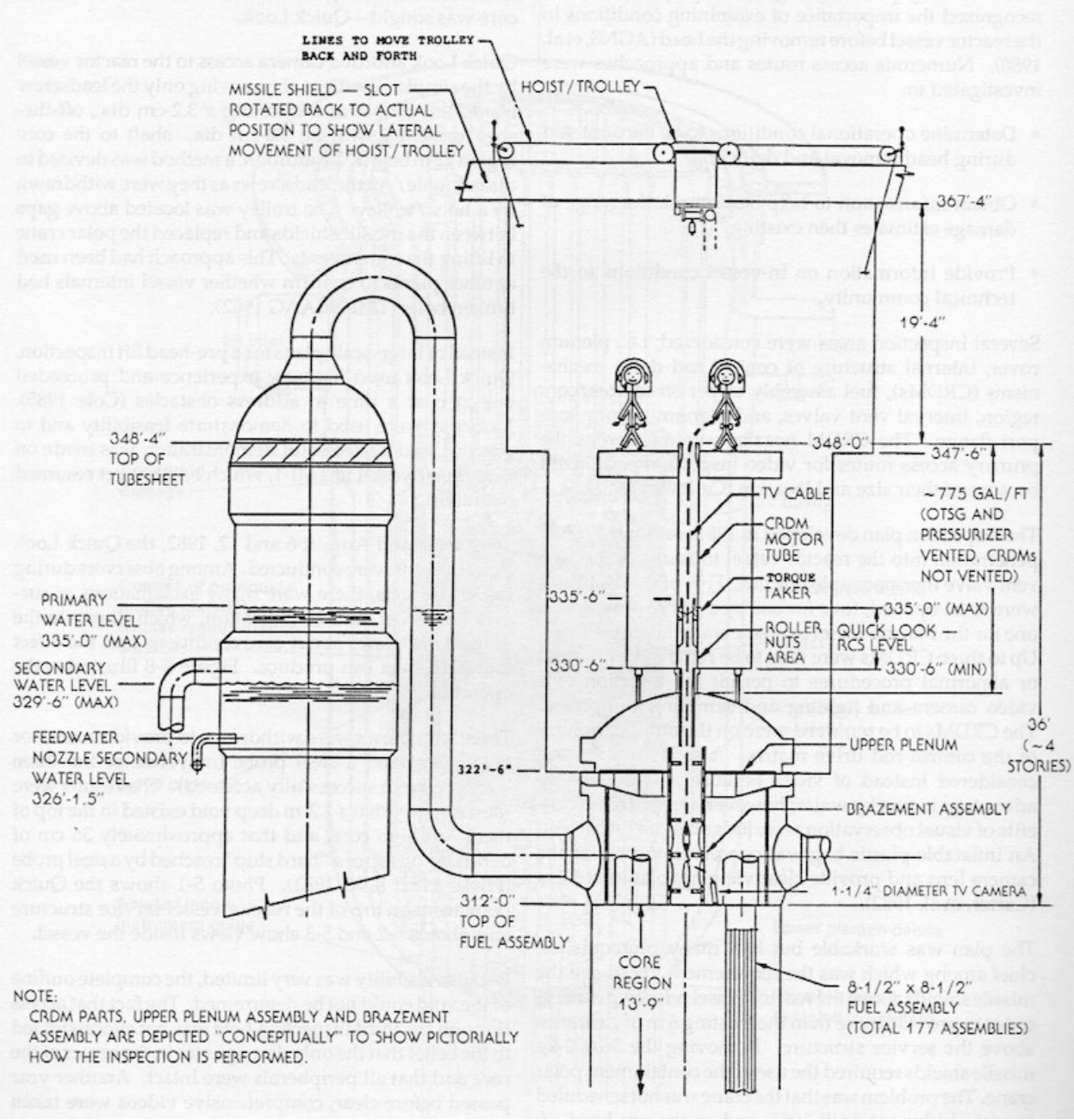

Figure 2. Quick-look video schematic cartoon. (EPRI-NP-6931).

Figure 3. Quick-look video image of debris bed. (EPRI-NP-6931).

Following the Quick-Look video work, debris samples were removed from the vessel using long-reach tools inserted through control-rod drive penetrations, as shown in Figure 4. Figure 5 shows the elevation view of the sampling locations.

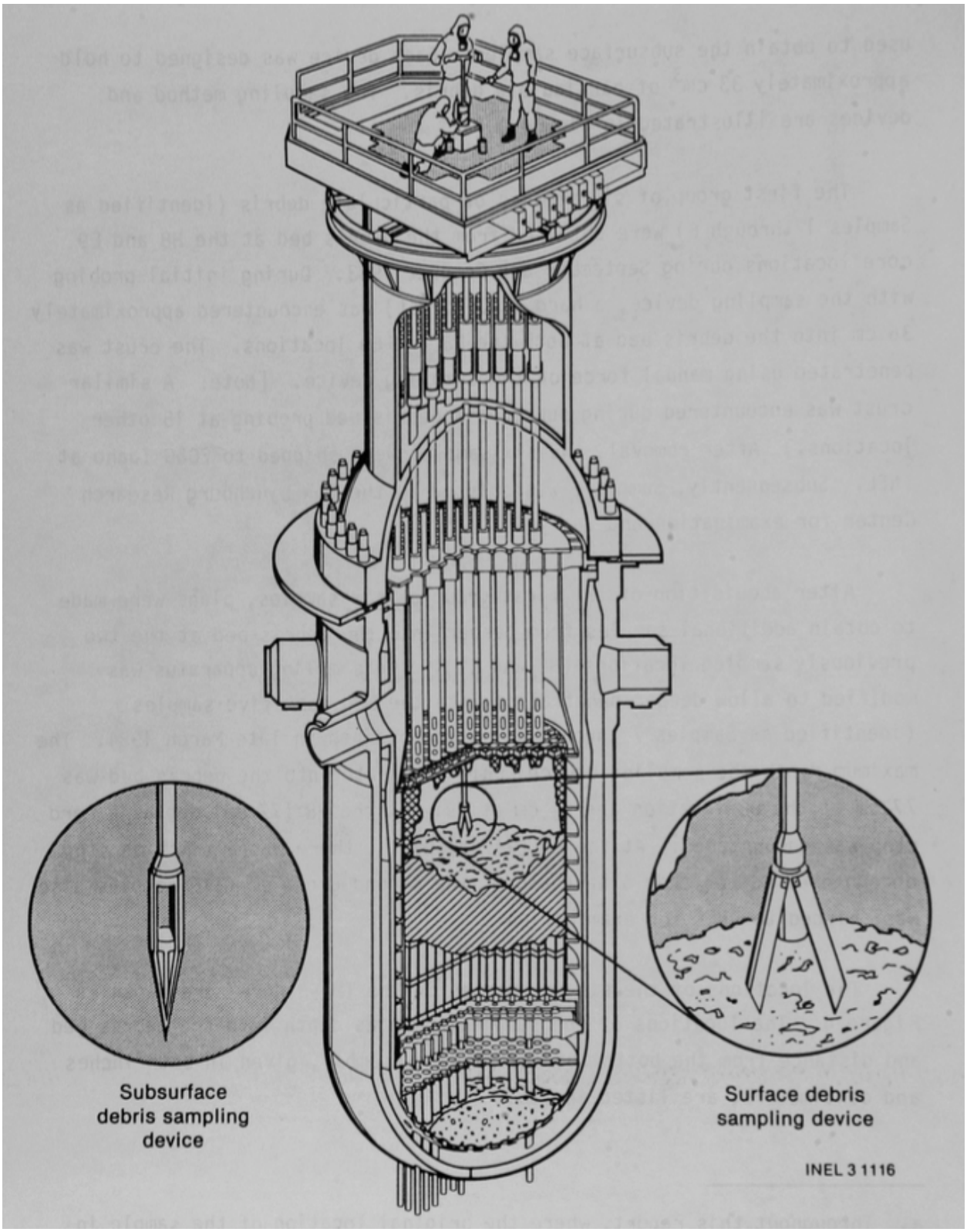

Figure 4. Loose debris grab sampling (EGG-TMI-6853 PT-1) October 1983 and March 1984.

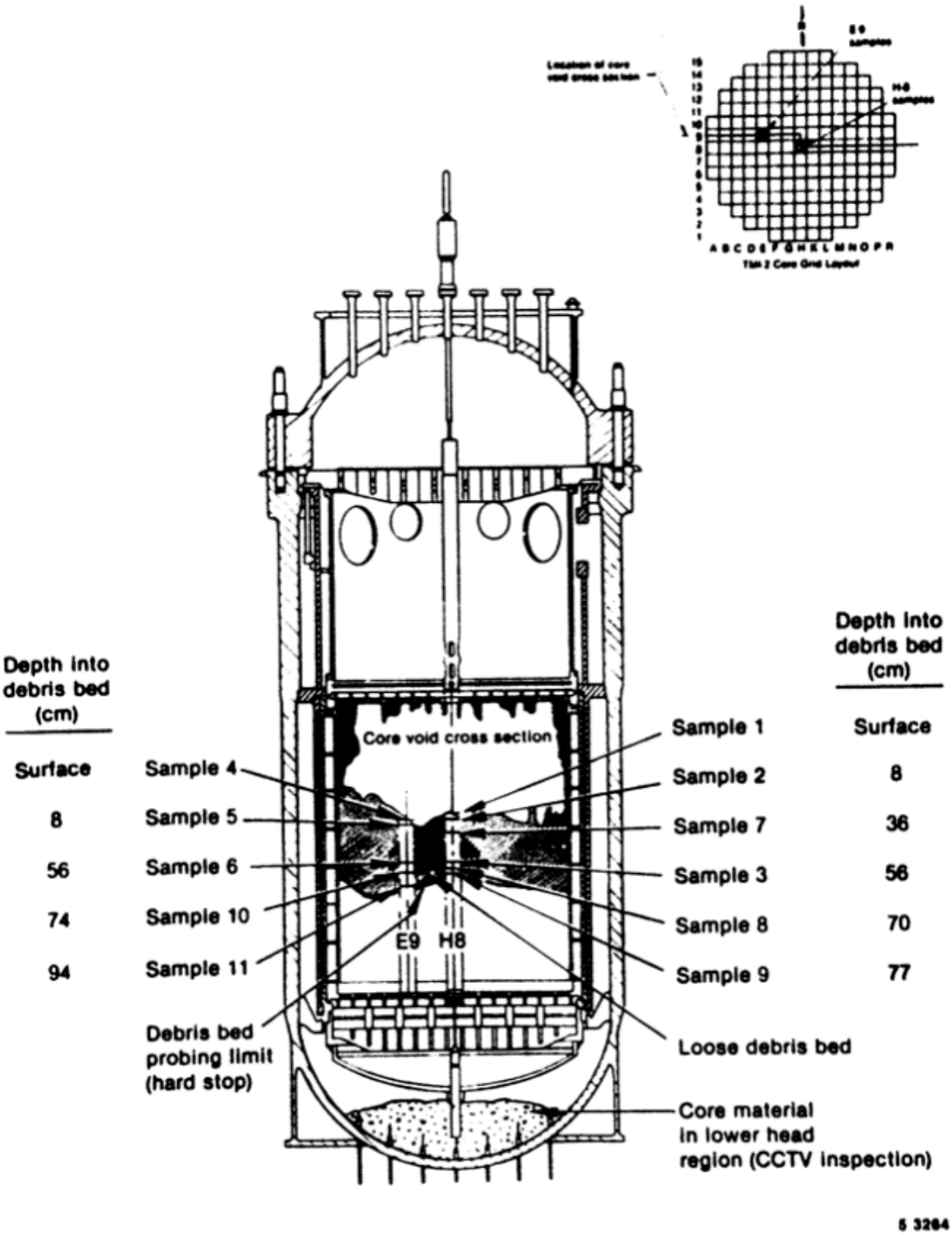

Figure 5. Loose debris sampling locations (EGG-TMI-6853 PT-1).

2.2.3 Reactor Pressure Vessel Head Removal

By mid-1984, the polar crane certification was completed; the reactor pressure vessel (RPV) head could be jacked up a small distance, allowing conditions to be evaluated. The upper plenum was inspected, and it was determined that it had only sustained a small amount of damage. By late 1984, it was raised and inspected, and by mid-1985, it was removed, followed by the upper spacer grid. The upper spacer grid had remnants of fuel elements stuck in it, requiring operators to push the stubs back into the vessel prior to removing it. A view of the underside of the upper spacer grid fuel bundle removal is shown in Figure 6. Some melting of the grid is visible.

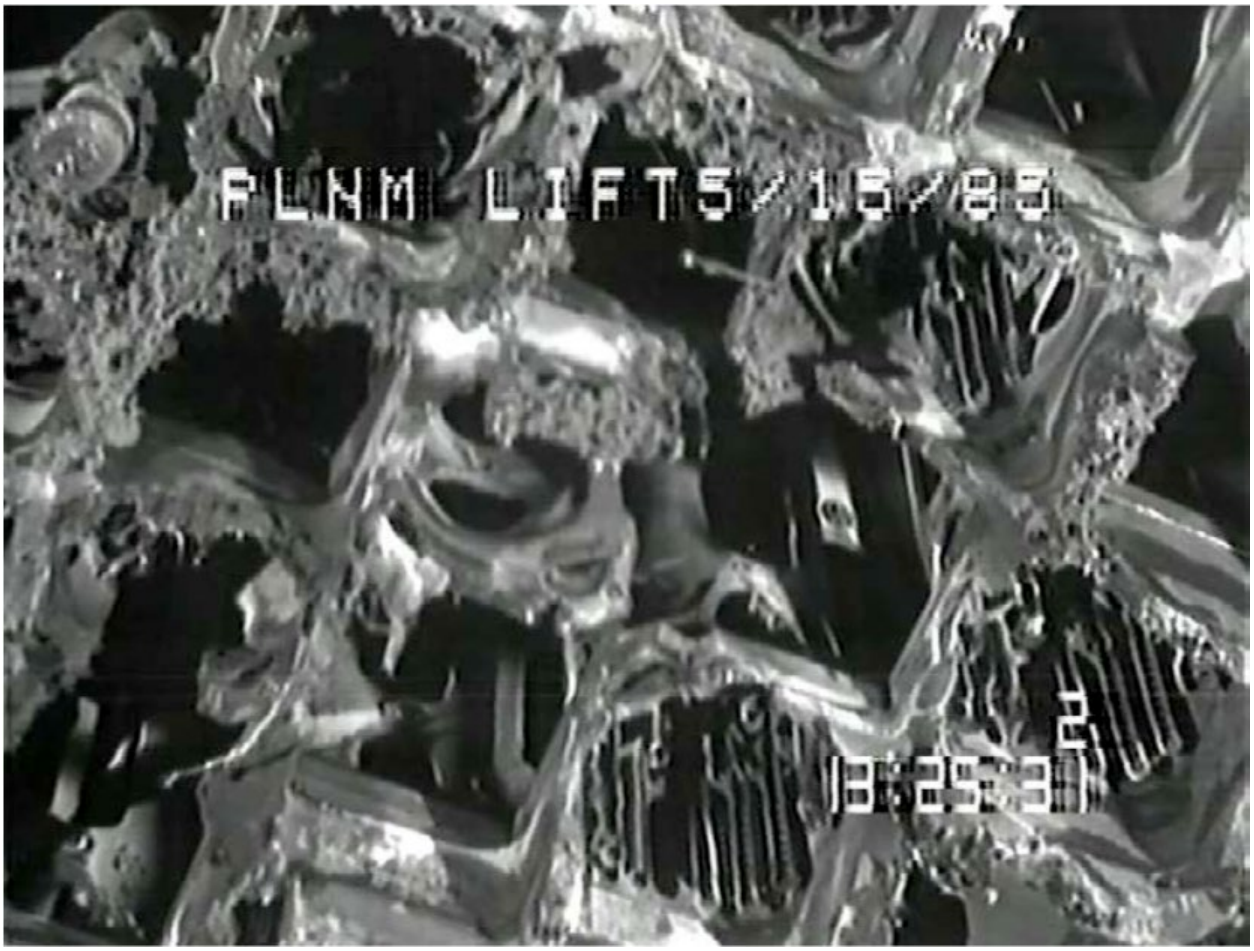

Figure 6. Underside of Upper Fuel Grid showing Evidence of Melting.

3. CORE STRATIFICATION SAMPLING PROGRAM

The Core Stratification Sampling Program adapted a commercial core-boring machine—typically used for geologic operations such as oil exploration—for the job of confirming the composition of the melt below the upper surface. In 1986, ten cores were bored at selected locations in the core. The drilling machine was instrumented to monitor changes in drive-motor torque as an indication of changes in material composition. The cores samples were shipped to Idaho National Engineering Laboratory (INEL) to be analyzed for chemical and radiological composition. From the core data, it was possible to determine that the melt varied in thickness from 1.5 m in the core center to 30 to 60 cm toward the outer edge of the core. The solidified melt amounted to approximately 10% of the core.

To accommodate materials ranging from metallic to ceramic, the core-boring system was based around a Norton Christensen Chrisdrill bit that used a combination of industrial diamond and tungsten carbide, silver-soldered into the drill body. The drive unit for the core-boring system used a hydrostatically driven spindle and hydraulic-drill string raising and lowering mechanism. A 50-hp electric motor drove a hydraulic pump that ran the multigear spindle as well as the hydraulic pump for raising and lowering. Drill operations were monitored for rotational speed and torque applied, as well as vertical force applied to the bit. The drill could operate from 0 to 500 rpm, with a torque from 0 to 3000 ft-lb and a vertical force of up to 10,000 lb. applied to the bit. The system was designed to work with the shielded defueling platform and reach any position within the central 8-ft of the core diameter. The system was constructed in modules to allow it to be transported into the containment via the 1 m × 1.9 m airlock doors.

The core bores were acquired using a 3.5-in. (OD) core barrel attached to a sectional drill string that allowed the bit to be driven to the full depth of the reactor vessel to extract a 2.5-inch OD core. During operation, the drill bit was cooled, and chips flushed by using a six gpm flow of the borated water that filled the reactor vessel. The selected equipment was a Longyear Corporation 38EHS unit, and used a Megalo head spindle, which allowed for adjustment of the jaw diameter to the required diameter of the drill string casing. A 4.5-in. OD casing was inserted into each hole that was bored to provide stability for the drill string and keep the hole open if video viewing was to be performed. The core barrel length was 132 in. to assure that it would be able to fit inside the debris canister.

Due to preinstallation testing using mock materials, the spindle torque and vertical force values provided an indication of whether the drill was running through standing fuel arrays, loose rubble, metal, or ceramic debris.

The system was mounted to the defueling platform in a manner that allowed radial and rotational position of the drill location to be precisely controlled. That position was confirmed by use of a surveyor’s theodolite. Figure 7 shows an elevation view of the drill orientation on the platform and its position in the vessel. Figure 8 shows the coring operation extending through the core support plate to the lower head.

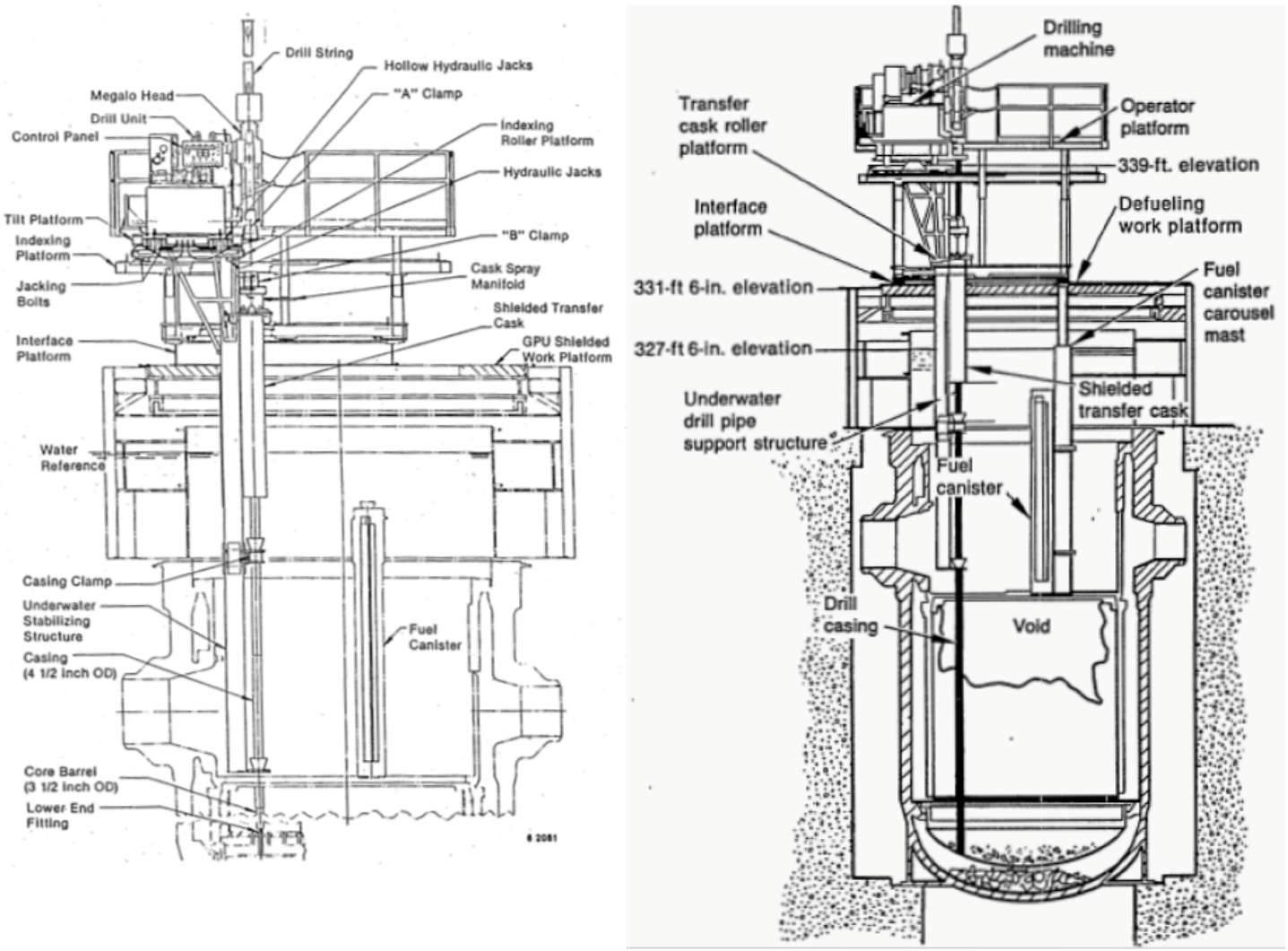

Figure 7. Elevation views of core stratification core bore system.

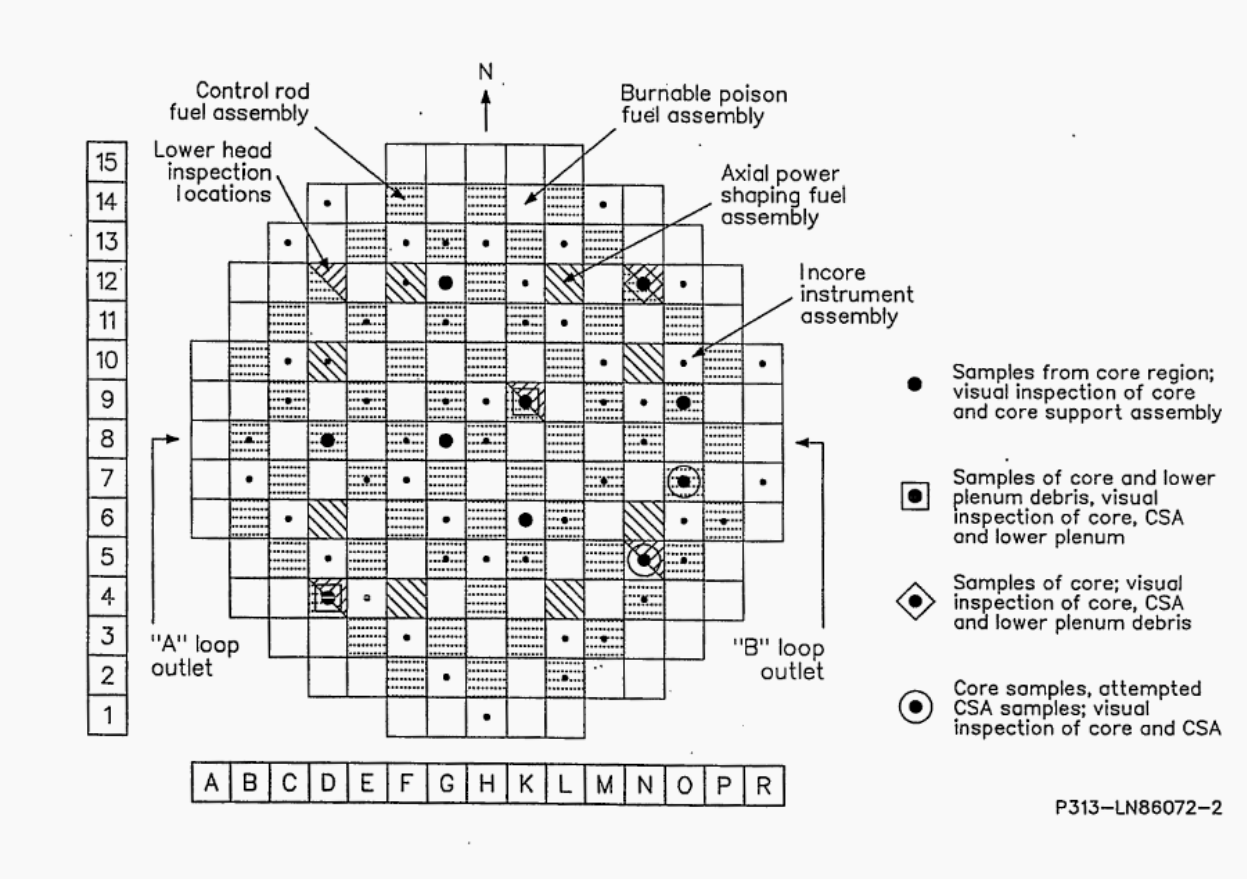

Figure 8. Plan view of core-drilling locations.

3.1 Core Bore Characterization

Analysis of core bore samples provided confirmation that interactions between the materials of the reactor core resulted in melting temperatures that are often far lower than the melting temperatures of the individual materials. In samples of core bores from the main melt, ceramic and agglomerate materials have characteristics of indicative of having been exposed to temperatures in excess of 2000 K. Figure 9 shows the range of material types encountered in a core bore from the periphery of the main core region.

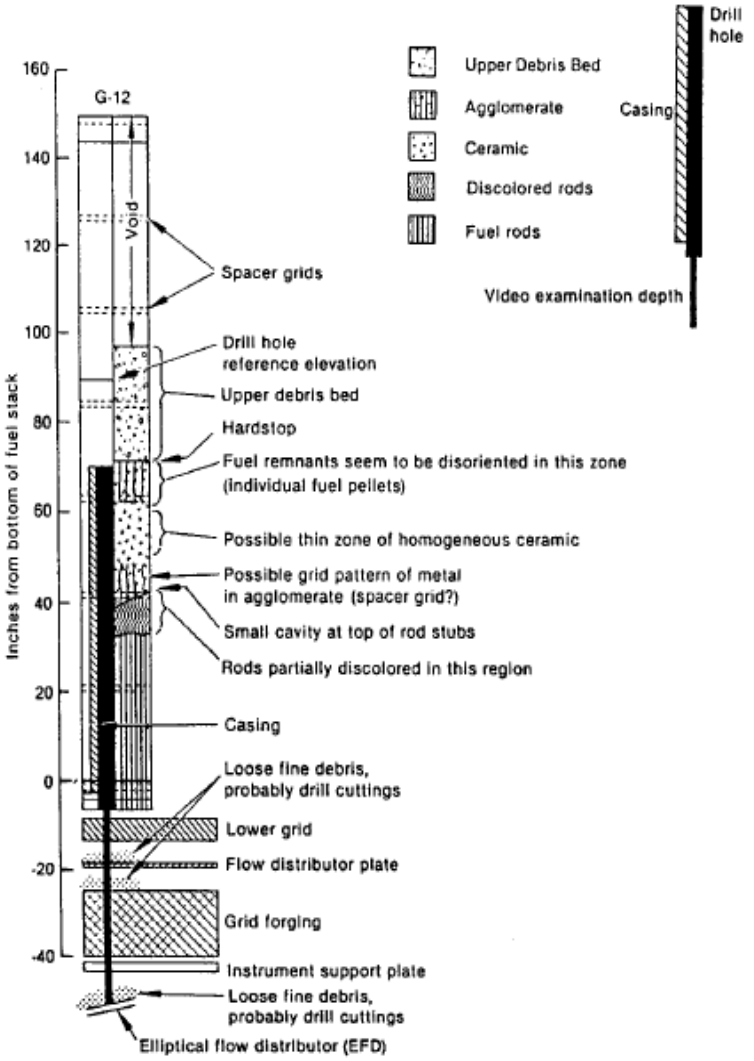

Figure 9. Example core bore material diversity.

Rod sections that were not completely melted contained silver, indium, and cadmium constituents of adjacent melted control-rod, imbibed into the fuel-clad gap, and precipitated in cracks in the fuel pellet. It is assumed that when clad integrity was lost, these relatively mobile species entered this space and condensed there. The relatively low temperature (860°C) indicated by the zirconium-phase oxygen ratio suggests that a eutectic between zirconium and stainless-steel allowed this uptake of molten metal to occur (Hofmann et al. 1989).

Analysis of the fuel pellet indicated no change in oxygen stoichiometry and no release of cesium content.

Core bore rocks were noted to be either ceramic or agglomerate types. The “homogeneous” ceramic types were predominately uranium and zirconium oxide, the relative concentrations of which varied widely (UO_2 62–82 wt%, ZrO_2 18–53 wt%) over the sample volume. Confirmation of the ceramic characteristics was done by X-ray diffraction; this showed the fluorite face-centered cubic form of UO_2 and the monoclinic of ZrO_2, with a dispersed spinel cubic phase representing the iron, nickel, and tin

inclusions in the rock sample. These inclusions in the homogeneous rock appear at the grain boundaries and, in some cases, as discrete inclusions in void spaces.

When compared to a calculated UO_2 radionuclide inventory, an example of ceramic rock showed that it was depleted in cesium by two orders of magnitude, but slightly enriched in cerium. The agglomerate rock was depleted in cesium by one order of magnitude, and the concentration of ^{106}Ru exceeded the expected model concentration by 60%, while ^{125}Sb concentration was 25 times higher than predicted. This is presumed to be due to selective dissolution of ruthenium and antimony into the metal phase. (Trotobas et al. 1989) Figure 10 shows another example of the variation of the composition of the melt.

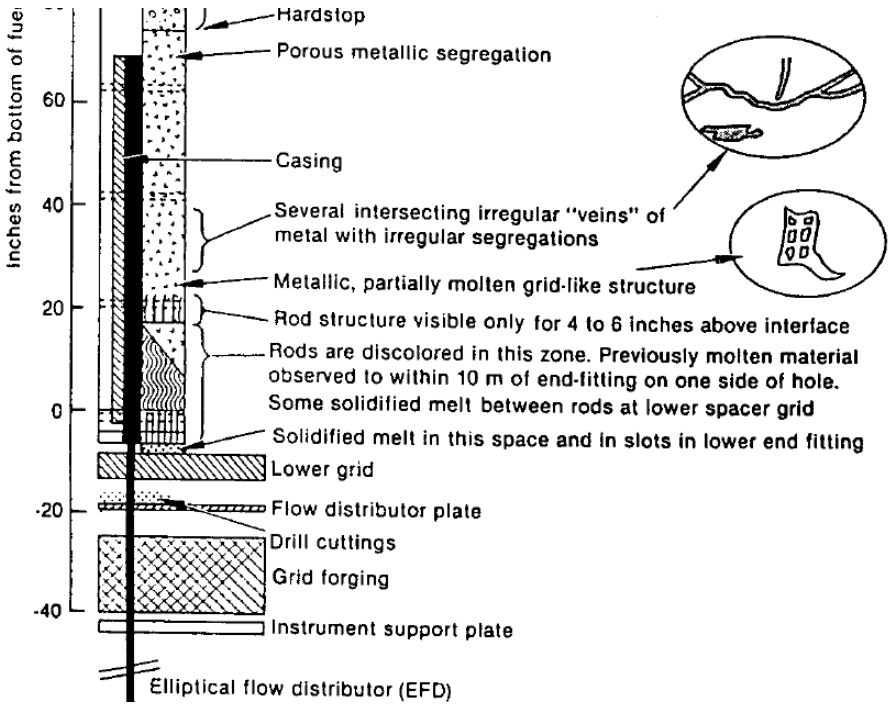

Figure 10. Section of core bore K9. (EGG-7385).

Standing fuel-rod sections varying from 0.2 to 1.5 m long were noted as being located around the periphery of the resolidified primary melt.

For hanging rod section examples, such as that taken from reactor core position K9, significant alteration of the Zircaloy clad at the location of the melt partition, with a wide range of zirconia thickness observed. Hydride formation was noted as relatively uniform, with a circumferential uniform hydride surface.

Sections of clad that did not undergo gross oxidation exhibited the expected beta phase of zirconium. In the highly oxidized zones, alpha-phase zirconium oxide (Zr[O]) was overlaid by a 14–52-micron layer of zirconia (ZrO_2). The large variation in zirconia thickness is indicative of the effect of a large thermal gradient. The oxygen ratio measured at the alpha-zirconium oxide/zirconium beta-phase interface indicated that temperatures may have exceeded 1100°C. (Trotobas, 1989)

Fission product ^{137}Cs and ^{134}Cs, and activation product ^{125}Sb and ^{60}Co-deposition were detected by gamma-ray spectrometry. Surface scrapings showed ^{238}U that may have been deposited during the samples' years-long exposure to uranium-containing water in the reactor vessel. (Jensen, GEND-INF-082, September 1987).

To establish these characteristics, core bores were subjected to axial gamma-ray spectrometry to identify the concentration and distribution of gamma-emitting fission products. The cores were examined for chemical content to determine what constituents had reacted to produce the melt.

Samples were selected for examination by U.S. DOE operators as well as multiple international laboratories, including ones in Japan, Germany, Canada, and France. The analysis included inductively coupled plasma, optical emission spectroscopy to determine elemental chemical composition, scanning electron microscopy to determine surface topography, and transmission electron microscopy and X-ray diffraction to identify chemical constituents and crystalline structure (Russell, EGG-TMI-7992, February 1988). An example of fuel-rod disarray is seen in a video image in Figure 11. Stubs of rods that had failed and remained positioned in the end fixture are shown in Figure 12.

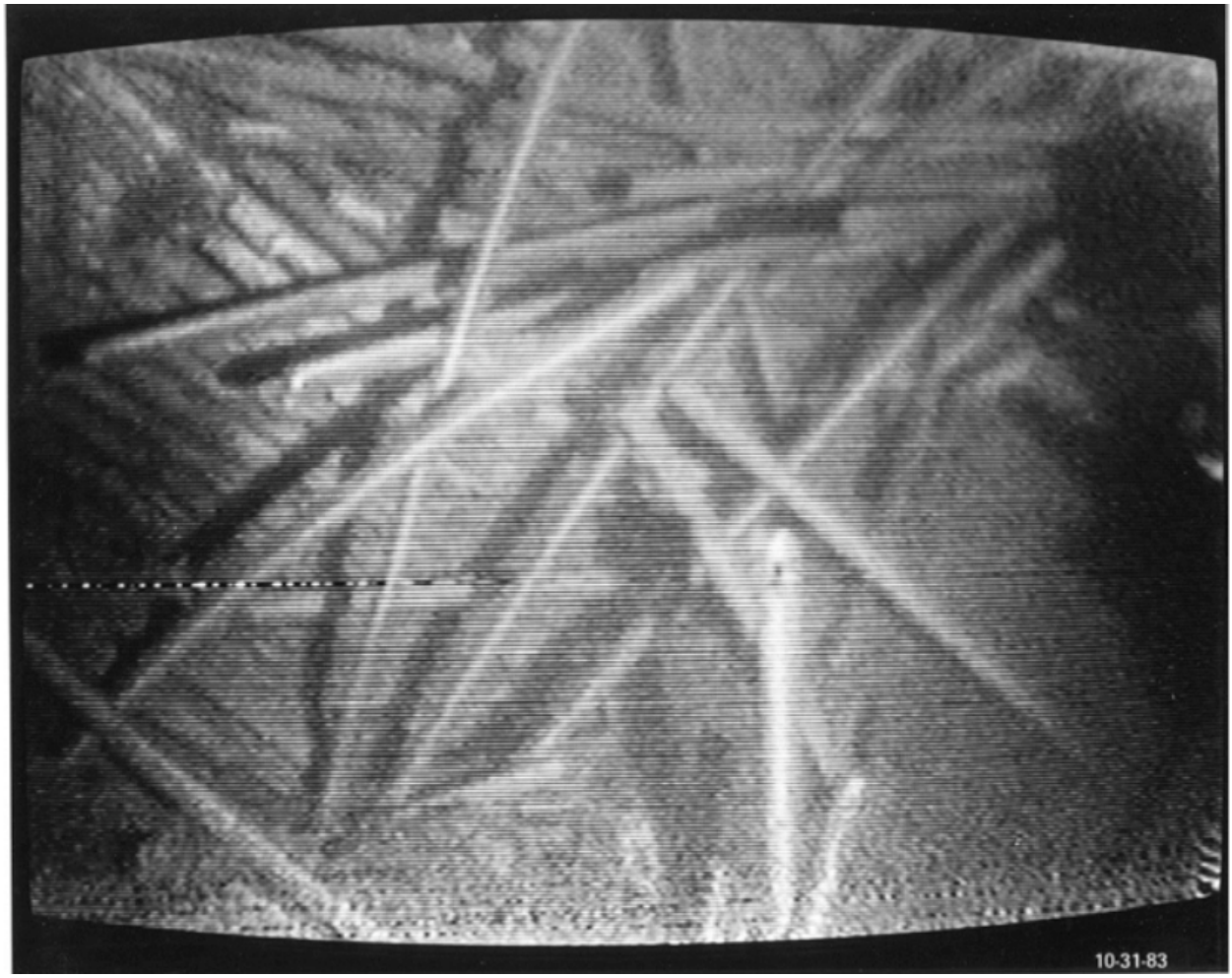

Figure 11.Video image of splayed fuel rods.

Figure 12. Standing remains of fuel assemblies.

The first indications that significant amounts of material were present in the lower head came from neutron detectors inserted between the biological shield and the reactor vessel.

The combination of quick-look video, ultrasonic mapping and bore analysis resulting in a reconstruction of the melt that is shown in Figure 13. An example of a metallographic image of mounted debris showing its multiple phases appears as Figure 14.

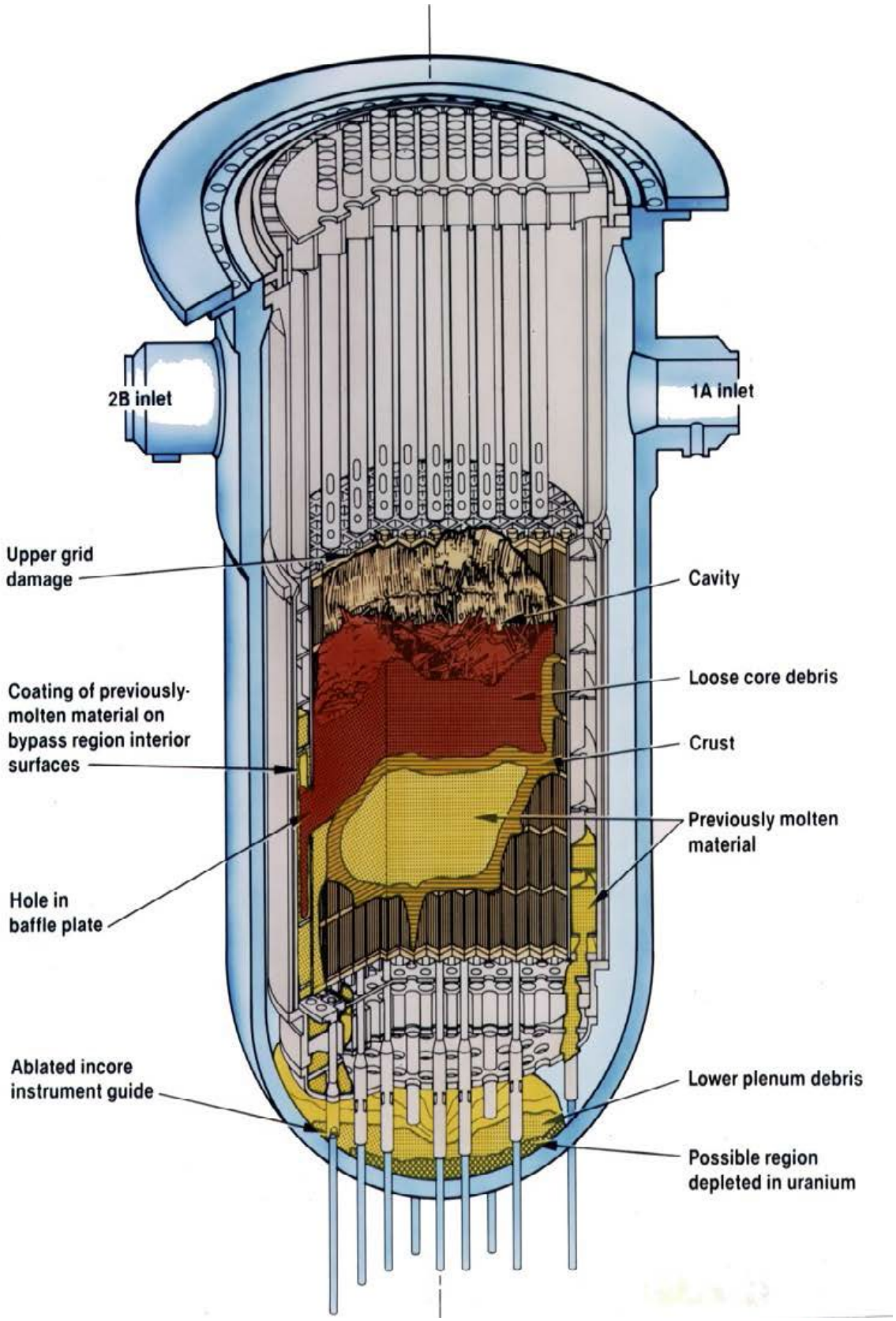

Figure 13. Final reconstruction of post-accident in-vessel debris configuration.

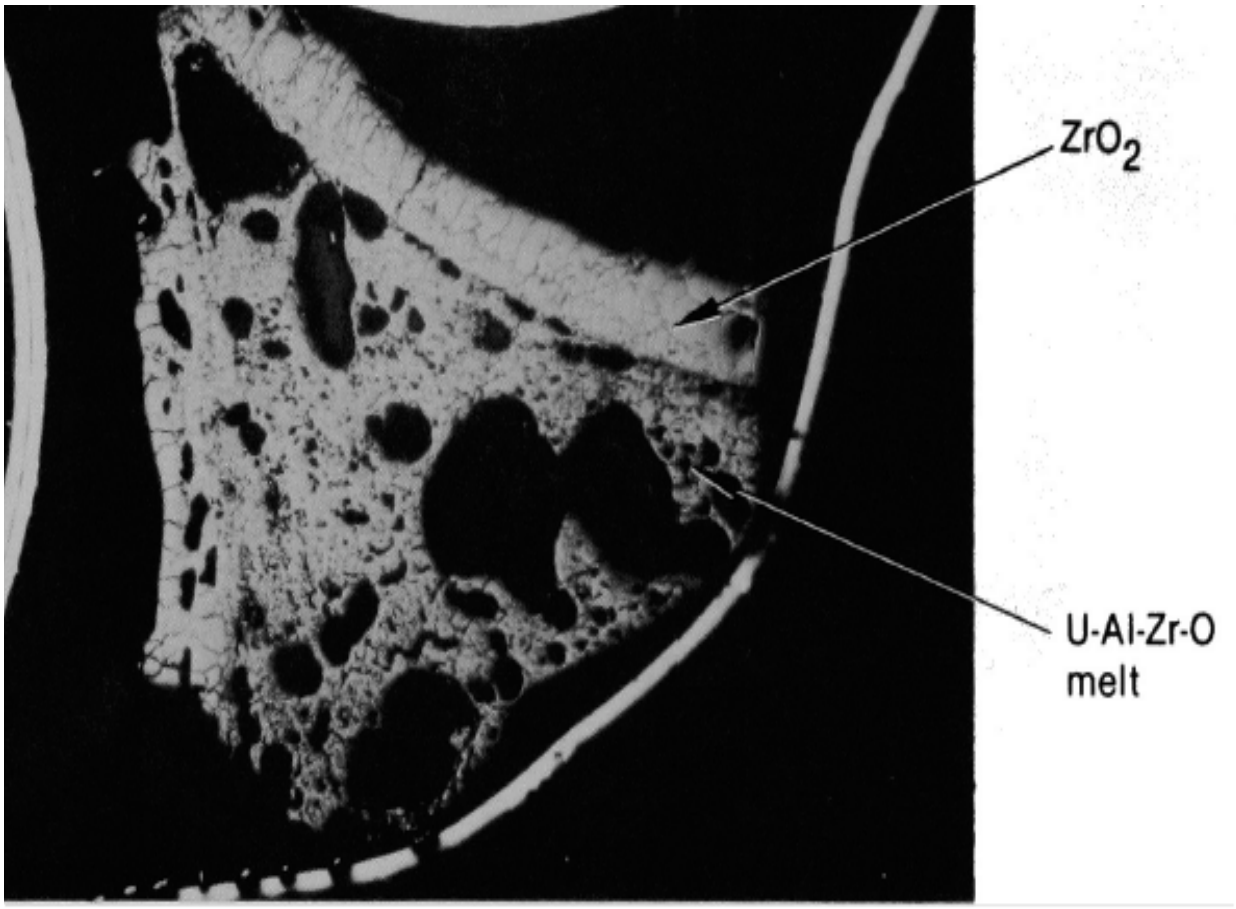

Figure 14. Optical metallograph of melted core sample.

A summary of the distribution material throughout the reactor vessel is shown in Table 1.

Table 1. Debris Composition and Distribution (Akers, 1990).

Core material repositories	Core material distribution of fuel material [(a)]			Core material distribution of control-rod materials [(a)]		
	Uranium	**Zirconium**	**Tin**	**Silver**	**Indium**	**Cadmium**
Upper reactor plenum	(b)	(b)	(b)	1.0	(b)	(b)
Upper core debris	24	13	(c)	1.8	(c)	(c)
Upper crust region						
• Ceramic	1.3	1.2	2.3	1.2	3.6	0.65
• Metallic	--	0.3	6.1	2.4	3.3	0.39
Consolidated region						
• Ceramic	12	18	--	10	27	6.1
• Metallic	--	0.2	5.8	1.6	2.1	1.1
Lower crust region						
• Ceramic	3.6	2.8	9.3	7.3	7.2	1.4
• Metallic	--	5.6	26	11	16	2.9
Intact fuel rods (d)	33	33	33	11	11	11
Lower reactor vessel head	15	11	(c)	(c)	(c)	(c)
Lower core support assembly	4.6	3.3	(c)	(c)	(c)	(c)
Upper core support assembly	3.3	2.4	(c)	(c)	(c)	(c)
TOTAL	**97**	**91**	**82**	**47**	**70**	**23**

(a) Percentage of the total amount of the element originally present in the core
(b) Insignificant amount (<0.1 wt%) based on the upper plenum measurements
(c) Elemental constituent not detected based on detection limits of approximately 0.1 wt%

Only 70% of the partially intact fuel assemblies contain control material as the balance (22.7%) are peripheral assemblies which do not contain control materials

Characterization of the various sampled materials provided an indication of the distribution of radionuclides that were retained in the core as shown in Table 2.

Table 2. Reactor System Fission Product Distribution (Akers, 1990)

Fission Product Repositories	**Fission product distribution** **Low volatility fission products** **Percent of inventory [a]**			**Fission product distribution** **Medium volatility fission products** **Percent of inventory [a]**			**Fission product distribution** **High volatility fission products** **Percent of inventory [a]**		
	Ce-144	**Eu-154**	**Eu-155**	**Sr-90**	**Ru-106**	**Sb-125**	**Cs-137**	**I-129**	**Kr-85**
Ex-vessel Containment atmosphere, basement, and tanks	0.01	(b)	(b)	2.1	0.5	0.7	(b) 47	(b) (47) [c]	54 (b)
Reactor coolant system	(b)	(b)	(b)	1	(b)	0.2	3	1	(b)
Auxiliary building	(b)	(b)	(b)	0.1	(b)	0.7	5	7	(b)
In-vessel									
Upper reactor plenum	(b)	(b)	(b)	(b)	(b)	(b)	(b)	(b)	(b)
Upper core debris-A	26	30	24	23	14	13	5.3	5.9	6
Upper core debris-B [c]	20	19	19	19	16	24	4.3	5.3	(b)
Upper crust region • ceramic • metallic	1.4	2.0	1.6	 0.73 (b)	 0.8 3.8	 0.5 7.8	0.41	0.27	(b)
Consolidated region • ceramic • metallic	24	32	22	 8.3 (b)	 2.2 9.0	 3.1 6.9	0.77	2.1	(b)
Lower crust • ceramic • metallic	5.9	7.9	5.1	 4.5 (b)	 5.7 24	 7.4 36	1.4	3.5	(b)
Intact fuel rods	30	30	30	30	30	30	30	30	30
Upper core support assembly	3.4	4.5	(d)	3.9	0.23	0.22	0.46	0.12	(b)
Lower core support assembly	4.7	6.3	(d)	5.3	0.32	0.30	0.63	0.16	(b)
Lower head-reactor vessel	16	21	(d)	18	1.1	1.0	2.1	0.54	(b)
TOTAL	**105**	**122**	**110 [d]**	**93**	**94**	**119**	**95**	**97**	**91**

(a) Percentage of total amount of the fission product inventory calculated from comparisons with ORIGEN2

(b) Insignificant amount (<0.1 wt%) based on the upper plenum measurements

(c) Two sets of bulk sample measurements were performed on the upper debris bed. The A series was performed on 16 cm^3 sample from near the center of the core at a variety of depths whereas the B series were bulk samples from near the bottom of the debris bed. The data provide a range. For the totals, the B series data were used.
(d) Measurements not performed for this radionuclide at this core location. The total shown value in parenthesis is a total which assumes the same distribution as Eu-154 for the repositories where measurements were not performed

Chemical analysis was performed to establish chemical composition, radionuclide content, and provide a basis for nuclear material accountancy. Several approaches were used to dissolve the samples for analysis. These included grinding the samples to get a sample mass that could be readily dissolved, dissolution with sequential application of nitric acid to dissolve metal and uranium, followed by hydrofluoric acid to dissolve remaining silicates and oxides of niobium, tantalum, titanium, and zirconium, then any remaining undissolved material was melted in a pyrosulfate fusion, which can be dissolved in acid to provide a solution for analysis.

3.1.1 Core Removal

Multiple approaches for core removal were considered prior to receipt of the first characterization data. Five official predictions of the degree of core damage were compiled into a single report known as GEND-007. This report was used as a basis for development of design concepts for defueling. These were the dual telescoping tube/manipulator system, the manual defueling-cylinder system, the indirect defueling-cylinder system, the flexible-membrane defueling system, and the dry defueling system. The dual telescoping tube system would have mounted two telescoping tubes on the TMI-2 defueling bridge and remotely operated them by closed circuit video. The manual defueling system was a design with a rotating cylinder supported on the top flange of the reactor vessel with a slot through which operators would perform manual removal of the core. The indirect defueling-cylinder system was to have inserted an X-Y bridge with a telescoping tube in place of the manual tools of the previous design. The flexible-membrane defueling system would have incorporated an X-Y bridge using a single telescoping tube operating through a conical contamination control membrane and used a separate tank whose support arms were to have pivoted out over the reactor vessel to hold manipulators canisters, buckets, and tools in support of the manipulation function of the telescoping tube. The dry defueling system was to insert an indexable shield ring on the top flange of the reactor vessel that used an access port to remove debris via a heavily shielded transport cask (Sec. 8.2.2 EPRI-NP 6931).

Considerable discussion about the merits of manual versus automated core removal included the possibility of using the Westinghouse remotely operated service arm (ROSA) to shred the melted core and transfer the result by vacuum to canisters outside the reactor vessel. One of the negative aspects of this approach was the dispersal of the core nuclides, increasing the dose potential and placing a greater demand on the water-cleanup systems. Several variations of the remote and manual core recovery systems were proposed, but all had the problems of complexity and delays due to development and testing of tools to size materials that were poorly understood and not well characterized.

Due to the expected delay in the automated-tool system development and the cost and availability of the polar crane, it was decided that the manual defueling approach was the most expedient. The manual shielded defueling platform was fabricated and installed on the top of the reactor vessel to perform core recovery. The platform was a shielded turntable with slots through which extended reach tools could be used to pick up individual pieces of debris and accumulate them in baskets that were used to fill the fuel debris canisters. The platform also supported the canister handling system and included specific ports for canister removal. An isometric view of the platform is shown in Figure 15. The work elevation was nine feet above the upper flange of the reactor vessel, as seen in Figure 16. Figure 17 is a photograph of the deployed system from above.

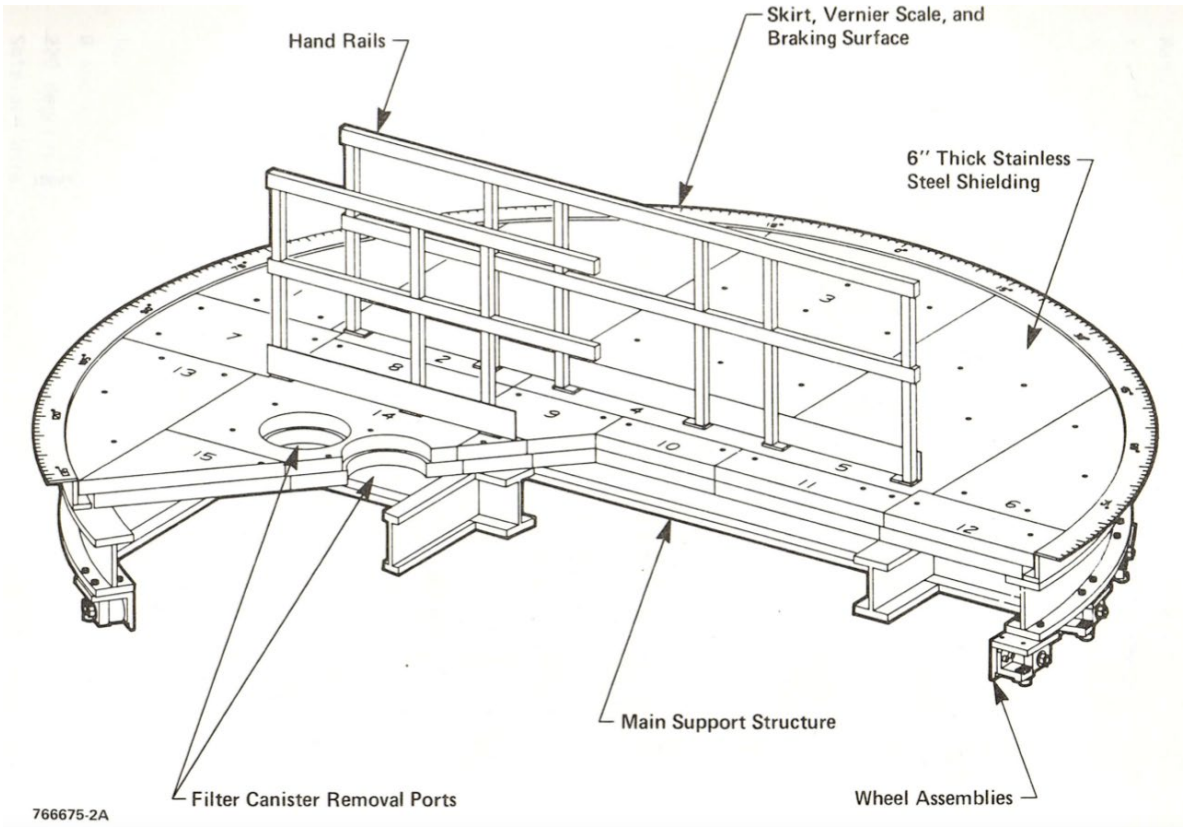

Figure 15. Manual shielded defueling platform.

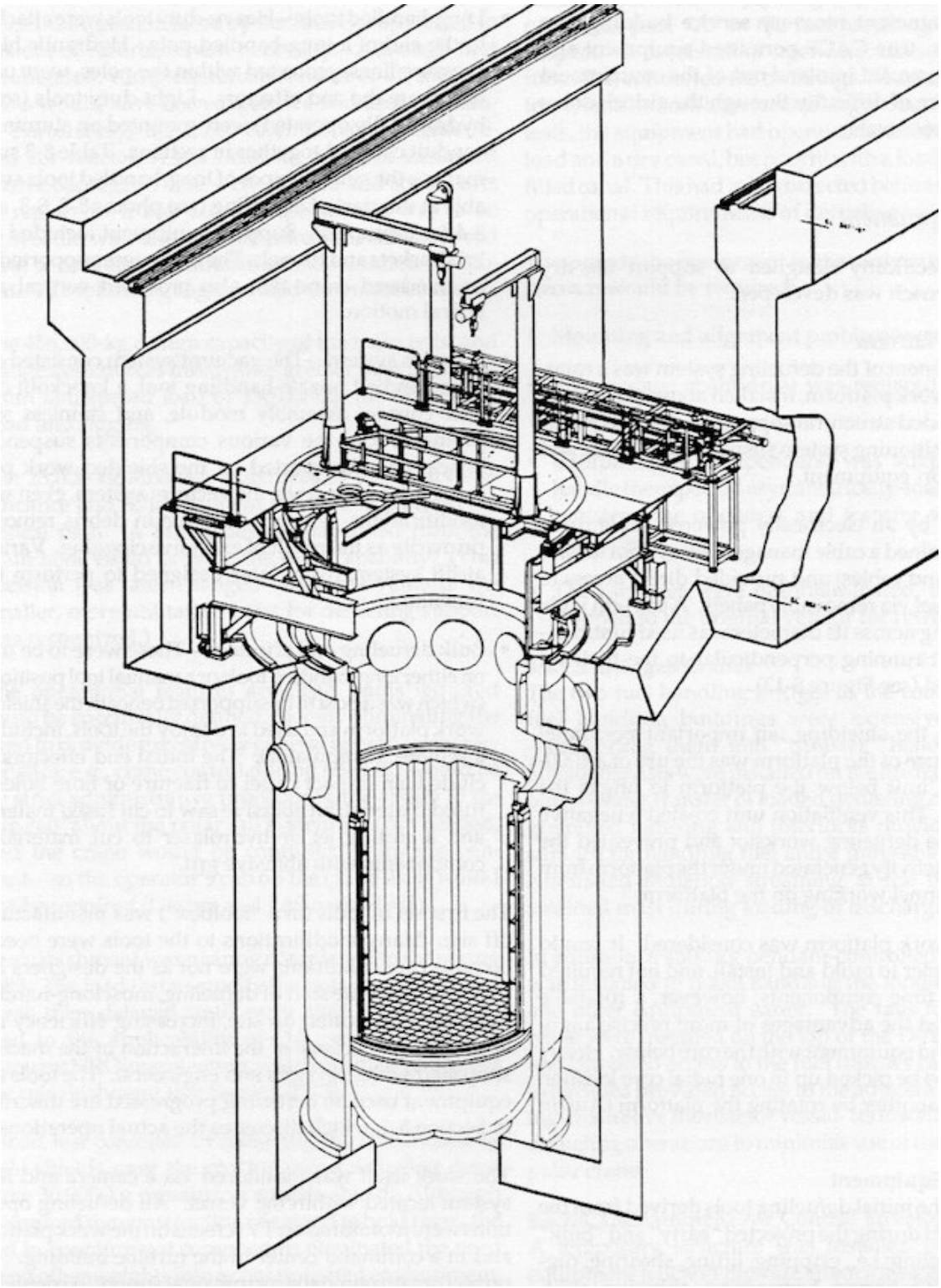

Figure 16. Defueling platform schematic in position on reactor vessel.

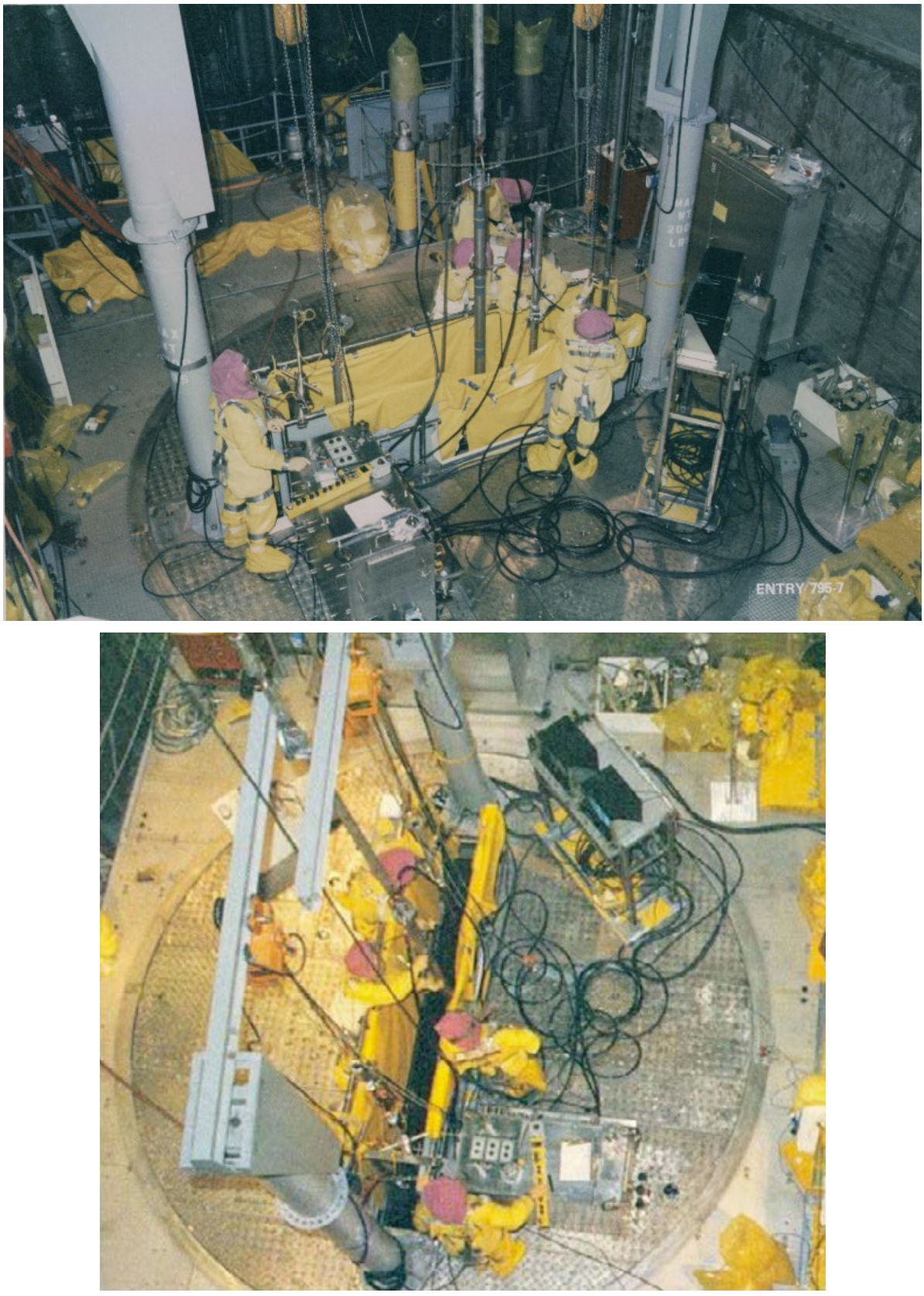

Figure 17. Photos of shielded defueling work platform.

The platform also supported a five-canister turret system that allowed multiple canisters to be loaded, as shown below in Figure 18. Once loaded, the canisters were weighed and then selectively transferred to the fuel pool for dewatering prior to loading into the transport cask.

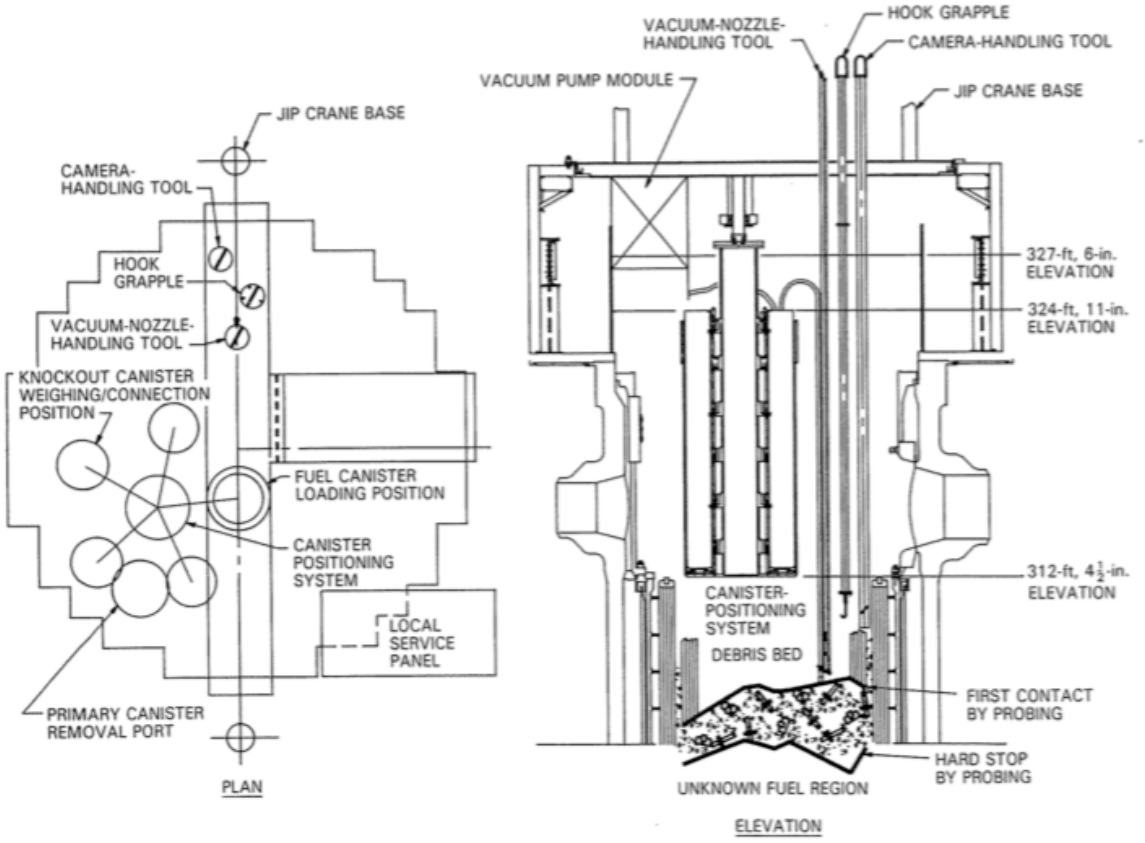

Figure 18. Canister-positioning system.

Once a canister had been filled to the desired limit, it was closed, lifted out of the reactor vessel through the penetration in the defueling platform, wiped down, and raised into the shielded transfer device, which then transferred the canister to the refueling canal within the reactor-building. As shown in Figure 19, the canister would be loaded into an upender that rotated it to the horizontal orientation, allowing it to be moved through the fuel transfer tube to the fuel-handling building pool.

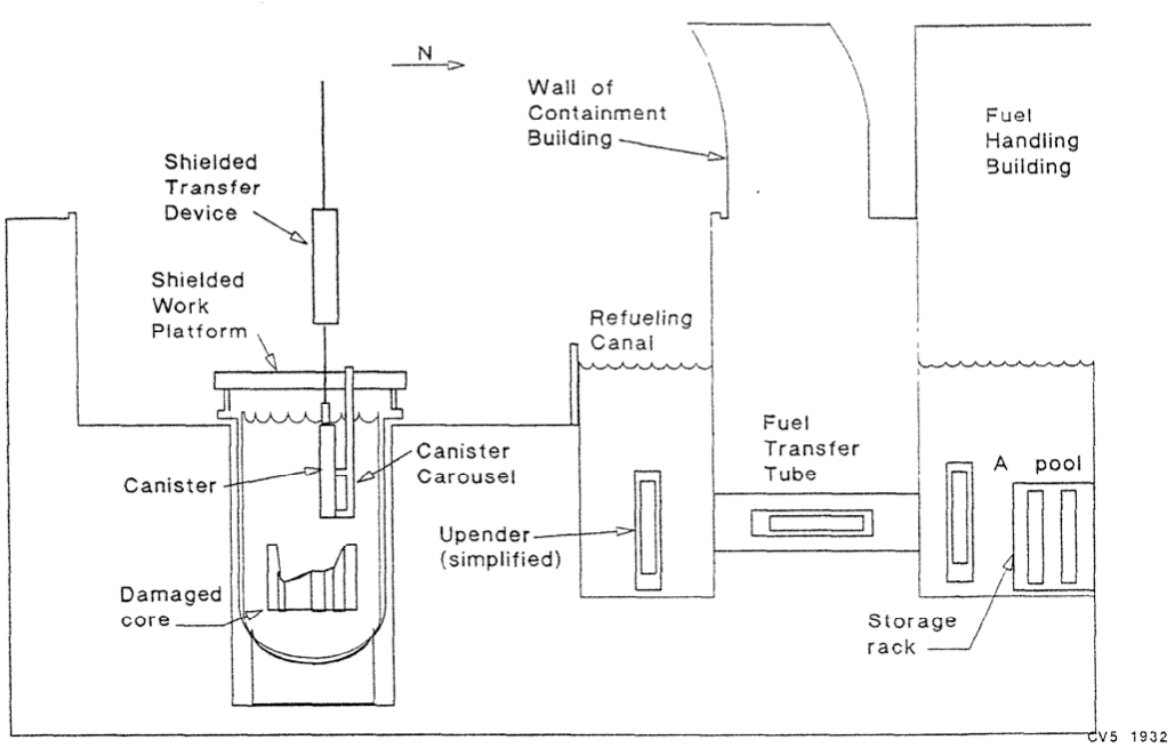

Figure 19. Schematic of canister transfer from reactor to fuel-handling building.

Debris canisters were filled piecewise by filling buckets, which were then transferred to the canisters. A graphic (Figure 20) shows operator notes on filling a canister, including the location and type of material added to Canister D-188.

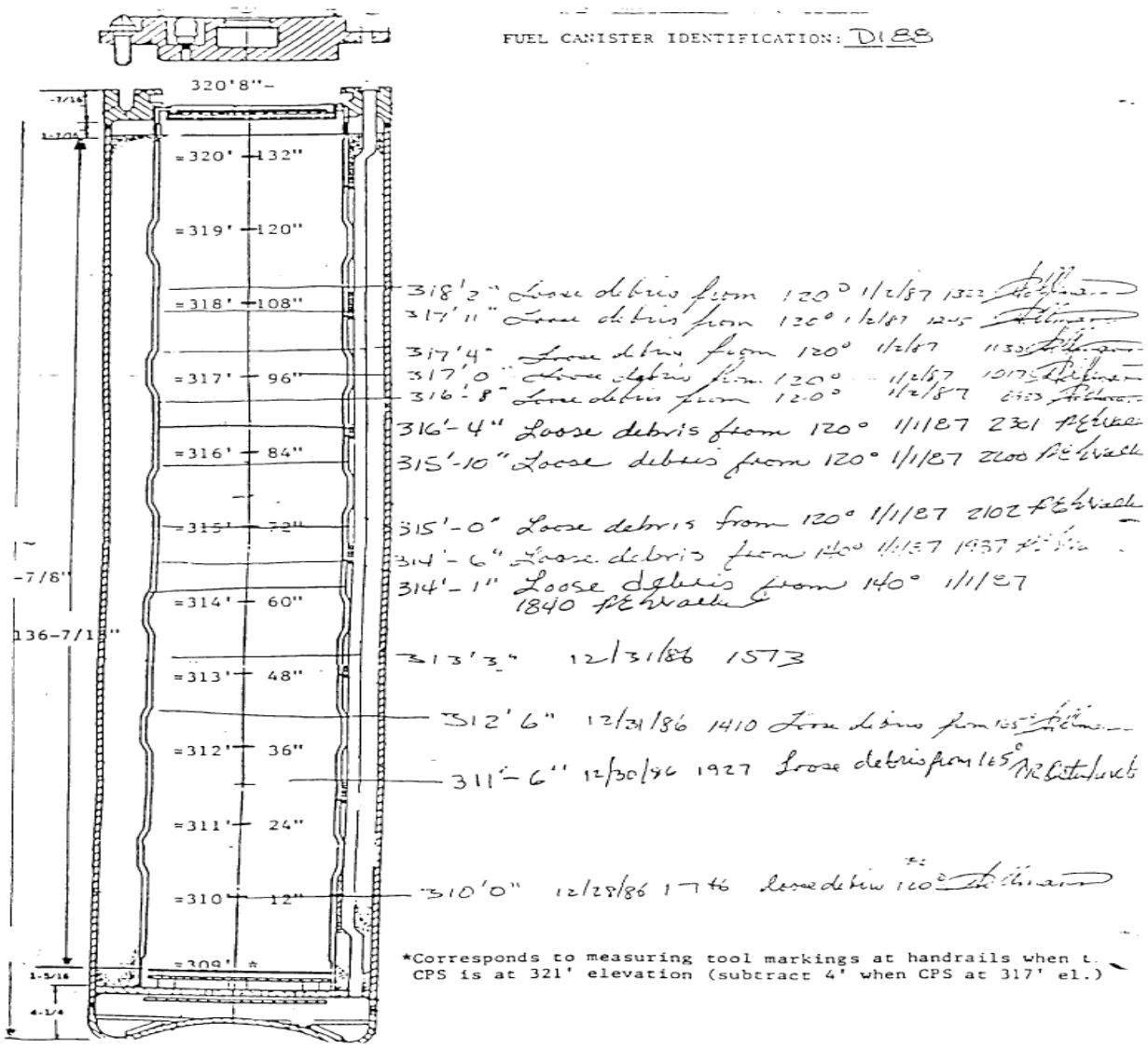

Figure 20. Operator log graphic of Canister D-188 loading.

3.1.2 Defueling Tools

A variety of specialized tools were developed for debris retrieval and sectioning of the melted core, including a water jet cutter, an abrasive saw, bolt and bale cutters, hooks, pliers, and an underwater plasma torch. Numerous changes in tool design occurred as the core conditions became better understood. Early design bases assumed a degree of consistency in the material to be retrieved when, in fact, the diversity of melted, broken, and shattered material was significant. Only 15% of the fuel retained a recognizable rod and assembly configuration. Examples of the tools, including a clamshell spade bucket, a spike tool, and a gripper tool, are shown in Figure 21.

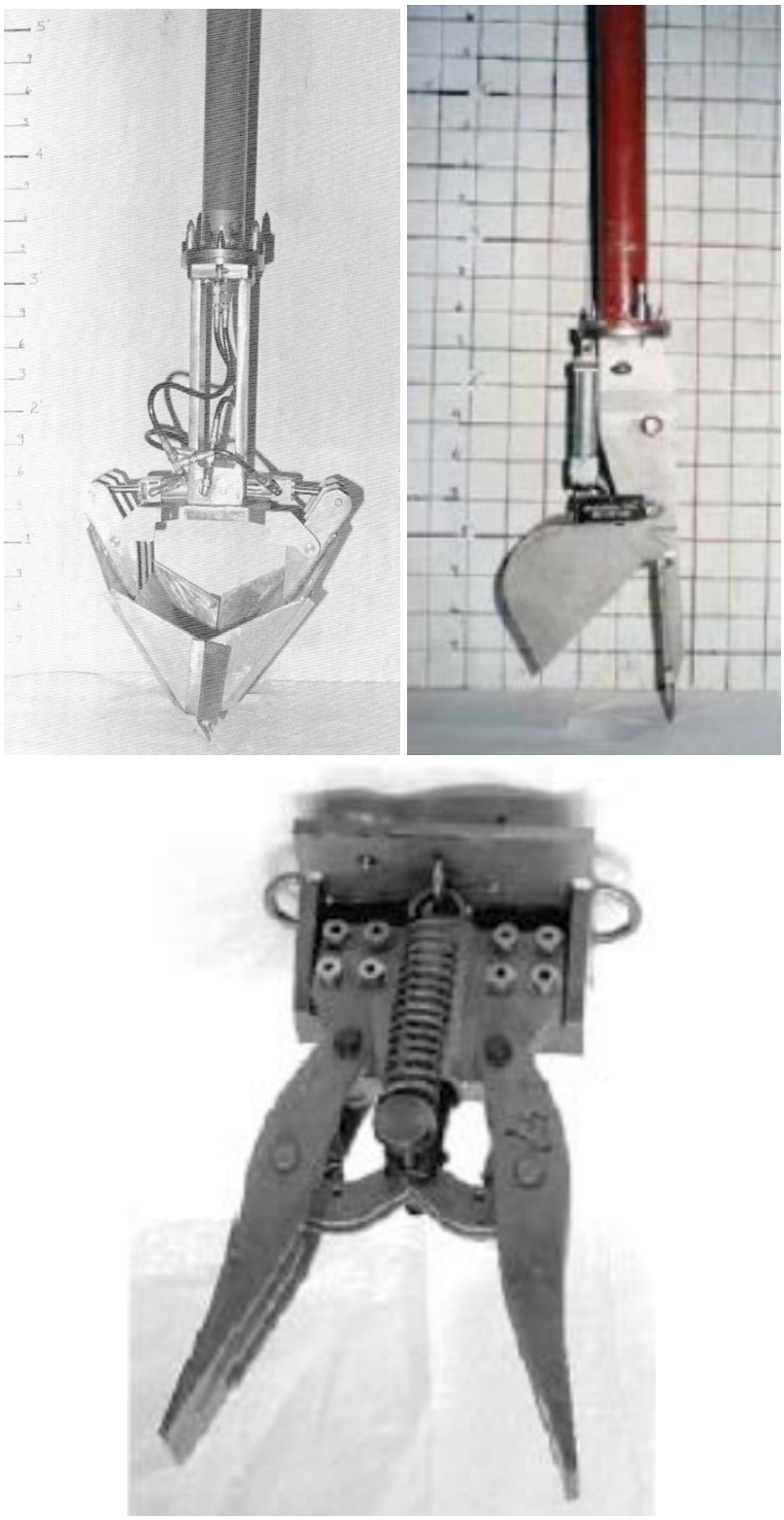

Figure 21.Spade bucket tool, spike tool, and gripper tool.

The debris were recovered by manual tools, including scoops, pliers, and hook tools. The material was collected in reusable buckets or baskets, which were transferred to the debris canisters using a funnel.

The canisters were weighed during loading to assure that the design weight limit was not exceeded as well as to provide a running total of fuel recovered.

3.1.3 Debris Removal

Primary fuel-removal operations began October 30, 1985 and concentrated on making room for installation of the canister-positioning system. Much initial effort amounted to removal of fuel end fittings. The process of loose debris removal using a spade bucket tool proceeded until April 1986 when the hard layer of formerly molten fuel was reached. Several tools, including a hydraulic impact chisel and a 135 kg impact tool, were tried on the crust, but none was able to penetrate it.

The core-boring machine that had been developed for the purpose of taking ten characterization cores was fitted with solid-face drill bits, and in October 1986, it was used to begin the process of boring 409 holes to break up the center of the solidified melt. This operation was made more difficult by poor visibility conditions due to a loss of water clarity that resulted from microbial growth and small particulates that plugged the water-cleanup sintered-metal filters. The microbial bloom was attributed to the introduction of river water during the early recovery response.

Following breakup of the central monolith, water clarity was improved by use of an additional water-filtration system. At that time, it was possible to see that there was a ring of large pieces that had been only partially broken up. These pieces were estimated to weigh as much as 1200 kg. Thus, they weighed too much to be handled with the manual long-reach tools. Because the pieces were overlaid on debris, hammering, and chiseling them in place was ineffective; the loose material absorbed most of the impact energy. A special thick-walled funnel was designed for the canister top. Large chunks were placed in the funnel and broken up using a 198 kg jackhammer fitted with a 3.6-meter-long chisel.

Pieces as large as 5 cm were retrieved using an underwater suction system that used an air-driven diaphragm pump connected to a 10-cm-diameter suction pipe. The schematic and isometric sketches of the configuration are shown in Figure 21. This suction system worked with the knockout and filter canister system to recover pieces too small to be easily picked with manual grab tools. The system had a maximum flow rate of 288 L/min. A flow rate of 227 L/min was demonstrated to be sufficient to pick up 9.5 mm OD x 16 mm long UO_2 fuel pellets. Operator care was needed to prevent plugging of the suction uptake due to the random size and geometry of the material that could be moved. Using this system, as much as 14,500 kg of debris was removed in a single month. (GEND-INF-073) This system was operated from late 1986 to mid-1987.

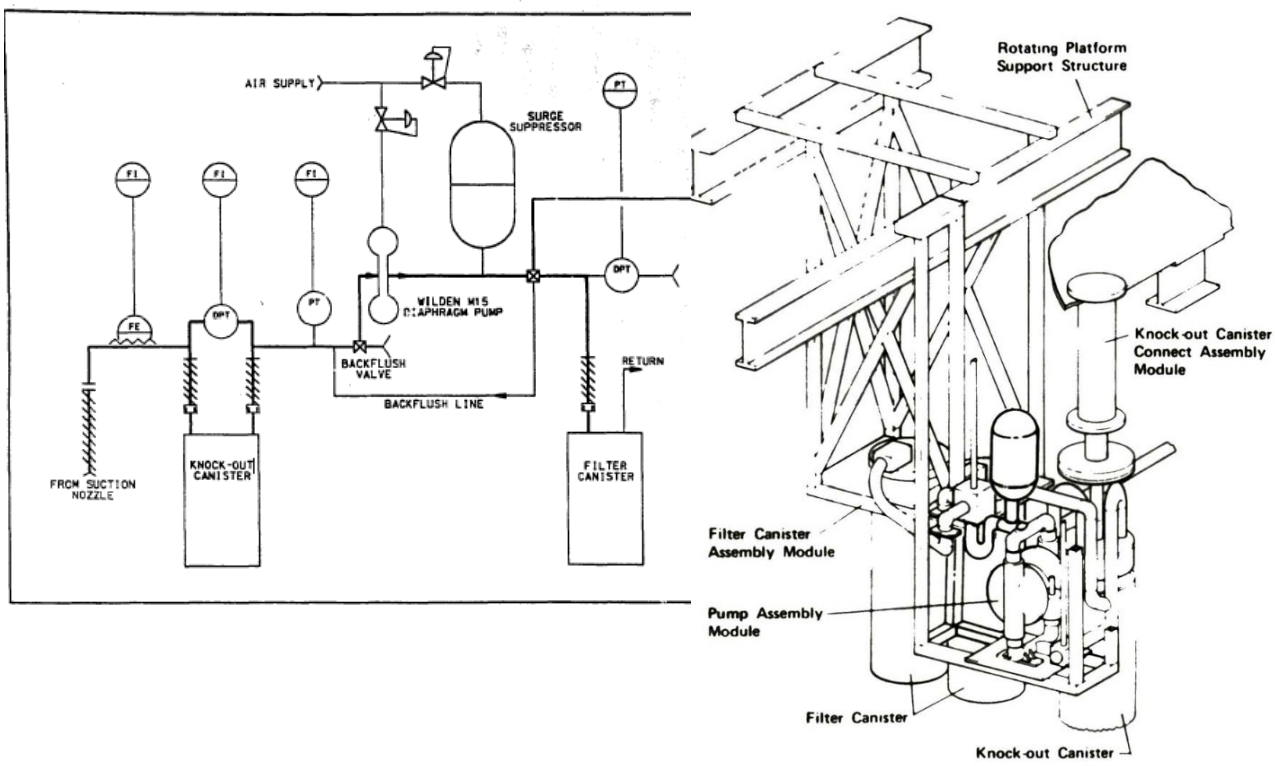

Figure 22. Suction System Schematic (GEND-INF-073 and GEND-INF-062).

Due to distortion of the end fittings of some assemblies, a decision was made separate those discrete non-fuel components to the extent possible and dispose of them separately from the fuel debris that were placed in canisters. The separated end fittings were shipped to the U.S. Department of Energy site at Hanford, Washington, and buried as low-level waste.

3.1.4 Stub or Partial Assemblies

The next type of fuel debris remaining after the central monolith and perimeter melted zones were removed was the partial or stub assembly region around the periphery of the reactor vessel and the pieces remaining below the melt. Some sections were partially stuck together. Most of this material was removed using long-handled tools that screwed into the top, attached as a clamshell, and then using pry tools to tilt partial assemblies away from each other. In some cases, largely intact assemblies could be removed after a spike was pressed into the top of the assembly and a tool with two fingers grasped it at the base. Except for two significantly melted locations, all of the stub assemblies were removed by November 1987.

3.1.5 Lower Core-Support Assembly (LCSA)

Once the stub assemblies were removed, it was possible to see that between 9000 and 18,000 kg of debris had fallen through the lower core-support framework. Initial design assumptions had been that only easily suctioned pieces would be present under this structure. Video revealed that, in addition to the debris that fell through during the stub assembly and nozzle removal, a substantial quantity of melted, solidified core mass was present under the LCSA.

Because its purpose was to support the entire core, the LCSA was massive: 3 m in diameter and fabricated in five stainless-steel plates, 90 cm deep. The components included the lower-grid top rib,

lower-grid distributor plate, lower-grid forging, in-core guide support plate, and in-core guide tubes, as shown in Figure 23.

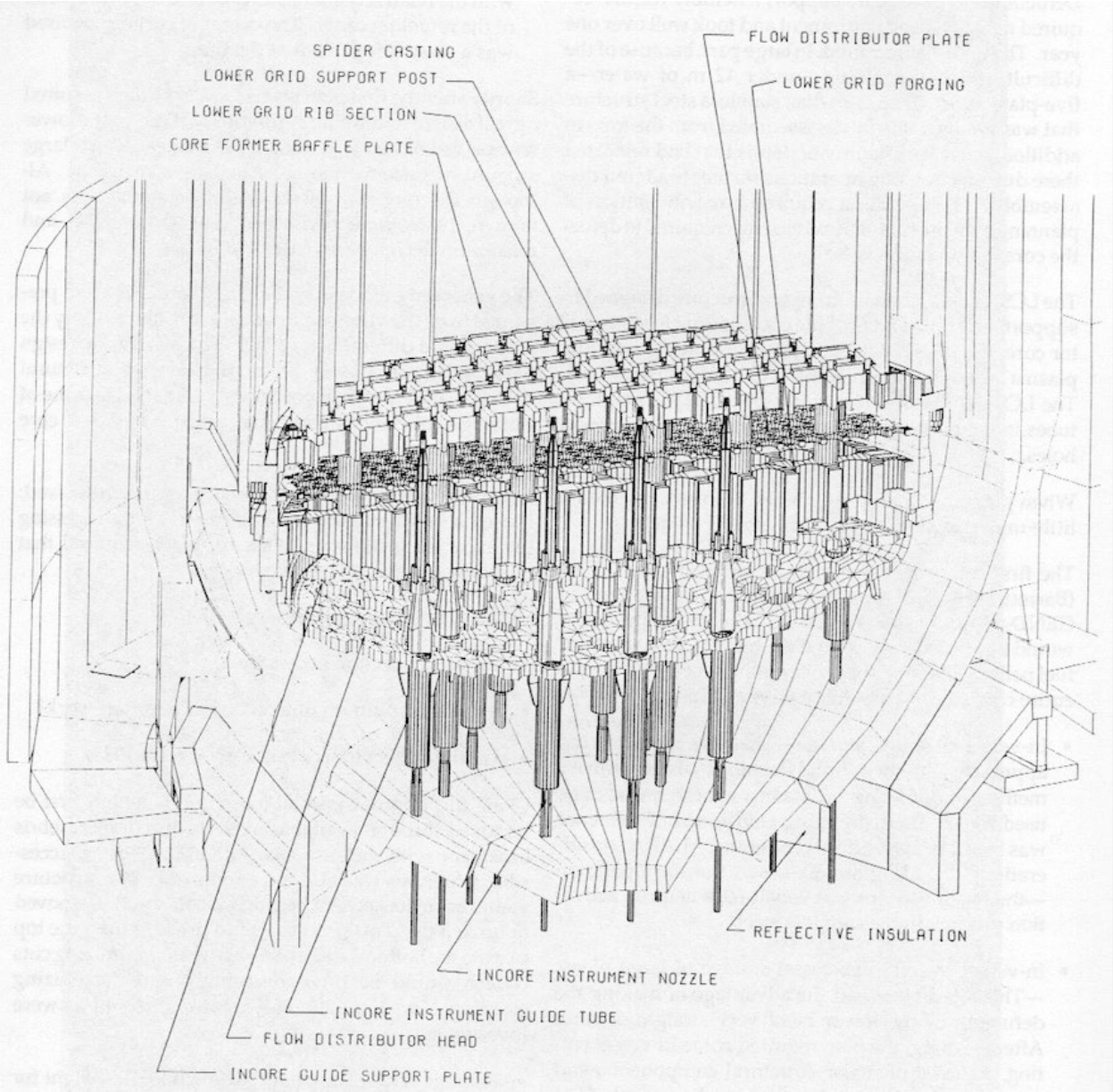

Figure 23. Lower core-support assembly model.

A large number of alternatives was considered for the removal and sizing process, ranging from sawing, and shearing to thermal, abrasive, plasma, and explosive cutting. After additional demonstration testing, the plasma arc cutter was applied for the primary portion of this task. The work was performed under 12 m of borated water. It was estimated that opening an access hole with an area of 1.2 m^2 would require 890 cuts. Because of the large number of cuts necessary to create an opening through which the debris could be removed, an automated cutting system (ACES) was developed to deploy the plasma torch. The ACES system is shown in Figure 24. One alternative design included a multi-axis dual-arm system (MANFRED) that ultimately was not used due to its complexity and the expected problems of decontaminating the multitude of hoses and cables that operated the arms. The plasma torch was deployed

using an X-Y bridge, which was lowered into the reactor vessel to a short distance above the lower core support to position the torch.

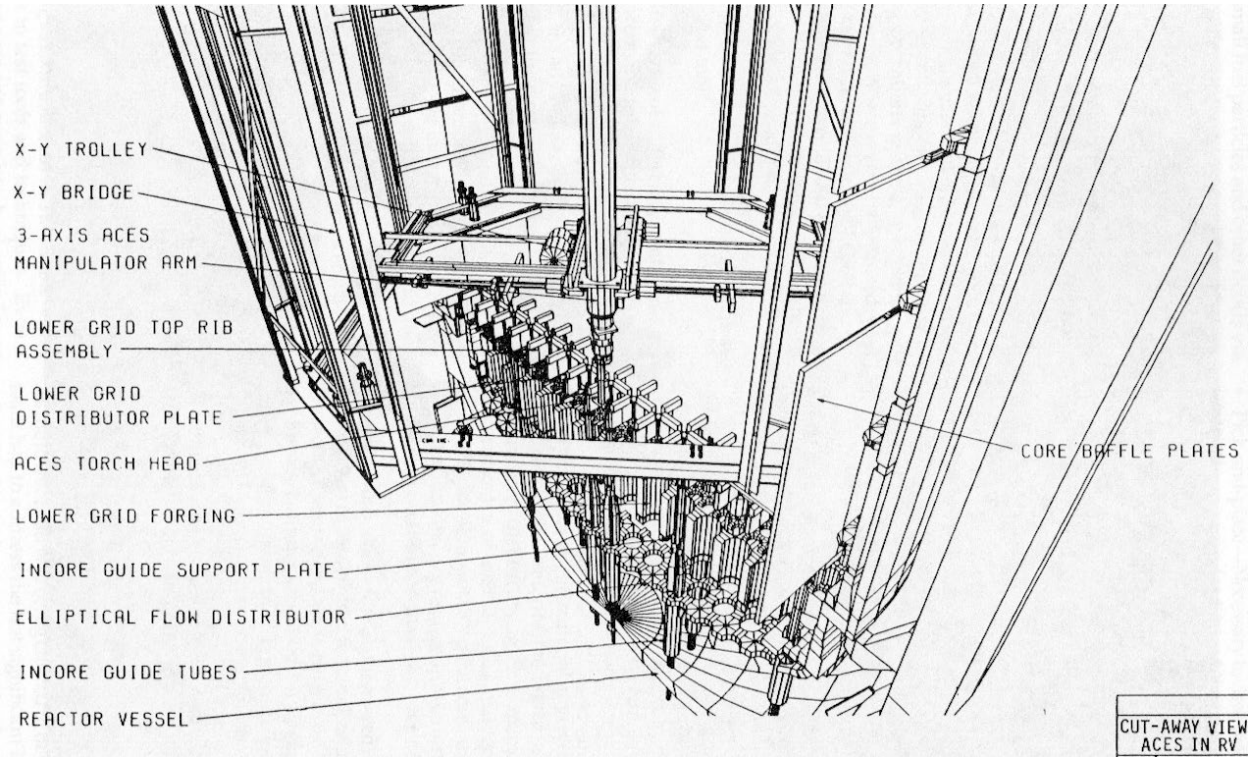

Figure 24. Automatic cutting equipment system (ACES).

Prior to deployment of the plasma arc torch, numerous concerns were raised, including problems of maintaining subcriticality, potential for hydrogen evolution, pyrophoric reaction of zirconium in water, the potential to damage the reactor vessel lower head, and unexpected spread of contamination. Through analysis, these concerns were discounted, and the torch was deployed.

Prior to using the plasma torch, the plan was that the core-boring machine would be used to drill out fifteen of the 52 in-core guide tubes and all 48 distributor plate support posts. Due to problem of discharging drilling chips, the bits became fouled, and not all of the in-core tubes were able to be cut. Despite that setback, the core-boring machine was used to cut the lower-grid rib plate into thirteen pieces.

The lower-grid distributor plate was disassembled and removed in four pieces in June and July 1998. Due to problems with torch failures attributed to adherent debris, the torch controls were redesigned. Cutting of the 34-cm-thick lower-grid forging plate required the use of an abrasive saw to perform vertical cuts while the plasma torch completed the horizontal cuts. The forging was removed during August to December of 1988.

The in-core guide support tube plate was removed in four pieces between December 1988 and February 1989.

The flow distributor plate was removed as 26 pieces during February through April of 1989.

Prior to removal of the core former baffle plates, it was necessary to remove debris generated by previous defueling activities.

3.1.6 Lower Head Debris Removal

The primary tools used for core removal were long-handled grippers, scoops, and tongs. Between pick-and-place actions with these tools and vacuuming using the airlift, 12,400 kg of debris were removed from the lower head in May 1989. This cleanup revealed a formerly molten monolithic mass on the bottom head of the reactor vessel. Although this mass was as much as 0.6 m thick at the center, it was determined to be brittle as it was fractured using an impact hammer. Figure 25 is a schematic view of the melt.

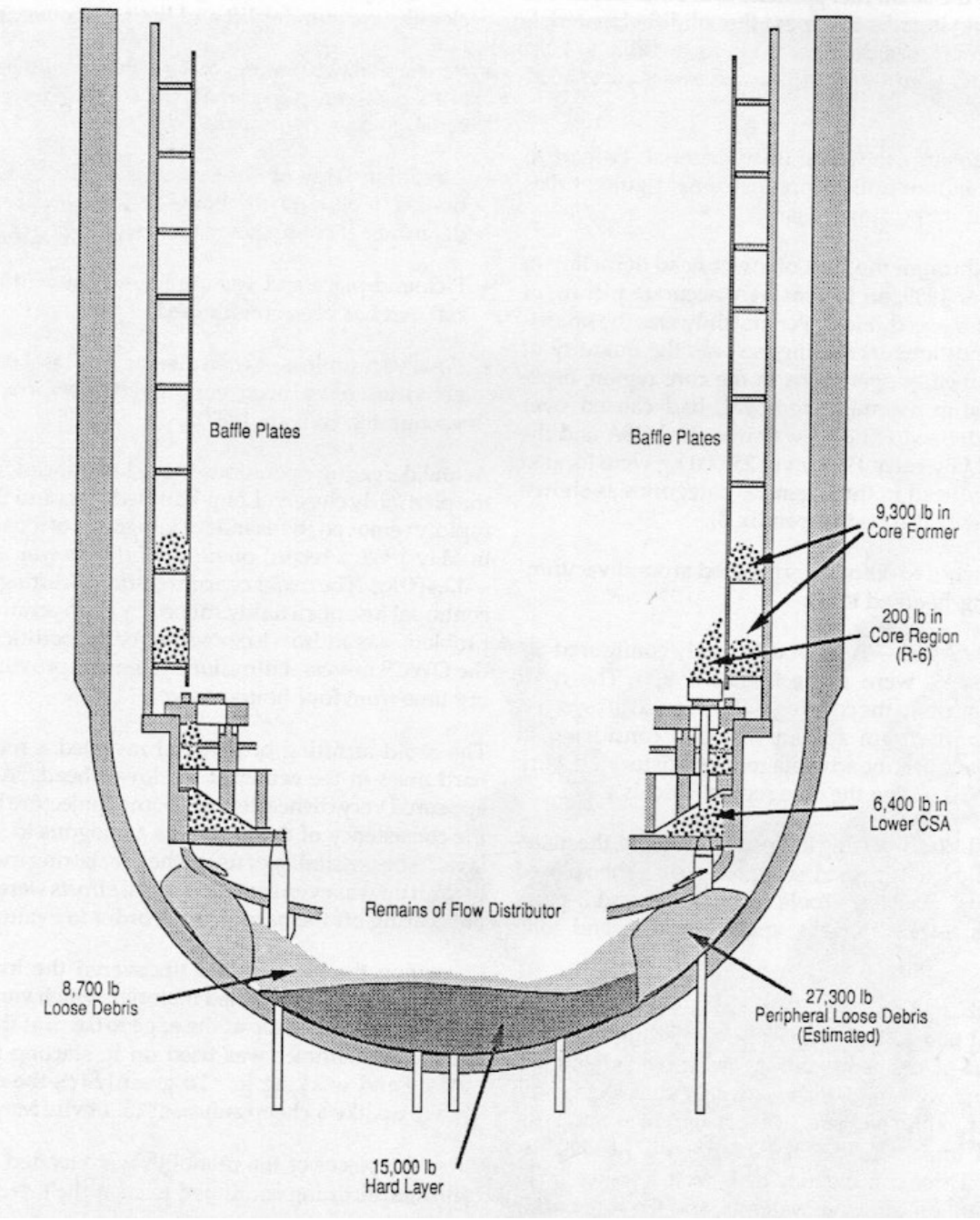

Figure 25. Debris located below the lower core support assembly.

It had been estimated that 4000 kg of debris was located behind the core former baffle plates. Removing the 4-m long baffle plates involved removing the bolts that held them in place and moving the eight pieces out of position to allow vacuuming of the debris. An airlift and cavitating water jet were used to recover the debris.

In all, the debris at the bottom of the vessel were tabulated as follows: 4218 kg behind the core former plates, 2903 kg was found in the lower core support area, and 3946 kg of central and 12,383 kg of peripheral loose debris, and 6804 kg of previously-molten monolithic hard layer, adding up to 30,254 kg.

4. CANISTER DESIGN

As a matter of system integration, the common component from the reactor to the current storage configuration was the canister. The canisters function as a discrete fuel-handling unit, provide confinement of fission and activation products, and maintain subcriticality. Design-requirement specifics are provided in Appendix A.

The canisters were designed by a team from Babcock and Wilcox and fabricated to American Society of Mechanical Engineers (ASME) Section VIII pressure vessel standards. The canisters were central to the retrieval process at the reactor, needed to be compatible with the INEL interim storage pool, and were the initially expected to be a confinement barrier in transportation.

Canisters for general debris, granular material, and filtered water were designed to be handled by the fuel-handling equipment at the reactor while being compatible with the interim storage pool at INEL.

The fuel debris canister was designed to accommodate partial fuel assemblies as well as debris. Some initial design assumptions considered the possibility that a significant fraction of assemblies were intact. The original approach was to use 457-mm-diameter canisters, but that was reduced to 456 mm due to handling limitations within the reactor vessel.

The knockout canisters were used to receive pieces suctioned from the reactor vessel that were too small for remote manual pick-and-place recovery; these ranged from fuel pellet size to 140 microns.

The filter canister was designed to remove particulate as small as 0.2 microns from the suction stream. Cross sectional views of the canister types are shown in Figure 26–Figure 28. The canisters were designed to allow remote dewatering and prevent hydrogen buildup resulting from radiolysis of retained water during transportation.

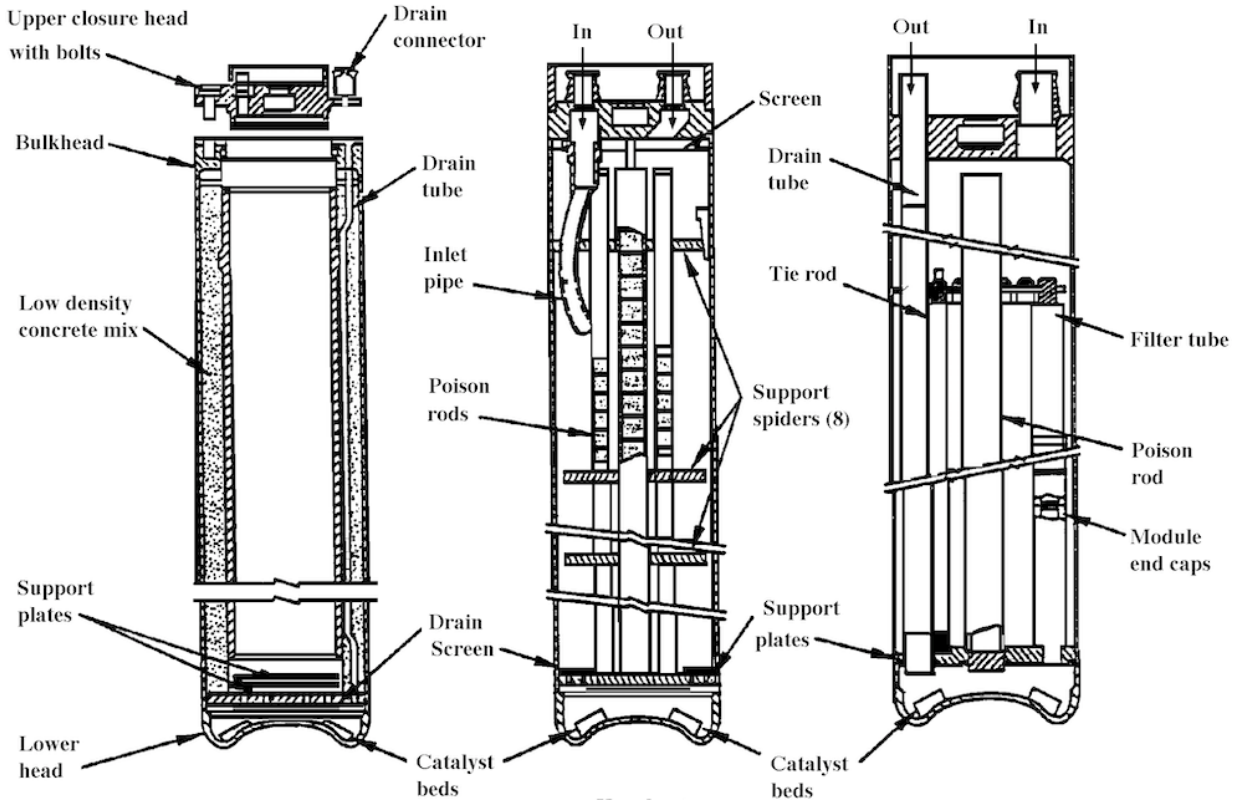

Figure 26. Fuel debris, knockout, and filter-canisters elevation view.

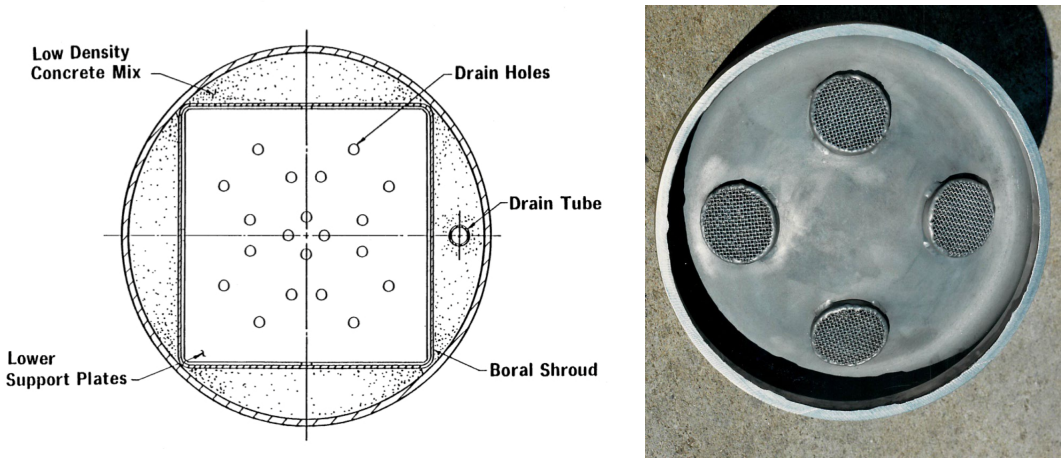

Figure 27. Cross-section view of fuel debris canister and lower head with catalyst bed.

Figure 28. Internal structure of knockout canister.

Concerns were raised regarding the properties of the debris being recovered. One uncertainty was the potential for pyrophoric reaction of unoxidized Zircaloy in air. This was determined to be unlikely because the debris were submerged in water, which would oxidize any zirconium surface immediately. To address this as a transportation issue, the canisters were backfilled with argon during dewatering. There was also the possibility of achieving a flammable concentration of radiolytically produced hydrogen. Numerous alternatives were suggested, but the choice was a platinum-palladium catalyst recombiner material that would convert hydrogen and oxygen back into water.

Assuring subcriticality (k_{eff} less than 0.95) in the nonhomogeneous mass of debris, whether as a single canister or in an array, was achieved by the use of boron neutron poisons in several configurations. The square tube of the fuel debris canister was constructed by sandwiching a layer of stainless-steel over plates of borated aluminum. The structure of the filter canister includes a center rod that is filled with B_4C pellets. In the knockout canister, four rods arranged around a large central rod, all filled with B_4C pellets function to prevent criticality (Babcock & Wilcox 1985).

5. CANISTER SHIPPING PROCESS

As part of the defueling, it was decided that a sort of post-mortem examination of the fuel needed to be performed. The core needed to be removed and stored to allow completion of the reactor-building cleanup.

To achieve a resolution of the final destination for the debris, negotiations in 1981 between NRC and DOE led to a memorandum of agreement under which DOE would take a portion of the debris for

research, and the balance would be retained onsite. In 1982, the decision was made to transfer the entirety of the core to DOE for research and storage until the national high-level waste repository was operational.

It was determined that the then-INEL had the requisite combination of facilities that could store the core debris and do the necessary research on the materials that were recovered. The laboratory also had experience doing research on severe accidents for the NRC and the nuclear industry.

To move the core and debris the 3540 km from Pennsylvania to Idaho, it was decided to design and construct two specialized rail casks. Rail as chosen to limit the number of shipments, allowing seven canisters to be shipped at once, versus one in a legal-weight truck cask. The shipping cask was designed and fabricated by Nuclear Pacific.

Because the fuel cladding was damaged or absent, the debris canisters were initially designed to be the primary barrier to dispersal. Due to concerns about the ability to achieve adequate sealing with the bolted-head canister design, it was concluded that the cask would need to provide double containment. The cask design provided two barriers in the form of internal and external cask modules, complete with individual impact limiters for the canisters. Double containment was mandated because the primary fuel-clad barrier was no longer present, and the transportation regulation requires double containment for Pu-containing materials. Three casks were fabricated for rail service. Forty-nine cask loads were transferred in 22 shipments. An elevation view of the general facility configuration for transfers to the shipping cask is shown in Figure 28.

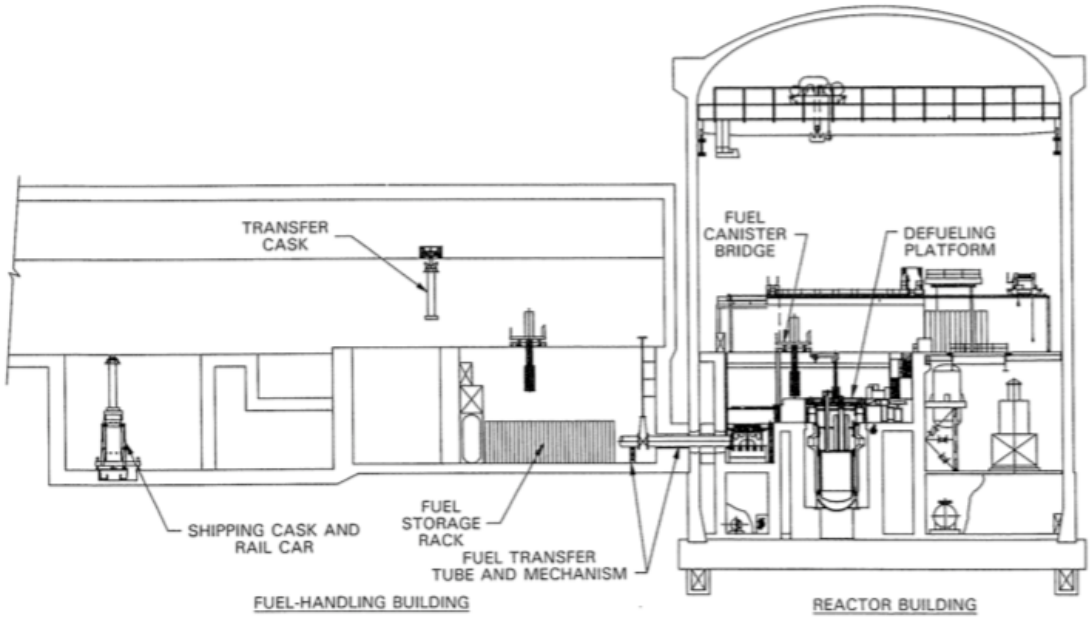

Figure 29. Reactor and fuel-handling building arrangement for canister shipping.

Once a canister was identified for shipping, it was dewatered using argon purge gas and loaded into the fuel transfer cask. The cask was moved to the fuel-handling building loading area, where the shipping cask was staged. The shipping cask was rotated from its horizontal transport position, and a loading collar was installed. A mini-hot cell was mounted to the loading collar and used to remove the shield plug from the shipping cask position designated to receive the canister that was ready for shipping. The fuel transfer cask was mated to the loading collar, the canister was lowered into the position in the shipping cask, and the shield plug was replaced. The loading collar and mini-hot cell configuration is shown in Figure 30, and the upended rail shipping cask with the fuel transfer cask attached is shown in Figure 31.

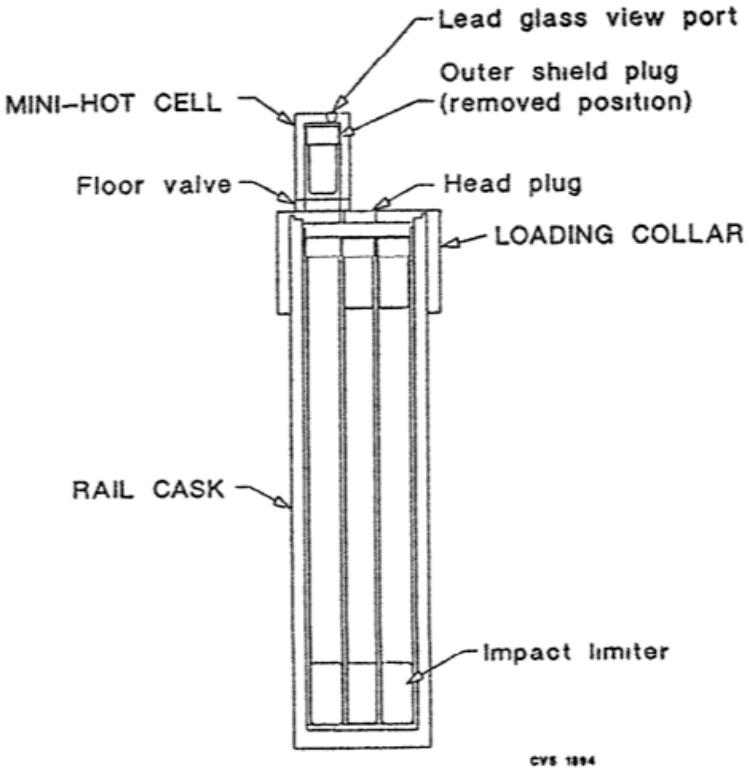

Figure 30. Schematic of mini-hot cell with rail cask and loading collar.

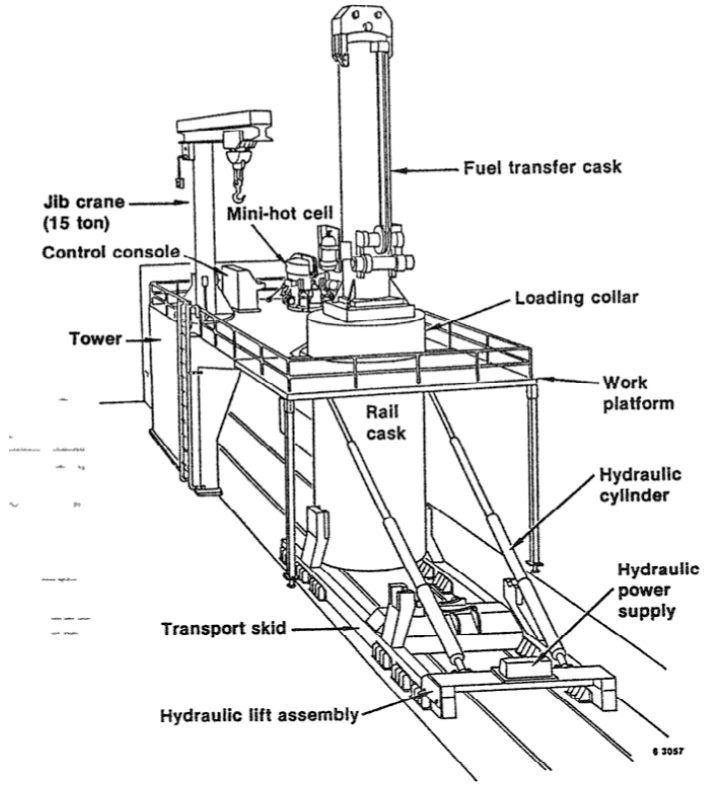

Figure 31. Equipment for dry transfer of debris canisters to rail cask.

On arrival of the empty cask, the impact limiters were removed before pushing the rail car into the fuel-handling building's truck bay. Then the rail car was pushed into a specific location in the truck bay under the cask-unloading station, where four screw jacks raised the cask and skid from the rail car. The rail car was then removed from the truck bay. The cask-unloading station was then removed from the skid and set aside using an overhead crane. The cask hydraulic-lift assembly was attached to the railcar skid to rotate the empty cask from a horizontal position to a vertical orientation. This unit comprised a pair of hydraulic cylinders that pushed on the upper trunnions to rotate the cask. A work platform was attached around the cask, allowing removal of the outer and inner cask lids using a jib crane.

Loaded debris canisters were operationally limited to a gross dewatered weight of 1272 kg, with a typical debris load of 750 kg.

Concerns about residual water retention were validated based on differences between empty and loaded, dewatered containers, as shown in Table 3. As may be expected, the filter canister (F-462) has the greatest remaining water.

Table 3. Sample canister water retention.

Canister ID	Canister Weight Empty (kg)	Full (kg)	Dewatered (kg)	Core Debris (kg)	Water Remaining (L)	Total Pay Load	Void Volume (L)
D-180	542	1,393	1,315	743	29	772	72
D-188	542	1,405	1,317	746	29	775	81
D-330	538	1,406	1,327	767	22	789	78
F-462	662	1,218	1,101	310	111	439	120
K-506	458	1,471	1,324	842	23	865	146

As part of the validation process for specifying transport conditions for potential radiolytic hydrogen production, eight of the canisters were sealed and monitored for pressure and periodically sampled for headspace composition. The test canisters remained sealed for between sixteen to 205 days. Pressure values reached as high as 198 kPa in as few as 16 days for the D-188 debris canister. The headspace gas was analyzed at INEL and indicated that, over time, the hydrogen concentration could reach as much as 9 vol% with only 0.2 vol% oxygen in 87% argon after 205 days sealed. The values are tabulated as shown in Table 4 and Table 5.

Table 4. Canister pressure samples sealed test. (Standerfer, 1987).

			First Sample		Second Sample		Third Sample		Fourth Sample	
Canister Number	Rail Shipment	TMI (psi)	psia	Days Closed	psia	Days Closed	psia	Days Closed	psia	Days Closed
D-144	-	29.54	26.33	147	-	-	-	-	-	-
D-148	4	29.52	29.13	26	28.83	48	-	-	-	-
D-145	5	20.54	29.33	27	-	-	-	-	-	-
D-180	6	29.38	18.33[a]	27	19.33	205	-	-	-	-
D-162	7	29.27	29.33	36	28.33	-	-	-	-	-
D-188	7	29.36	29.08	16	28.83	181	28.33	88	27.33	168
D-207	8	29.34	28.83	20	27.33	56	-	-	-	-

Table 5. Sealed Canister Headspace Composition (Standerfer, 1987).

	Hydrogen (% Volume)				Nitrogen (% Volume)				Oxygen (% Volume)				Argon (% Volume)			
Canister Number	1st	2nd	3rd	4th	1st	2nd	3rd	4th	1st	2nd	3rd	4th	1st	2nd	3rd	4th
D-144	0.77	-	-	-	0.90	-	-	-	0.08	-	-	-	98.20	-	-	-
D-148	1.15	1.47	-	-	0.36	0.70	-	-	0.07	0.13	-	-	98.40	97.70	-	-
D-145	0.74	-	-	-	0.585	-	-	-	0.09	-	-	-	98.6	-	-	-
D-180	1.23	9.05	-	-	1.07	3.75	-	-	0.13	0.02	-	-	97.5	87.19	-	-
D-162	1.005	1.01	-	-	4.36	2.22	-	-	1.02	<0.01	-	-	93.53	96.74	-	-
D-188	1.165	2.43	3.30	5.09	0.50	1.95	2.16	1.81	0.05	0.305	0.26	<0.01	98.26	95.29	94.25	93.1
D-207	0.20	0.46	-	-	0.475	3.82	-	-	0.04	0.72	-	-	93.40	89.66	-	-
D-267	0.12	0.25	-	-	0.90	0.52	-	-	0.17	0.01	-	-	98.80	99.17	-	-

6. TRANSPORTATION CASK

The transportation cask was designed by Nuclear Pacific as a multiple-barrier system. In a normal fuel shipment, intact fuel-clad can be credited as a containment barrier. Per transportation regulations, the fuel debris contained sufficient plutonium to require double containment. In this design, the canisters were not considered a containment barrier because the debris canisters had removable heads. To provide the necessary barriers, the NuPac 125-B casks were designed with an inner and outer vessel to provide double containment. The inner vessel weighed 15.4 metric tonnes, and the outer vessel weighed 43.5 tonnes.

Seven canisters were fitted inside the cask, each having its own upper shield plug and upper and lower internal-impact limiter. The internal configuration is shown in Figure 32. The casks were shipped cross country by rail as a dedicated shipment with as many as three rail cars, each cask on its own car. Figure 33 shows the package dimensions and impact limiter arrangement. A photo of the cask, with impact limiters in place on the rail car, in its skid is seen in Figure 34.

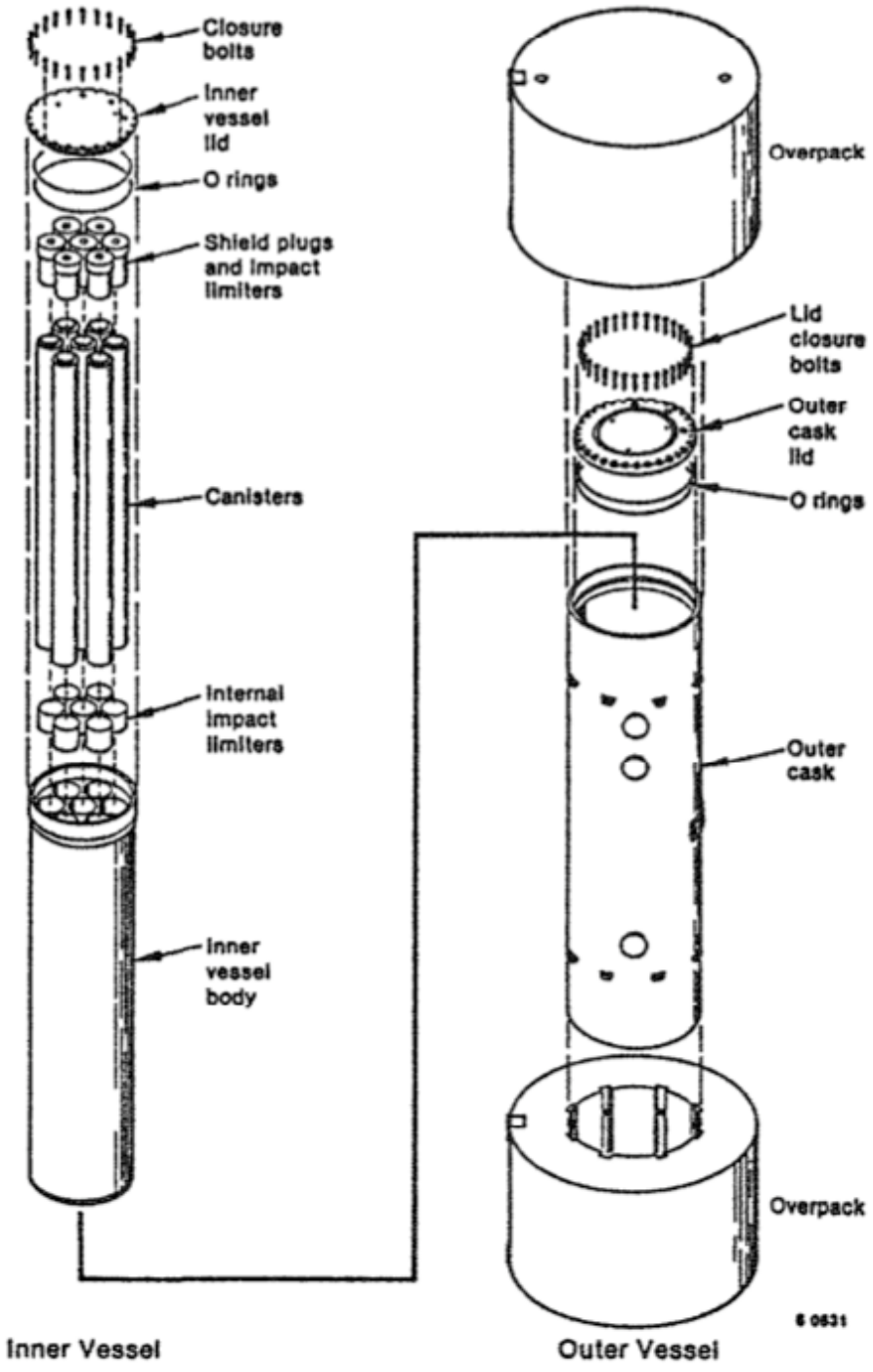

Figure 32. NuPac 125B schematic.

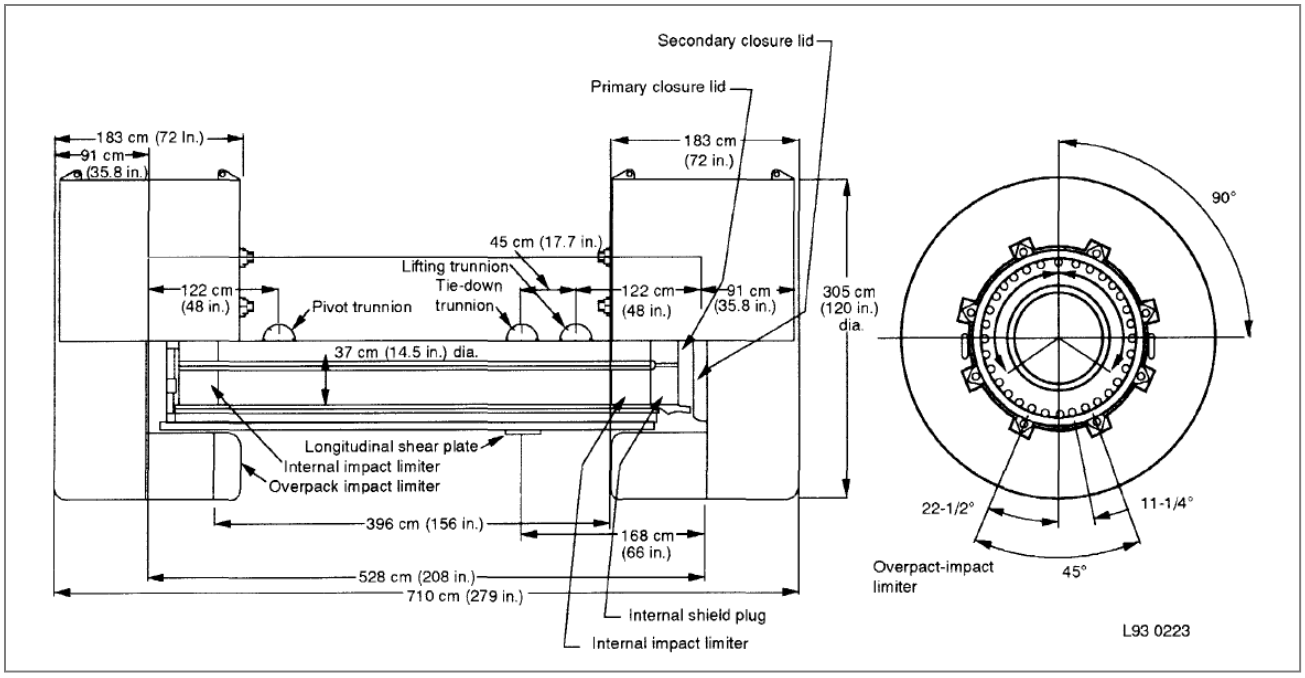

Figure 33. NuPac 125B dimensions and impact limiter orientation.

Figure 34. NuPac 125B cask on rail car.

The 125B cask was mounted to a skid that was in turn attached to a rail car, as shown in Figure 35.

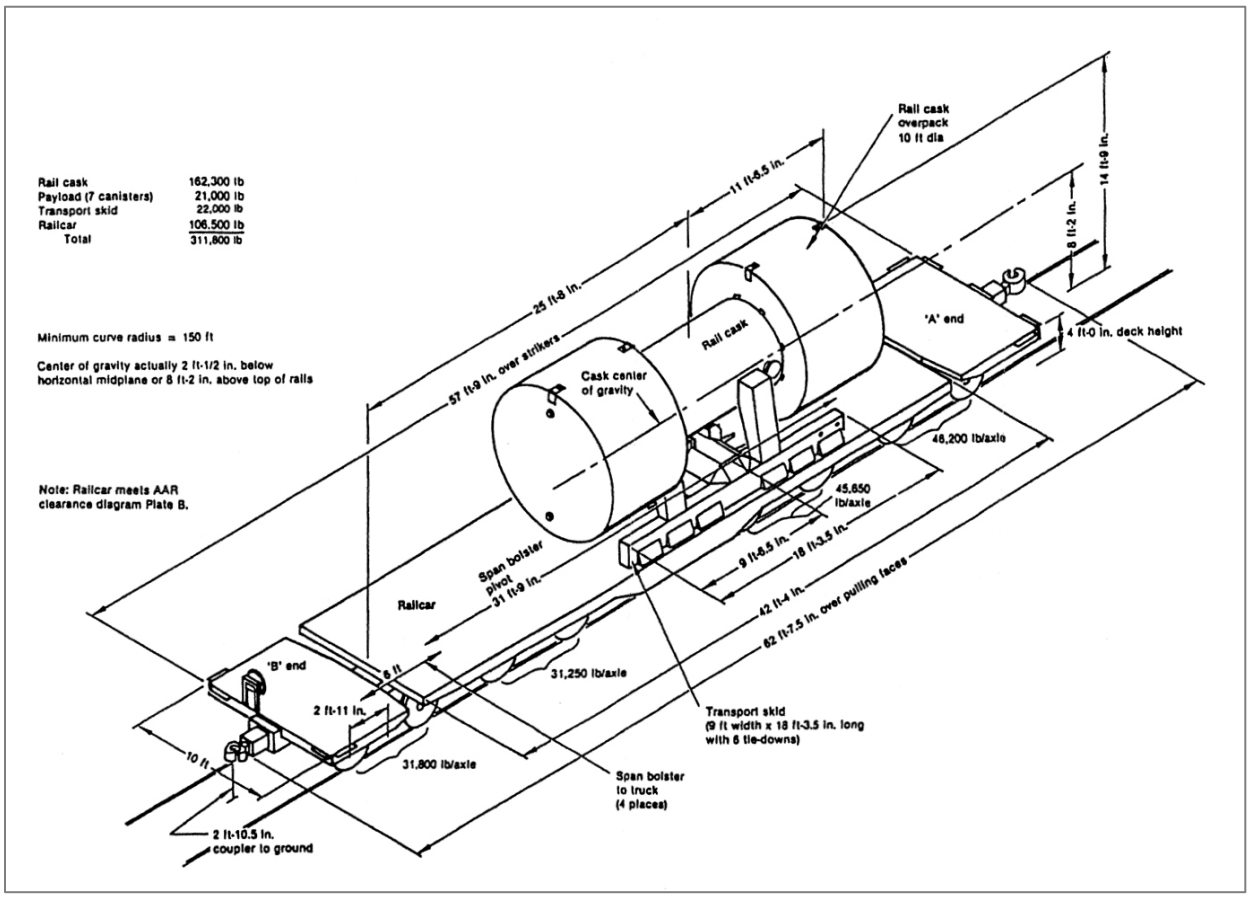

Figure 35.125B cask rail car configuration.

To perform the loading of the transport cask in the fuel-handling building, it was necessary to remove the 125B cask and its transport skid from the rail car. This was performed using the cask-unloading station fixture, as shown in Figure 36.

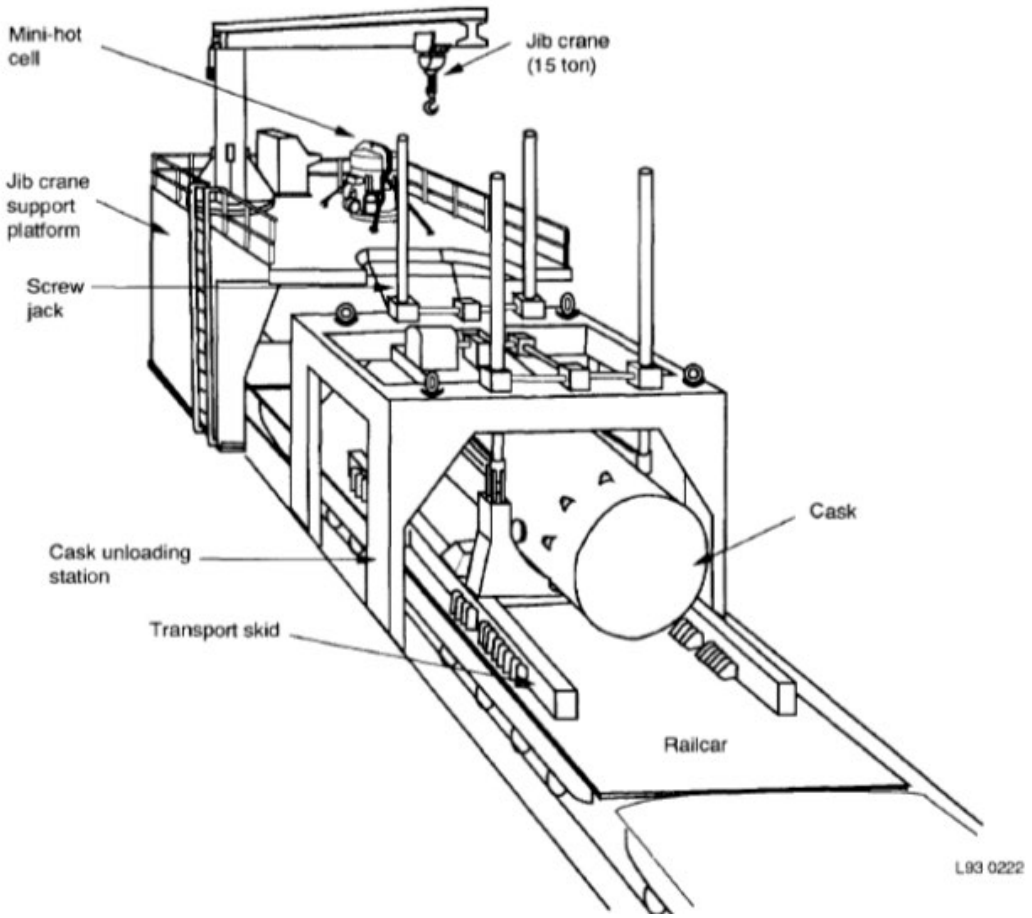

Figure 36. NuPac 125 B cask handling equipment at TMI-2 fuel-handling building.

6.1 Offloading at INEL

The casks were shipped cross country via rail, but when the shipment reached INEL, no rail spur was available to complete the journey to the TAN-607 hot shop and pool system. This meant that the casks needed to be unloaded from the rail cars and transported by truck approximately 48 km from the rail terminal at the INEL Central Facilities Area to TAN. The transfer process is depicted in Figure 37. A photo of the cask mounted to the transport skid, suspended from the Central Facilities Area gantry crane is seen in Figure 38. The cask and skid are shown mounted on the truck, being moved to TAN in Figure 39.

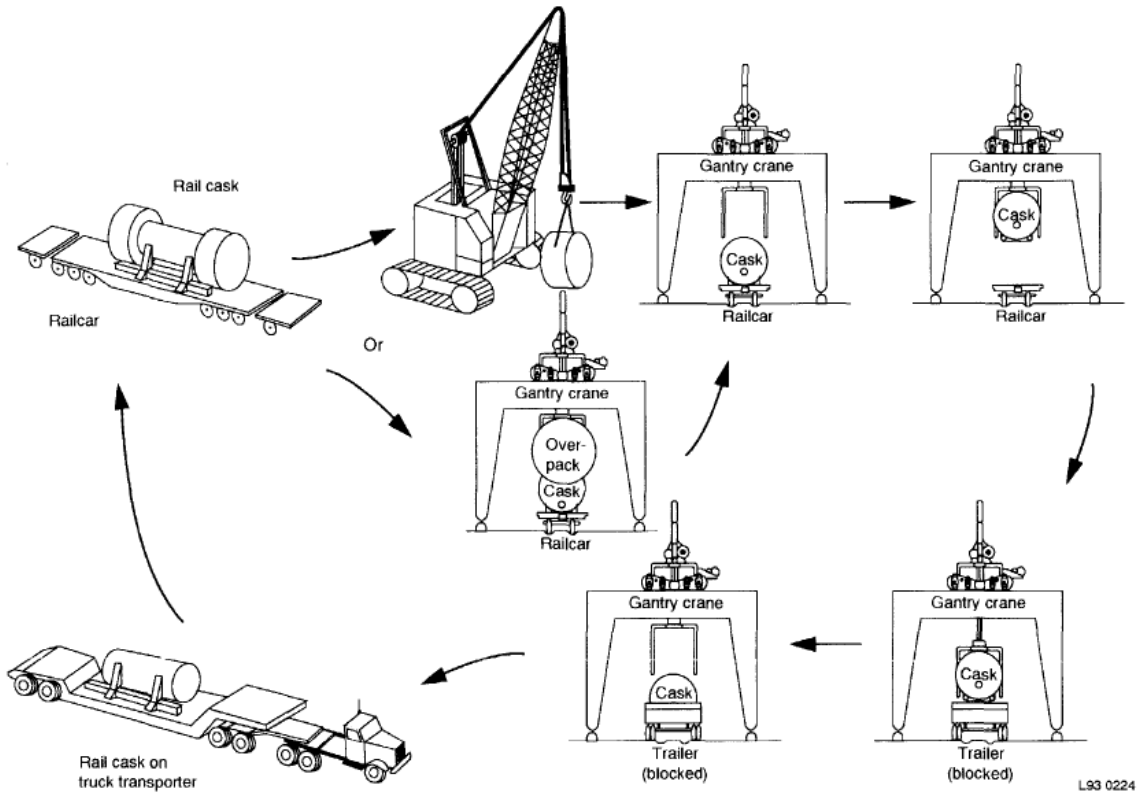

Figure 37. Cask transfer from rail car to truck schematic.

Figure 38. Gantry crane removing 125B Cask from rail car.

Figure 39. 125B cask on transport skid, loaded on trailer.

6.2 INEL Storage Site TAN-607

The TAN-607 building included a hot shop, which was originally designed for handling test nuclear reactors for a conceptual nuclear airplane. The hot shop was 15.5 m × 50 m × 16.76 m. It was a high-bay cell with a large entry lock sufficient to accommodate a large truck-trailer unit or a rail engine using rail tracks. It featured a 100-tonne bridge crane, nine shielded viewing windows, and one bridge-mounted and three wall-mounted electromechanical manipulators. The main overhead crane was used to lift and position the NuPac 125B casks upright. The manipulators were used to open the casks and retrieve the contents. The truck transport was carefully backed into the hot shop, and the casks were individually removed from the truck skid by rotating the casks upright using the main crane. The casks were placed on a work platform, where the lid bolts were removed, and preparations were made for the remote transfer of the canisters to the storage pool. The rotation and unloading process is shown in Figure 40 and 41.

Figure 40. Cask-unloading in TAN-607 hot shop.

Figure 41. NuPac 125B cask on the work platform.

The hot shop had a vestibule that provided access from the dry area to the storage pool. The pool was 14.6 m wide, 21.3 m long, and 7.3 m deep.

TAN-607 also had a hot cell 3.05 m wide × 35 10.7 m long × 6.1 m high. It was directly connected to the hot shop, which facilitated receipt of the TMI-2 canisters that contained core bores for inspection. An additional set of four hot cells allowed handling of subdivided samples for further analysis. The hot shop plan view is shown in Figure 42. A schematic of the canister transfer path from the cask to the storage racks in the vestibule is shown in Figure 43. Details of the pool storage systems are shown in Figure 44 through Figure 47.

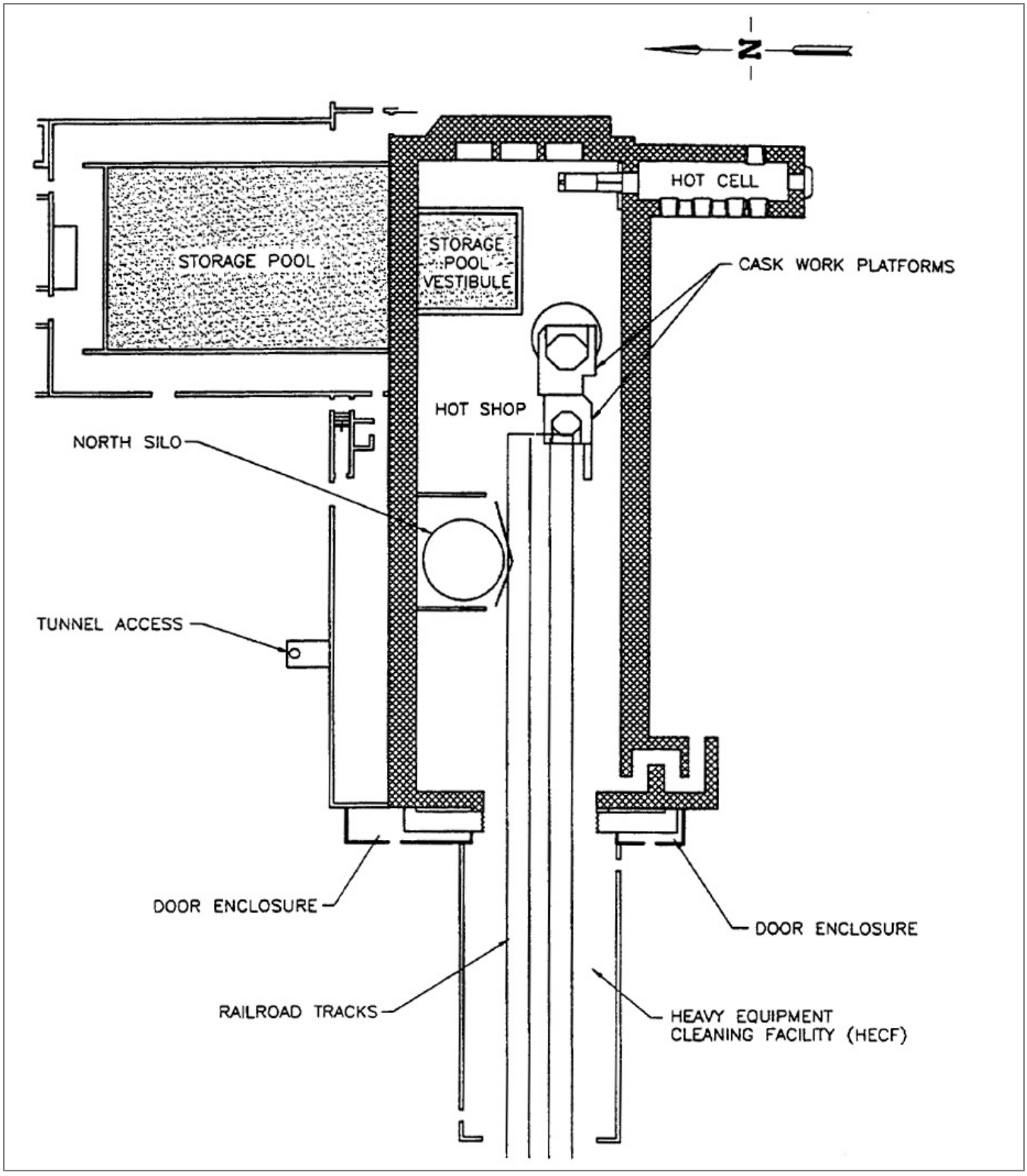

Figure 42.TAN hot shop, hot cell, and pool, plan view.

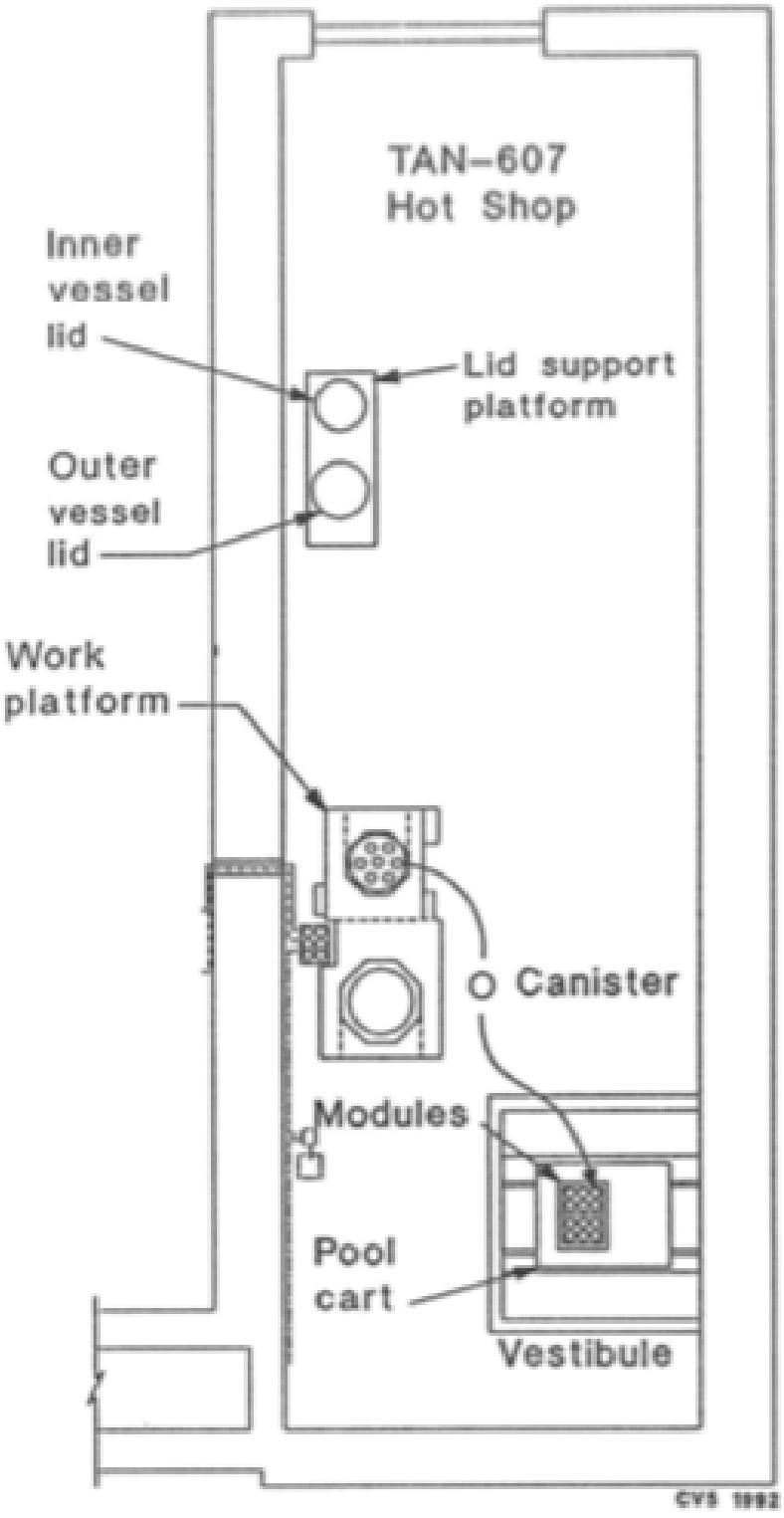

Figure 43.TAN hot shop plan view, showing canister transfer to racks in pool vestibule.

Figure 44.Canister being removed from 125B cask prior to transfer to TAN-607 pool.

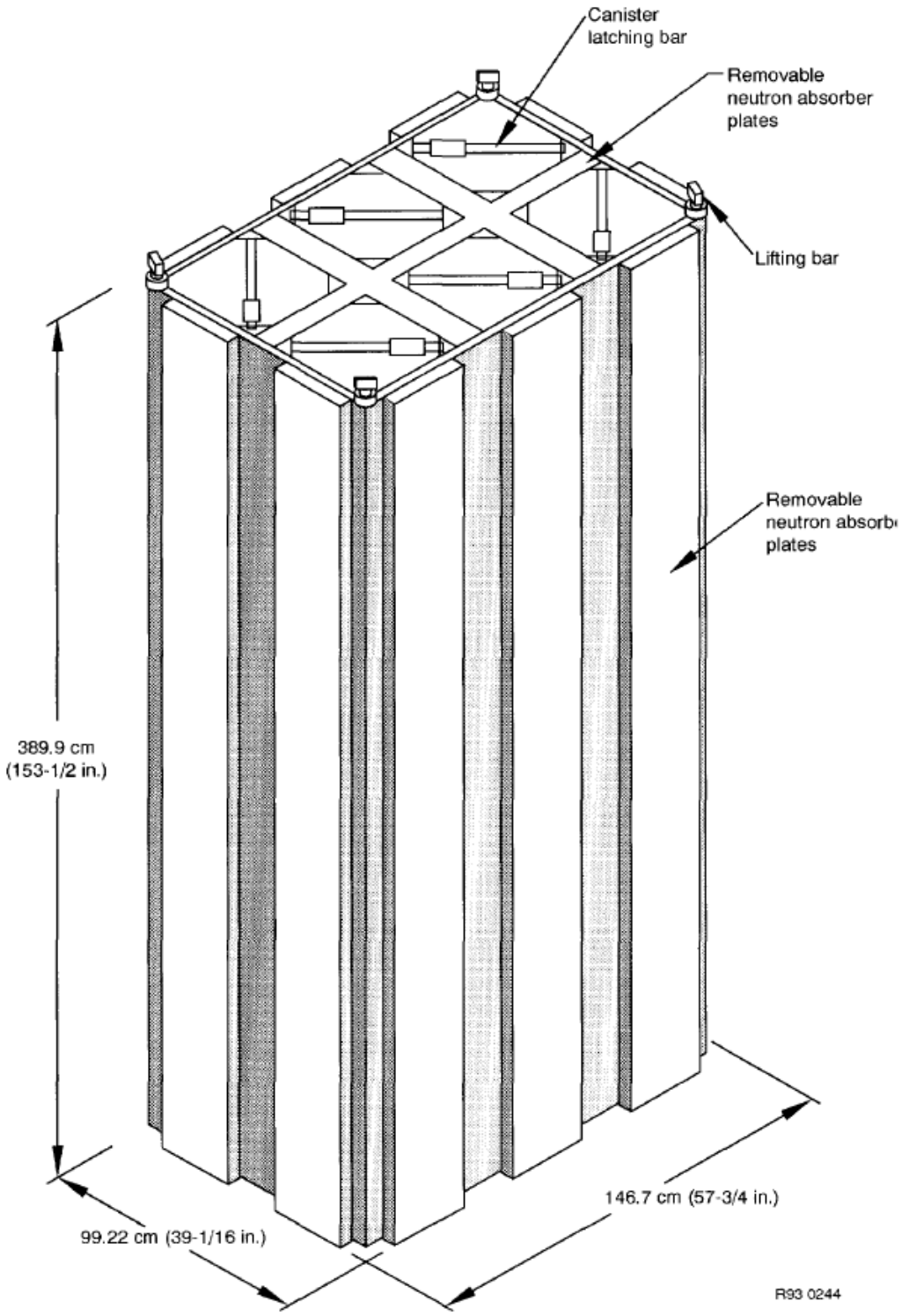

Figure 45. Six-pack canister rack for storage in TAN-607 pool.

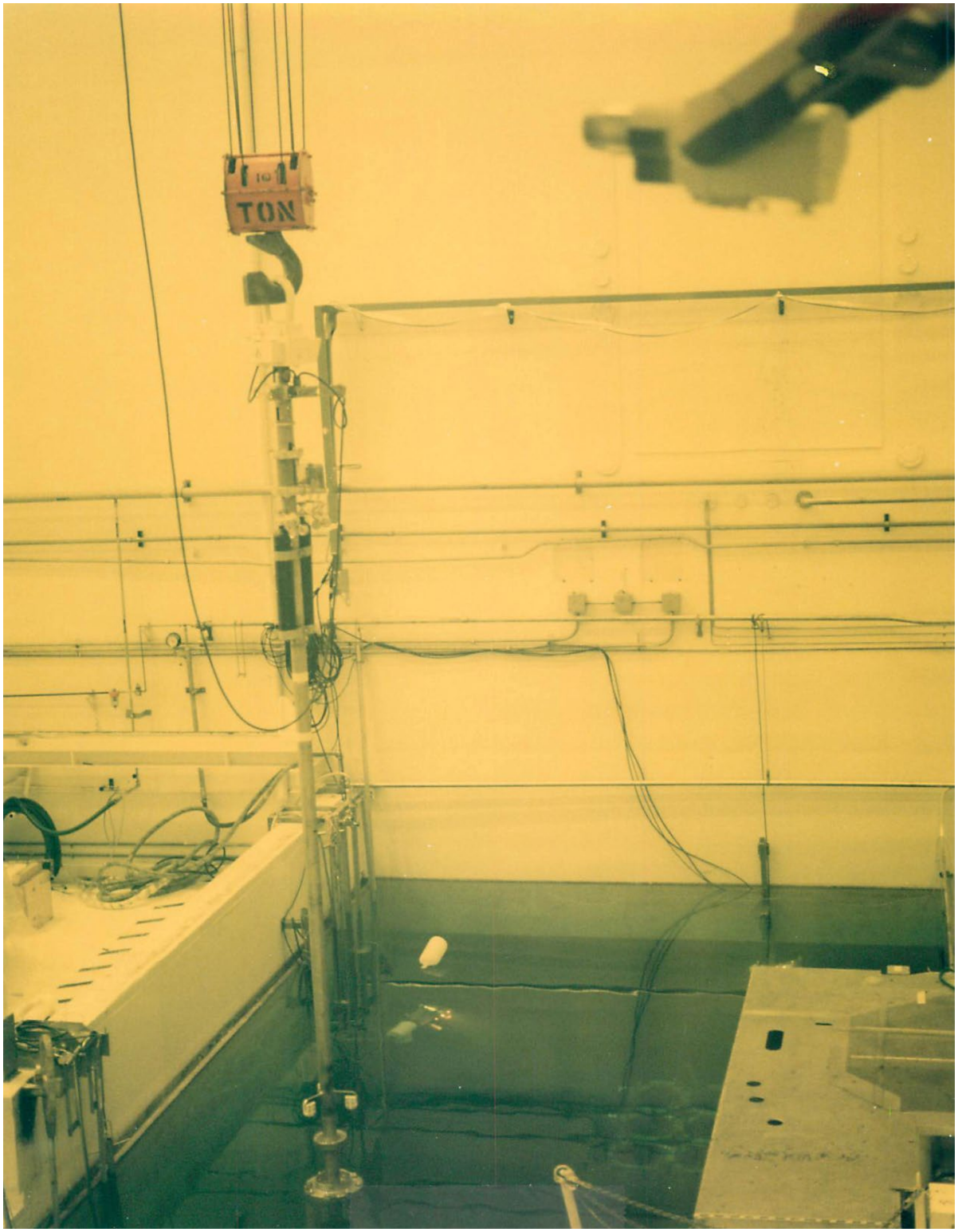

Figure 46. Canister being lowered into six-pack rack in TAN-607 pool.

Figure 47.TAN-607 pool, showing six-pack racks and individual canister-vent ports (orange caps divert water back into pool).

Storage of the canisters in the TAN-607 pool used the six-pack array, with each canister having an individual vent tube extending above the pool surface. The canister internals, including debris, were isolated from the pool water. The canisters were backfilled with deionized water through the vent tube. During the early stages of storage, release of gas from radiolytic hydrogen production caused the water in the canister to be kinetically expelled through the vent tube. Following observation of this phenomenon, the tops of the vent tubes were covered with plastic caps that diverted any expelled water back into the pool (see Figure 47).

6.3 Transfer to Dry Storage

At least in part due to legal action by the state of Idaho regarding the U.S. DOE management of nuclear material, a decision was made to transfer the fuel debris from wet to dry storage. This decision was made on the basis that dry storage is less expensive to operate and represents a lesser environmental risk; the TAN-607 pool was known to leak. Contaminated water could have eventually reached the Snake River Aquifer.

Design alternatives led to selection of the concrete-shielded Pacific Nuclear Fuel Services NUHOMS design. One primary consideration was the relatively low cost of the concrete shield and dry shielded canister design when compared to metal-shielded multipurpose cask designs.

A total of 342 stored canisters were dried and repackaged for dry storage in the hot shop. (A larger number of canisters, 344, were originally shipped from TMI to INEL, but two of the canisters were

handled separately because various epoxy-containing metallographic mounts that were produced during the characterization phase were loaded into these canisters. The two separate canisters contained a minimal amount of fuel debris, and they are stored in one of the 125B transport casks located on the CPP-2707 dry-cask storage pad.) The dry area of the hot shop included access to the wet storage pool, so the canisters were retrieved from the six-pack storage racks, dewatered, and brought into the dry hot cell for final drying in the heated vacuum drying system (HVDS). Dewatering was performed by removing the vent tube and attaching a gas line to the Hansen connector on the canister and displacing the water with air or nitrogen. The gas released during the dewatering purge process was vented through a high-efficiency particulate air (HEPA) filter and the TAN-607 air-handling system before being released through the TAN-734 stack. Sintered-metal filters were installed on 3/4-in. vent and 1/2-in. purge lines of the filter and knockout canisters in place of Hansen quick-connect fittings. This was a precaution to reduce the chance of fines being released from the canisters during drying.

It was calculated that there could be as many as 80 L of water retained in the canister following dewatering. The displaced water was not discharged into the pool to avoid introduction of contamination. The water from selected canisters was sampled and analyzed for dissolved chemical species to determine the degree of leachability of the debris. Canister sample pH was 8.0, except for D-330, with pH of 8.5. Canister data are shown in Table 4. The analysis is shown in Table 6. Table 7 shows tabulated radionuclide concentrations measured in the water. A calculated average radionuclide leach value for all sampled-canisters is shown in Table 8.

Table 6. Leach water from sampled-canisters, description.

Canister	Description	Contained Solid Mass (kg)	Contained Volume (l)	Solid Void Fraction	Volume of TMI Water Shipped (l)	Present Water Volume (l)
D-180	Fuel	742	191	0.404	29.02	77.21
D-188	Fuel	745	191	0.458	29.02	87.53
D-330	Fuel	766	191	0.411	21.77	78.55
F-462	Filter	309	281	0.416	110.66	117.07
K-508	Knockout	841	304	0.482	23.2	146.43

Table 7. Chemical constituents of canister water (HLW-100-1074/JDC-8-97).

Species or Elemental Component	D-180 (moles/l)	D-188 (moles/l)	D-330 (moles/l)	F-462 (moles/l)	K-506 (moles/l)
Boron	9.03×10^{-5}	7.24×10^{-2}	6.84×10^{-2}	7.97×10^{-2}	1.02×10^{-1}
Sodium	1.24×10^{-2}	1.07×10^{-2}	1.44×10^{-2}	1.16×10^{-2}	1.67×10^{-2}
Calcium	4.19×10^{-6}	4.07×10^{-6}	3.78×10^{-4}	1.25×10^{-5}	6.94×10^{-6}
Chloride	4.26×10^{-5}	9.00×10^{-5}	2.06×10^{-4}	1.35×10^{-4}	7.87×10^{-5}
Silicon	2.34×10^{-5}	2.16×10^{-5}	7.09×10^{-5}	1.24×10^{-4}	3.20×10^{-5}
pH (pH paper)	8.0	8.0	8.5	8.0	8.0
Hydroxyl	1.0×10^{-6}	1.0×10^{-6}	3.2×10^{-6}	1.0×10^{-6}	1.0×10^{-6}
Barium	1.49×10^{-7}	3.93×10^{-7}	7.03×10^{-7}	6.19×10^{-7}	2.37×10^{-7}
Cadmium	1.87×10^{-7}	1.78×10^{-7}	3.02×10^{-7}	5.16×10^{-7}	1.60×10^{-7}
Lithium	8.65×10^{-6}	1.08×10^{-5}	ND	ND	ND
Bromide	3.30×10^{-6}	ND	ND	2.79×10^{-6}	1.13×10^{-6}

Species or Elemental Component	D-180 (moles/l)	D-188 (moles/l)	D-330 (moles/l)	F-462 (moles/l)	K-506 (moles/l)
Chromium	1.06×10^{-7}	ND	ND	2.02×10^{-7}	3.37×10^{-7}
Arsenic	ND	ND	ND	ND	ND
Lead	ND	ND	ND	ND	ND
Magnesium	ND	ND	2.22×10^{-4}	ND	ND
Mercury	ND	ND	ND	ND	ND
Selenium	ND	ND	ND	ND	ND
Silver	ND	ND	ND	3.4×10^{-7}	6.0×10^{-6}
Uranium	ND	ND	ND	ND	ND

ND = not detected; below the limits of detection. Detection limits (molar) are Li 7.2×10^{-6}; Br $\times$ 1.110^{-6}; Cr $1 \times 10^{-7\pm}$; Mg 4×10^{-6}; As 2.7×10^{-6}; Pb 5×10^{-7}; Hg 5.5×10^{-7}; Se 2.5×10^{-6}; Ag 2×10^{-7}; U 2.5×10^{-8}.

Table 8 Canister Water Radionuclide Content December 1995, (Pincock, 2012)

	Canister D-180		Canister D-188		Canister D-330		Canister F-462		Canister K-506	
	Max (mg/L)	Min (mg/L)	Max (mg/L)	Min (mg/L)	Max (mg/L)	Min (mg/L)	Max (mg/L)	Min (mg/L)	Max (mg/L)	Min (mg/L)
Pu238	4.92E-06	0.00E+00	< 4.53E-08	0.00E+00	2.75E-06	0.00E+00	4.67E-06	2.71E-06	< 1.74E-07	0.00E+00
Pu239	6.10E-04	0.00E+00	1.18E-03	0.00E+00	3.57E-04	0.00E+00	7.67E-05	0.00E+00	9.41E-04	4.62E-04
Np237	1.02E-01	5.99E-02	1.79E-03	0.00E+00	2.07E-01	1.47E-01	1.90E-03	0.00E+00	1.88E-02	0.00E+00
Am241	3.40E-06	0.00E+00	1.26E-05	0.00E+00	1.22E-05	0.00E+00	9.65E-06	4.16E-06	5.73E-06	0.00E+00
Th228	1.11E-09	0.00E+00	2.53E-08	0.00E+00	2.06E-08	0.00E+00	2.27E-08	0.00E+00	< 5.11E-09	0.00E+00
Th230	3.93E-04	0.00E+00	9.85E-04	0.00E+00	< 1.27E-04	0.00E+00	8.23E-04	0.00E+00	7.46E-04	0.00E+00
Th232	1.14E+02	0.00E+00	< 2.22E+00	0.00E+00	<2.22E+00	0.00E+00	< 2.21E+00	0.00E+00	1.05E+02	0.00E+00
Tc99	6.48E-03	2.86E-03	5.94E-02	5.50E-02	1.93E-02	1.54E-02	3.49E-03	0.00E+00	4.27E-02	3.86E-02
Sr90	7.60E-03	7.60E-03	3.79E+03	3.79E+03	9.08E+02	9.08E+02	2.14E+03	2.14E+03	2.00E+03	2.00E+03
H3 (Tritium)	1.09E-06	1.09E-06	1.58E-06	1.58E-06	9.52E-07	9.52E-07	1.26E-06	1.26E-06	1.11E-06	1.11E-06
Cs134	4.22E-06	3.56E-06	5.37E-06	4.57E-06	1.73E-06	1.52E-06	No Data	No Data	3.80E-06	3.31E-06
Cs137	3.60E-02	3.30E-02	4.47E-02	4.11E-02	1.41E-02	1.29E-02	9.90E-04	9.16E-04	2.90E-02	2.66E-02

Table 9 Calculated Maximum Average Radionuclide Leach Rates

	Average (g/cm^2/day)
Pu238	3E-16
Pu239	8E-14
Np237	9E-12
Am241	1E-15
Th228	2E-18
Th230	8E-14
Th232*	< 3E-10
Tc99	3E-12
H3 (Tritium)	2E-16
Cs134	5E-16
Cs137	3E-12

* Excluding canister D-180 and K-506 for Th-232.

The data noted in the reference letter indicate that only a negligible amount of calcium was leached from the light-weight concrete in the debris canisters (i.e., D-180, 188 and 330). This may be related to the limited communication and surface area within the canisters.

In addition, the dewatering skid was fitted with a collimated sodium iodide gamma-ray spectrometer that was calibrated for ^{154}Eu detection. A correlation-to-uranium carryover was used to assure that minimal transfer from the canister to the dewatering system occurred during the water removal process.

Following dewatering, the canisters were raised out of the pool into the main hot shop, where the canisters were placed either into a shielded silo or directly into one of the four positions in the HVDS.

The HVDS was built by Exolon Systems under contract to VECTRA and was designed to receive four canisters at a time. The vacuum furnace vessel had a 388.62 cm internal length and was of 96.52 cm internal diameter. It was equipped with five thermocouples and heated by 54 kW of axial heating elements. The initial vacuum drying vessel was installed in the REA-2023 cask to provide shielding in the cell in the event that personnel entries were required. A second furnace was eventually procured and installed in one of the NuPac 125B casks. The process schematic is shown in Figure 48. The Control Screen and skid configuration are shown in Figure 48.

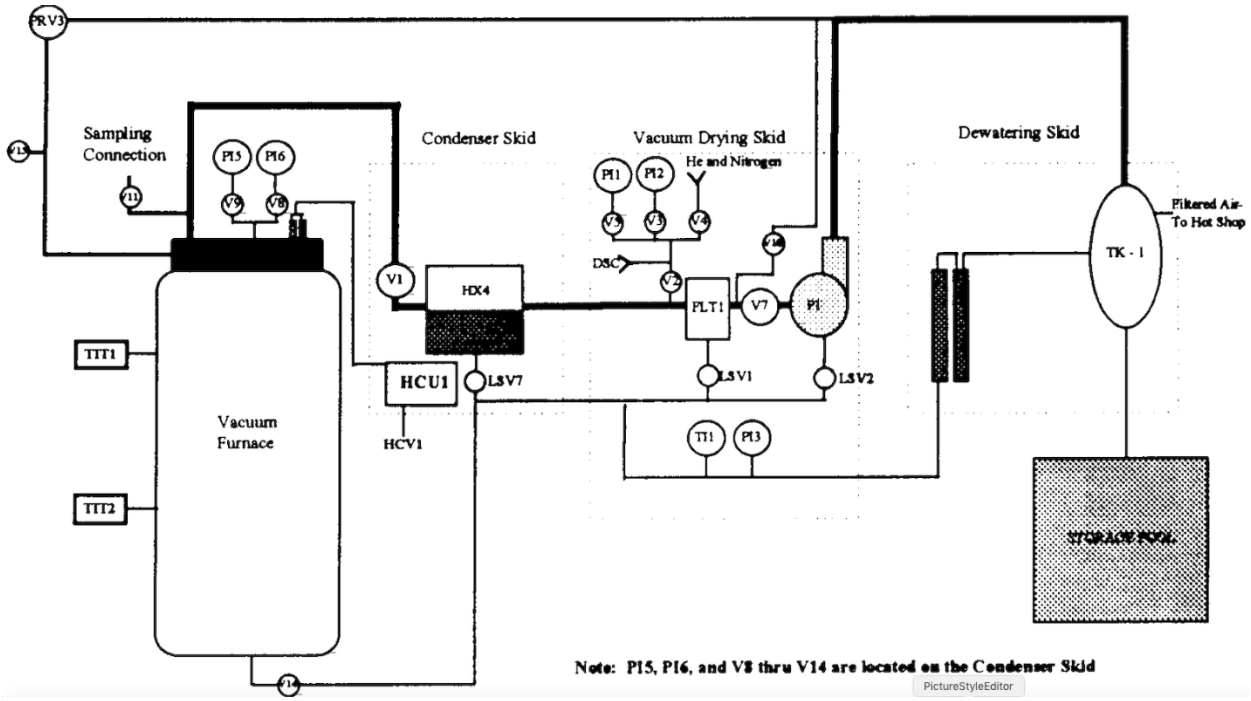

Figure 48. General schematic of dewatering and vacuum drying processes.

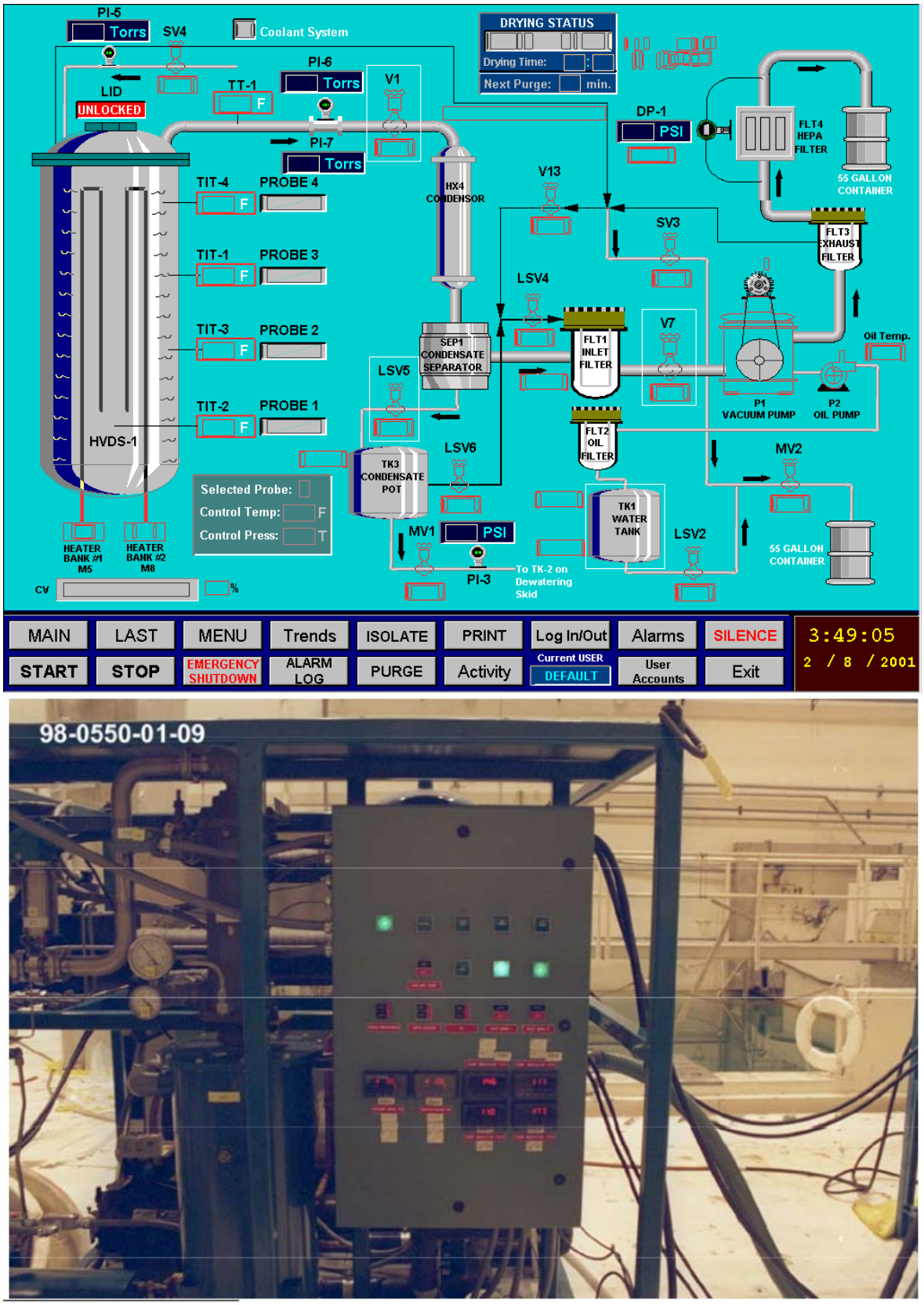

Figure 49. Process-control operational screen (upper); skid configuration in cell (lower).

Groups of four canisters were loaded into the HVDS, and the lid was secured. The system heated to 315°C and evacuated. The heater control temperature was a maximum of 482°C, and the debris temperature was estimated to be ~300°C. Because the heater was attached to the vacuum vessel, not to individual canisters, the temperature of the canister was determined by mathematical models. Design temperature was limited to minimize the potential for release of fission products such as ^{137}Cs, which becomes volatile in excess of 500°C. When a vacuum level of 3 torr was reached, the vacuum pump was isolated, and the vessel pressure was monitored. The drying cycles initially were expected to be able to maintain the standard identified in NUREG-1536 of 3 torr for 30 minutes of isolation. During early operation, these values were not achieved, requiring multiple evacuation cycles that took as many as 96 hours to reach the desired vacuum-isolation duration. Because it was impossible to determine whether the inability to maintain vacuum was due to inleakage from incomplete closure of the HVDS vessel head, an alternate approach was used. Due to schedule demand, it was determined that acceptable levels of drying could be achieved by observation of the change in temperature and pressure to identify the change from constant-rate drying to falling-rate drying. The latter is noted by a rise in bulk temperature and a consistent drop in pressure. Falling-rate drying is an indication that the bulk water has been fully evaporated from among the particles of a granular system such as the fuel debris. The HVDS system included a condenser for water removal and separate pump for removable of noncondensible gas. The system design included controls to prevent overtemperature conditions as well as to assure that flammable gas deflagration was not possible. The design allowed for intermittent purge capability, which was used periodically. The canister configuration in the HVDS was also analyzed to assure subcriticality.

The original assumptions used by the INEL Engineering Group (Palmer 1996) were predicated on maintaining the drying temperature below that which would cause failure of the O-ring on the fuel/debris canister head. When the drying and packaging contract was awarded to VECTRA, the decision was made only to take credit for the dry shielded canister (DSC) as the confinement barrier; no credit was taken for the fuel/debris canister O-ring, meaning that there was no need to run at a temperature (<150°C) that would not damage the O-ring. The four-canister configuration in the HVDS is shown in Figure 50.

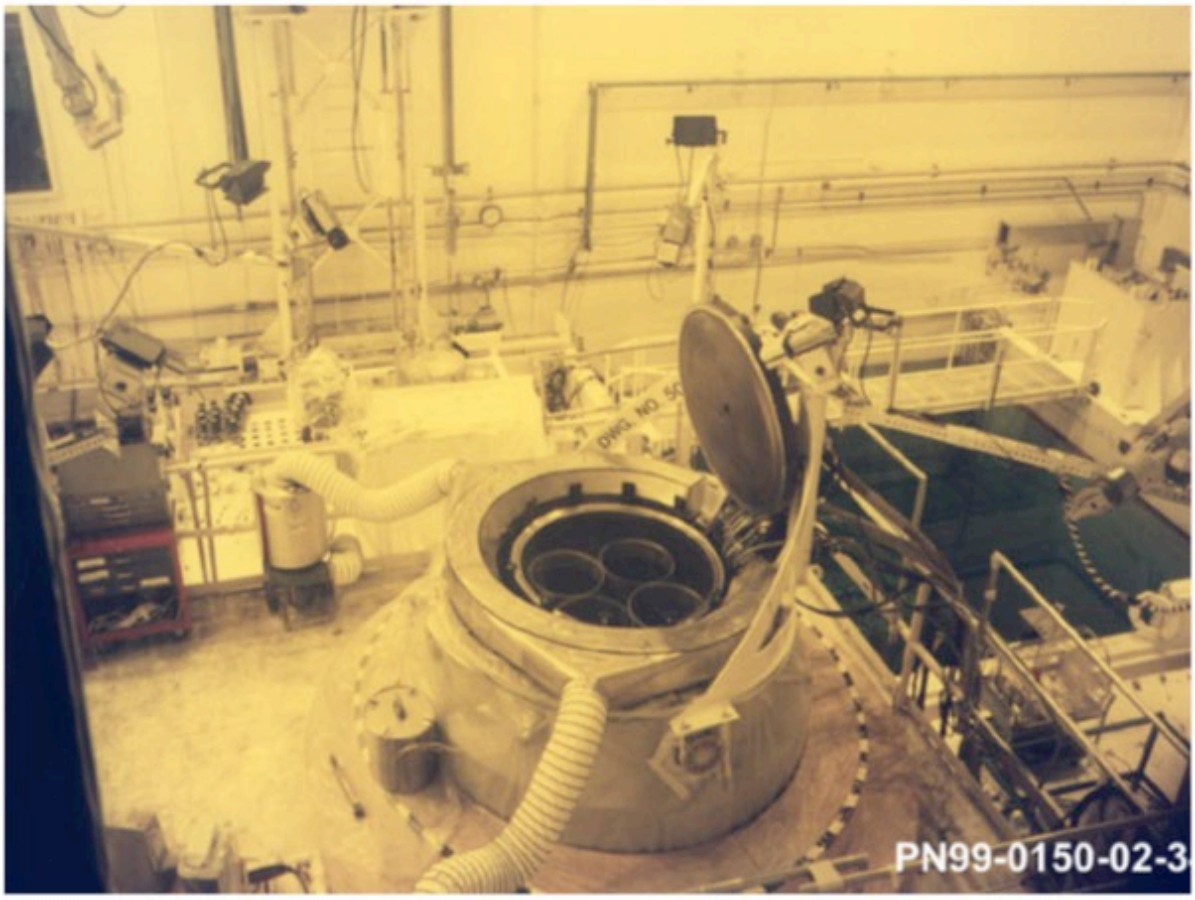

Figure 50. Heated vacuum drying system installed in REA-2023 cask in TAN hot shop.

Prior to award of the drying contract, several tests of different materials were performed at INEL, including thermal measurements of bucketed rods, tests on simulated fuel elements in buckets, canned rods, bucketed sand, and TMI-2 debris canisters containing lava rock using heated forced air and heated vacuum drying. Heated vacuum drying was selected as the preferred option.

7. NUHOMS DRY SHIELDED CANISTER

The NUHOMS design that was selected for interim dry storage is a modified variant of the standard NUHOMS design that accommodates 24 power assemblies per canister in stainless-steel DSCs. The NUHOMS-12T design uses an internal basket configuration that positions twelve of the TMI-2 canisters in a circular array.

The NUHOMS-12T DSCs were fabricated from SA-517, Grade 70 mild steel. The DSC main shell is fabricated of 1.6 cm-thick plate, rolled into a 170-cm-diameter, 426-cm-tall cylinder. The canister configuration is shown in Figure 51.

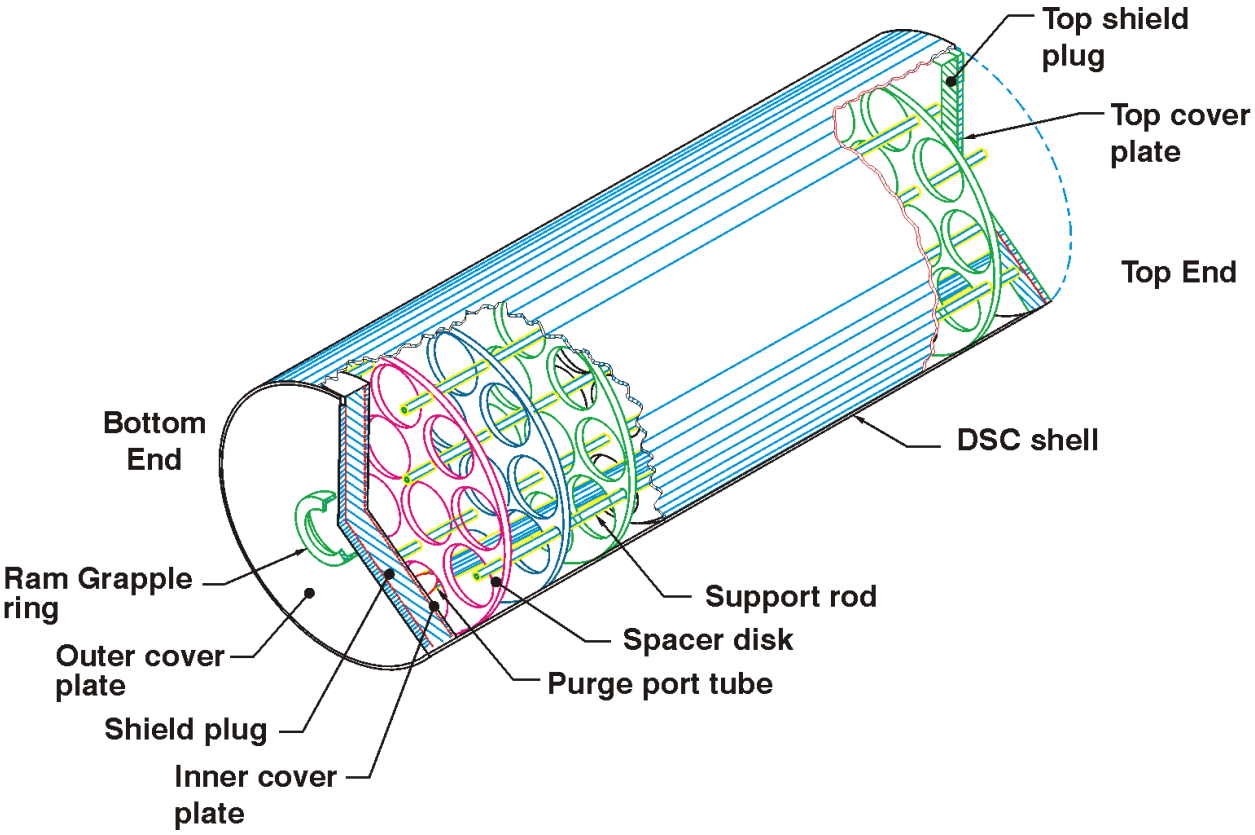

Figure 51. NUHOMS DSC schematic.

The DSC has a 2.54 cm-thick welded top plate and a multiple-piece bottom lid that incorporates a, 11.5-cm-thick radiological shield plug and two 3.8-cm-thick top cover plate that are welded to the shell to complete the final closure. The bottom end also incorporates a ring on which a hydraulic ram is attached that is used to push the DSC into place in the horizontal storage module as well as retrieve it at the end of interim storage. The ring is visible in the fabrication photo, Figure 52.

Figure 52.Photo of the DSC during fabrication.

The TMI-2 DSC design required separate certifications from the standard design, at least in part due to its manufacture from carbon steel, which was initially seen as a cost-saving measure. This additional certification included confirmation that certain fabrication welds could be made in a fully compliant manner.

The most unique part of the TMI-2 DSC design is the vent that was incorporated to allow any residual water or radiolytic hydrogen to be released from the debris canisters. This vent module is located near the edge of the non-shielded end of the canister and includes four Pall sintered stainless-steel filter units as well as an isolation and purge port. In the event that high hydrogen values are observed in a gas sample, the canister can be purged with nitrogen to reduce the concentration to less than the 4 vol% value. In the event that a filter fails to function, the original assumption was that the DSC could be returned to the hot shop, and the filter module, replaced. No filters have failed during testing to date.

Structurally, the entire system was evaluated for specific head load and canister-drop potential. Table 10 shows the design criteria.

Table 10. NUHOMS DSC design criteria.

Category	Criteria or Parameter (Dimensions Are Nominal)	Value
TMI-2 Canister Criteria:	Maximum Canister Weight	1,327 kg (2,926 lbs.)
	Size (Nominal): Length	3.81 m (150 in)
	Diameter	35.6 cm (15 in)
	Initial Maximum Enrichment (weight % without U-235)	2.98%
	Fuel Burnup (MWd/MTU)	3,175
	Gamma Radiation Source (photons/sec/canister)	$6.37x10^{14}$ (19 yr. cooled)
	Neutron Radiation Source	$6.90x10^{5}$ (19 yr. cooled)
	Thermal Characteristics	
	Max. Decay Heat/Canister	60 W
	Average Decay Heat/Canister	15 W
	Thermal Design Basis	
	Max. Decay Heat per Canister	80 W
	Total Decay Heat for DSC with 12 cans	860 W
Dry Shielded Canister:	Number of TMI-2 Canisters per DSC	Up to 12
	Size (Nominal):	
	Overall Length	4.15 m (163.5 in)
	Outside Diameter	1.71 m (67.2 in)
	Shell Thickness	15.9 mm (5/8 in)
	Heat Rejection	860 W
	Internal Atmosphere	Air
	Design Pressure	15 psig
	Equivalent Cask Drop Deceleration	75g Vertical (end) & Horizontal (side)
		25g Oblique (corner)
	Materials of Construction	Carbon Steel
	Service Life	50 years

7.1 DSC Loading and Welding

Dried canisters were then transferred to the NUHOMS-12T DSC in the TAN hot shop. The DSC was staged in the hot shop, positioned in the OS-197 onsite transfer cask with the lid off. The canister loading is shown in Figure 53.

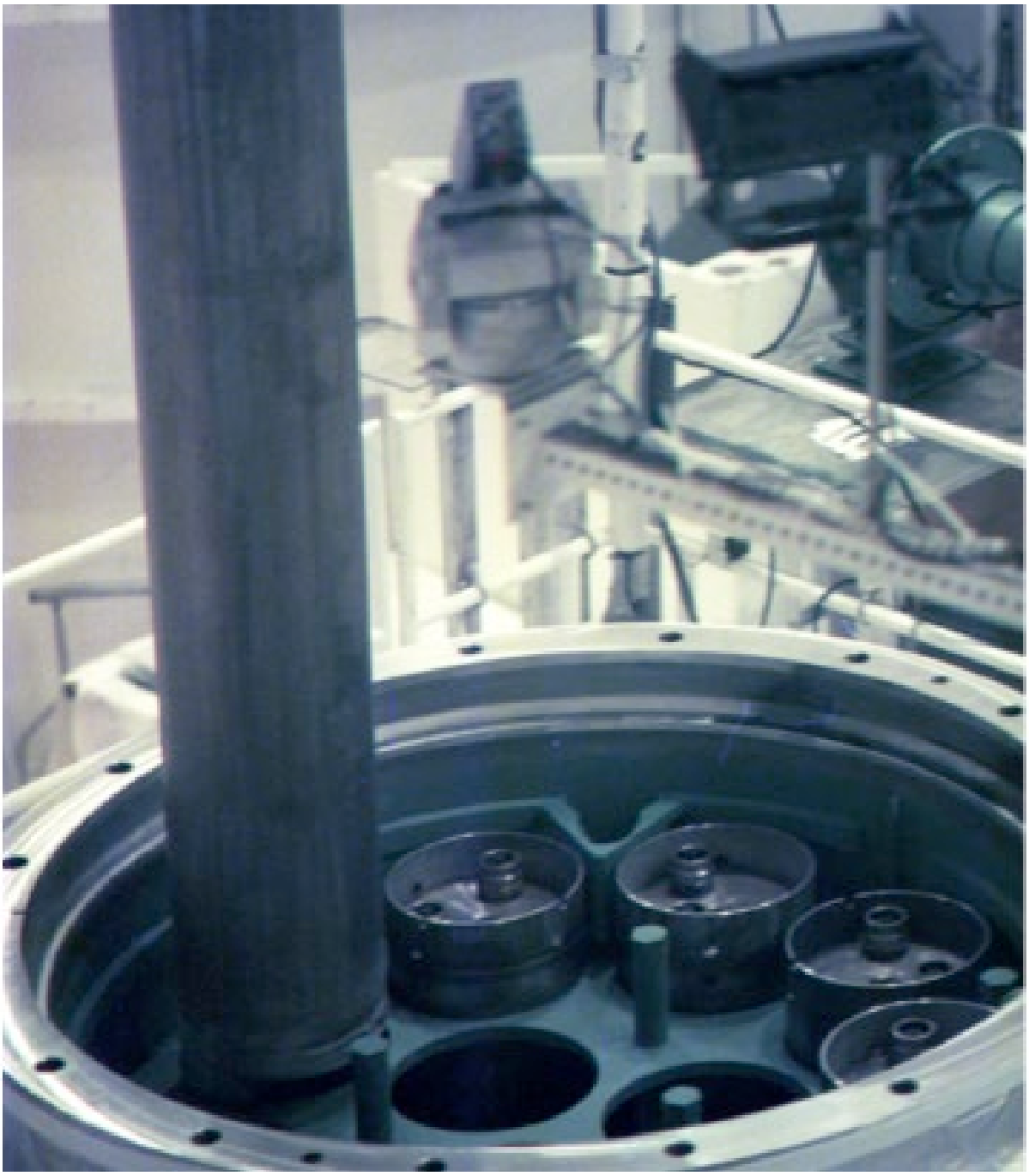

Figure 53. Dried debris canisters being loaded into a DSC.

Once the twelve-canister payload was inserted into the DSC, the radiological shield plug was inserted, and the final shield plugs were welded into place using the automatic welding machine. Initial welds were performed manually, but in the interest of radiological-dose reduction and improved weld consistency, an automatic welding machine was used. When the shield plug weld was completed, the weld was visually inspected by remote camera. Both the welding technique and the remote inspection process were validated using mockup canisters prior to implementation. The DSC was then evacuated to 10 torr using the vacuum drying system and backfilled with helium to a 151 kPa pressure, after which a helium leak check was performed. If the DSC failed the helium leak check, the point of leakage would be

repaired by grinding and rewelding. The DSC top cover plate was then installed, welded, and visually inspected. The vent and purge ports at the shield plug end of the DSC were then seal welded.

The less-shielded head of the DSC incorporates a replaceable sintered-metal HEPA filter that allows any gas that might be produced from water that was not removed during the drying process to be vented without pressurization of the DSC in storage. Following the top cover weld completion, this filter module was installed on the vent and purge ports. A cover was placed over the vent port to seal the canister, and the DSC was then backfilled for transportation.

The OS-197 top lid was installed and secured, and helium was leak checked. The cask was lifted, rotated to a horizontal position, and loaded onto the transport trailer. Following survey and decontamination, it was moved out of the TAN-607 hot shop and driven by truck the 30 km to the INTEC.

7.2 DSC Lid-Closure Weld

The final lid-closure weld was performed using gas tungsten arc-welding process using a semiautomatic rotary weld unit. This process uses a non-consumable tungsten electrode operating in an argon fill gas with an automatic wire feed for filler metal. The system used dual gas-cooled torches mounted on a rotary track that were monitored by video cameras. All communication and power-supply cabling was routed outside the cell to allow remote operation. After the first several canisters were assembled, operational issues were resolved, and during the latter stages of the TMI-2 DSC loading campaign, 25 DSC canisters were completed in eight months, amounting to completion of 3500 linear feet of welding with no detected flaws. The multisection lid arrangement is shown in Figure 54. A photo of the weld apparatus in operation with an observer is shown in Figure 55.

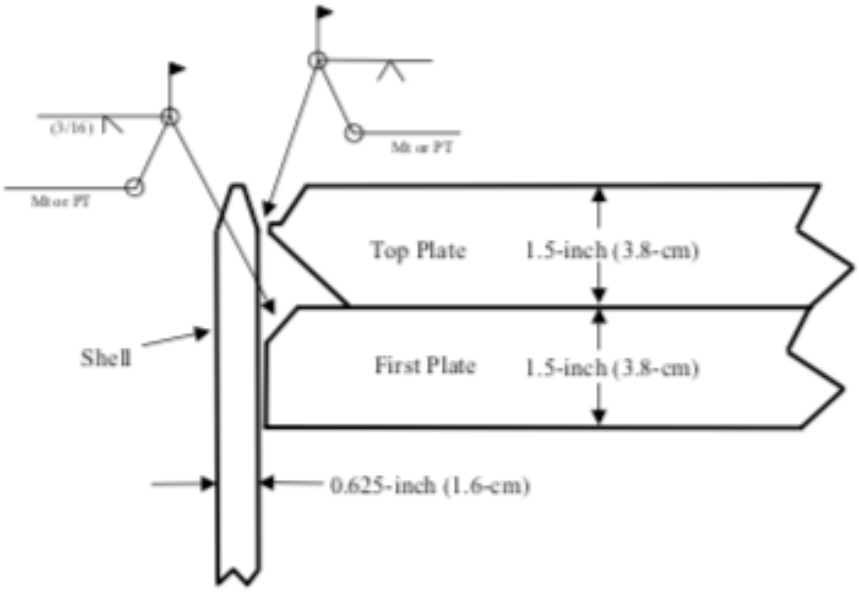

Figure 54.DSC lid-closure weld configuration.

Figure 55. Semiautomatic welding of DSC lid.

7.3 OS-197 Onsite Transport Cask

Because the fuel-loaded DSC is only radiologically shielded on the end that is exposed following loading into the horizontal storage module, shielding is required when it is handled in transport from loading to placement. The shielding around the cylindrical portion of the DSC is provided by the OS-197 cask. The design is intended to be adequate to meet U.S. Department of Transportation radiological-dose-rate values but is not expected to meet transport-accident criteria at highway speed because it lacks impact limiters. In the case of the TMI-2 canisters, the dose-rate limits were not likely to be challenged because the debris were from a low burnup core. Onsite transport speed was limited to less than 30 km/h to assure that an impact accident would not result in a radiological release.

One primary function of the OS-197 is to support the DSC during insertion into the horizontal storage modules (HSMs). The lid through which the DSC was loaded is removed, and a smaller plug on the opposite end is removed to allow the hydraulic ram to be attached to the DSC. The transport cask is positioned to precisely align with the HSM cavity, and the hydraulic ram is actuated to push the DSC into the concrete shield. As in several other respects, the TMI-2 installation is unique in that the DSC must be placed in a precise manner to allow the vent port on the DSC to align with the cutout in the concrete vault that allows access to it. Because the debris canisters were not uniformly loaded, it was discovered that certain DSCs tended to rotate out of alignment with the vent port during transport and insertion. Following this discovery, efforts were made to load heavier canisters in positions that would be the bottom when the DSC was rotated to the horizontal position. The specifications of the OS-197 are shown in Table 11. Figure 57 shows a cross-section view of the cask, and Figure 58 presents a photograph of the cask in transit between TAN and INTEC.

Table 11. OS-197 onsite transport cask design criteria.

OS-197 Cask:	Payload Capacity	37,000 kg (82,000 lbs.)
	Gross Weight	113,000 kg (250,000 lbs.) handling
		109,000 kg (240,000 lbs.) transport
		123,000 kg (271,200 lbs.) transport with impact limiters
	Equivalent Cask Drop Deceleration	75g Vertical (end) & Horizontal (side)
		25g Oblique (corner)

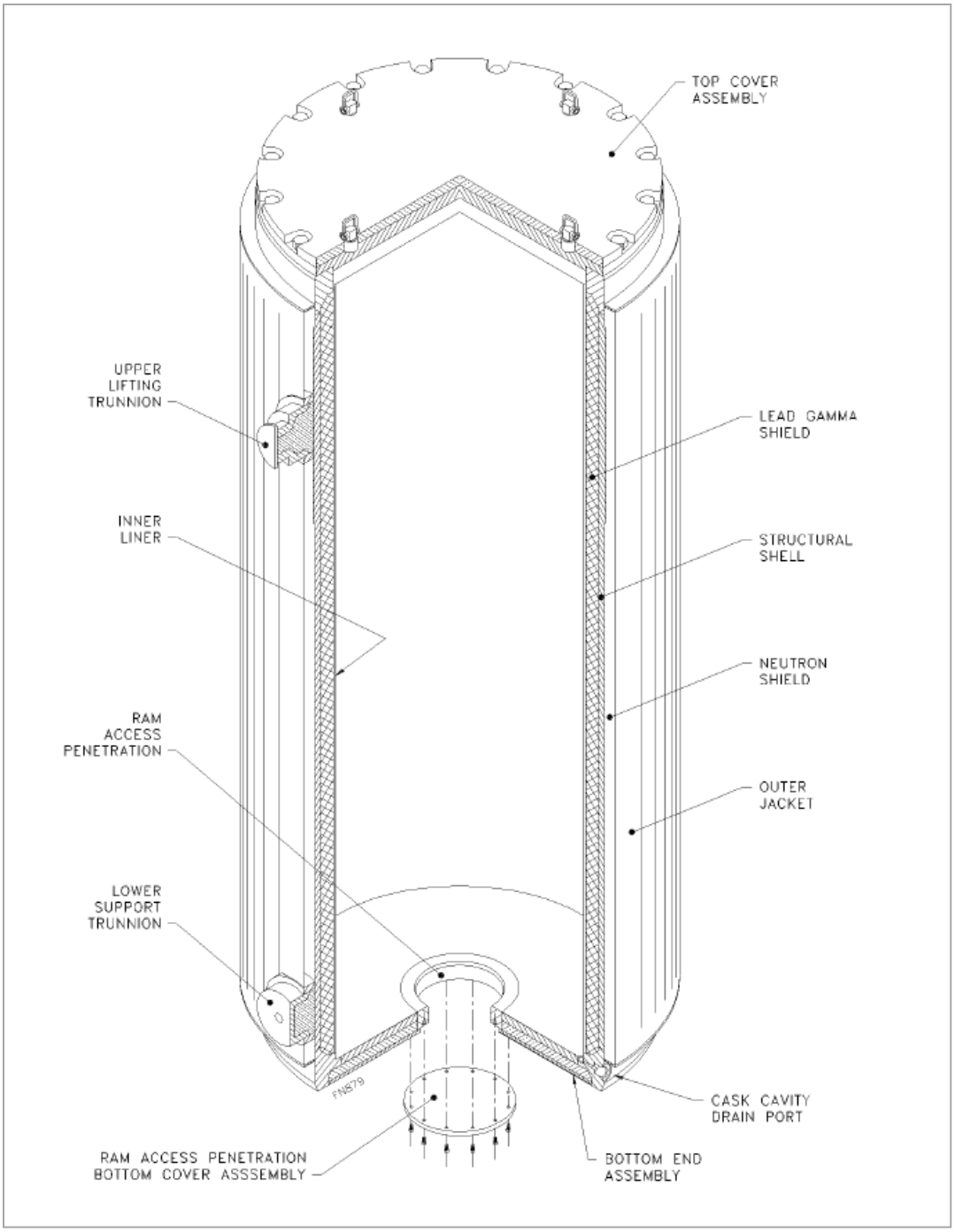

Figure 56. OS-197 onsite transfer cask.

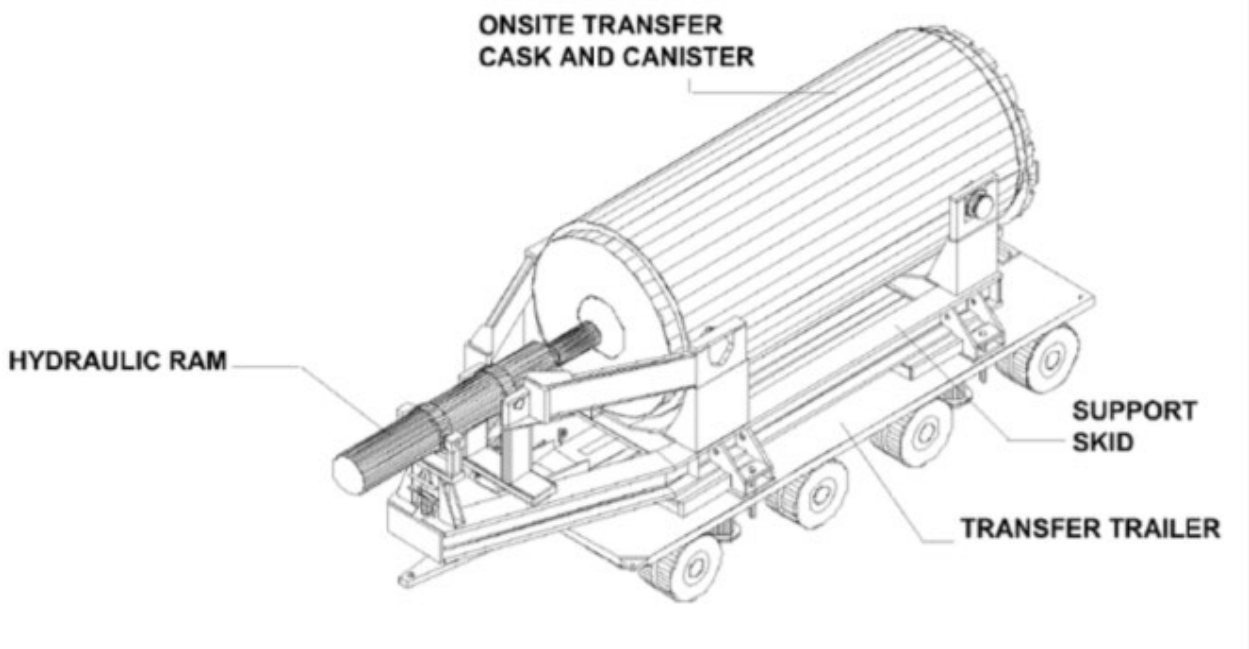

Figure 57. OS-197 As configured on transfer trailer.

Figure 58. OS-197 in transit between TAN and INTEC.

Once the OS-197 arrived at INTEC, the trailer was unhitched from the truck tractor that pulled it from TAN and was hitched to a rubber-tracked agricultural tractor that had the necessary traction and maneuverability to position the cask trailer accurately between the two rows of HSMs.

The TMI-2 installation (see Figure 59) requires HSMs to be exposed on both ends, one for insertion of the DSC, the other for access to the canister-vent.

Figure 59. Mating OS-197 to HSM at INTEC CPP-1774 ISFSI for DSC placement.

7.4 Horizontal Storage Module

As discussed in previous sections, the NUHOMS HSM is constructed of thick concrete sections that provide the primary radiological shielding for the DSC payload. The DSC rests on a steel-rail structure inside the concrete vault. The concrete panels that comprise the vault are bolted together to form the rectangular structure.

The TMI-2/CPP-1774 ISFSI uses a design that departs from the standard in that each module has access at both ends of the DSC and HSM to allow for loading as well as access to the vent port. The TMI-2 design also departs in that no convective-cooling vents are included in the concrete vault due to the low decay heat of the canister contents.

As shown in Figure 60, the vent module access panel includes the connections necessary for testing the filter, isolating the DSC headspace and headspace gas sampling. The design criteria are shown in Table 12.

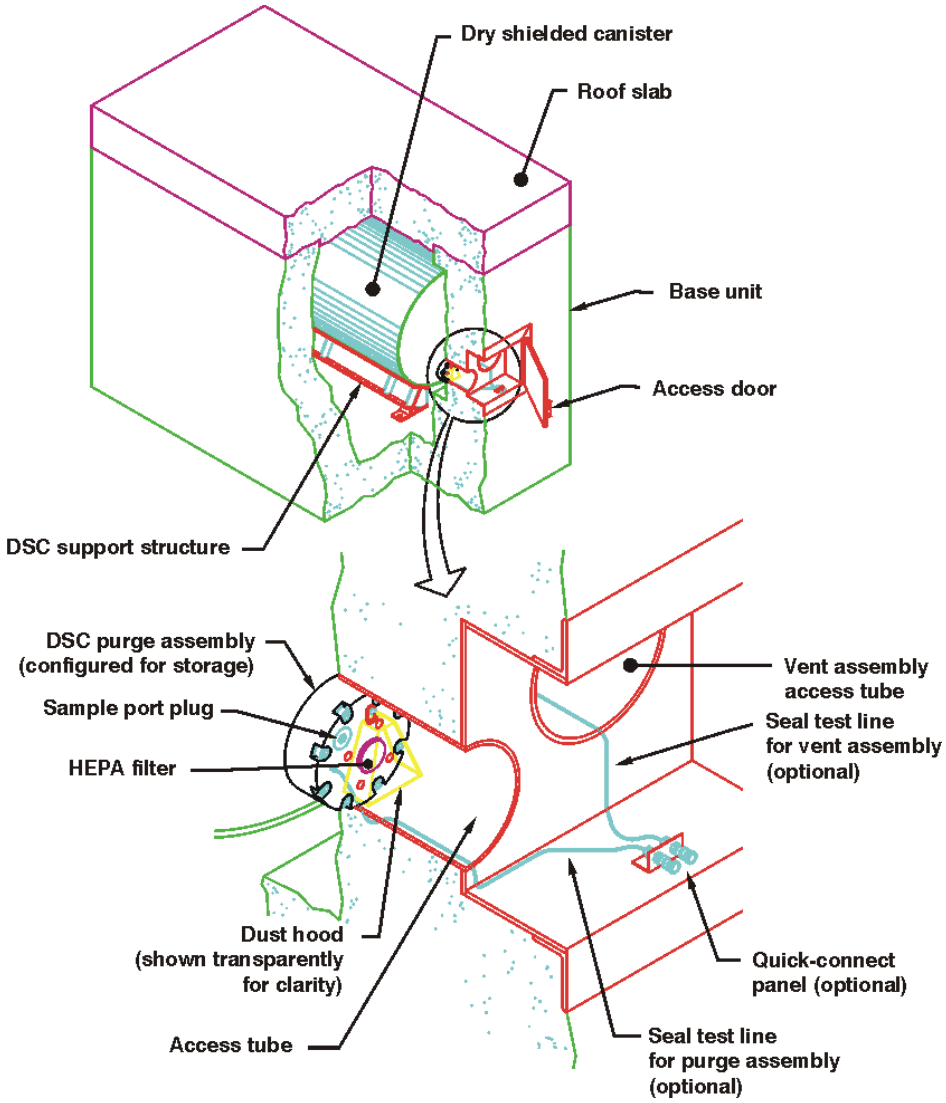

Figure 60. HSM cutaway diagram (top) and photograph showing purge vent and filter port (bottom).

Table 12. NUHOMS HSM Design Criteria

Capacity	One DSC per HSM
Array Size	Two rows of 15 modules
HSM Size (Nominal)	
Length	5.54 m
Height	4.42 m
Width	3.12 m
Surface Dose-Rate	ALARA
Heat Rejection Capacity	860 Watts
Materials of Construction	Reinforced concrete and structural steel
Service Life	50 years

The current (final) ISFSI two-row HSM configuration is shown in Figure 61. There are thirty HSMs, of which 29 contain loaded DSCs. The intent is to provide an additional HSM in the event that one of the DSCs should fail, and an additional position be necessary for any repackaged contents.

Apart from freeze-thaw effects of snowmelt on the bolt pockets that hold the HSM together, no significant degradation has been identified on the structure or systems. The bolt-pocket damage was remedied by use of an epoxy filler and covering with stainless-steel covers.

Figure 61. CPP-1774 ISFSI with HSMs.

7.5 Ongoing Sampling and Monitoring

In accordance with the safety analysis requirements, a portion of the stored DSCs undergoes headspace gas sampling annually. Due to uncertainty about the effectiveness of the drying process, the canisters were sampled monthly during the first year following loading. Although the canisters are vented, no radiological contamination and no detected release of airborne radiation has been detected by direct smears or air sampling. Gas sampling during the first year resulted in indication of as much as 3% hydrogen, but subsequent samples have stabilized in the range of approximately 0.4 vol%. Given the safety analysis report (SAR) assumptions about potential for radiolysis of residual water in the light-weight concrete (LICON), there is no indication that the hydrogen generation rates approach the predicted values (see Figure 62).

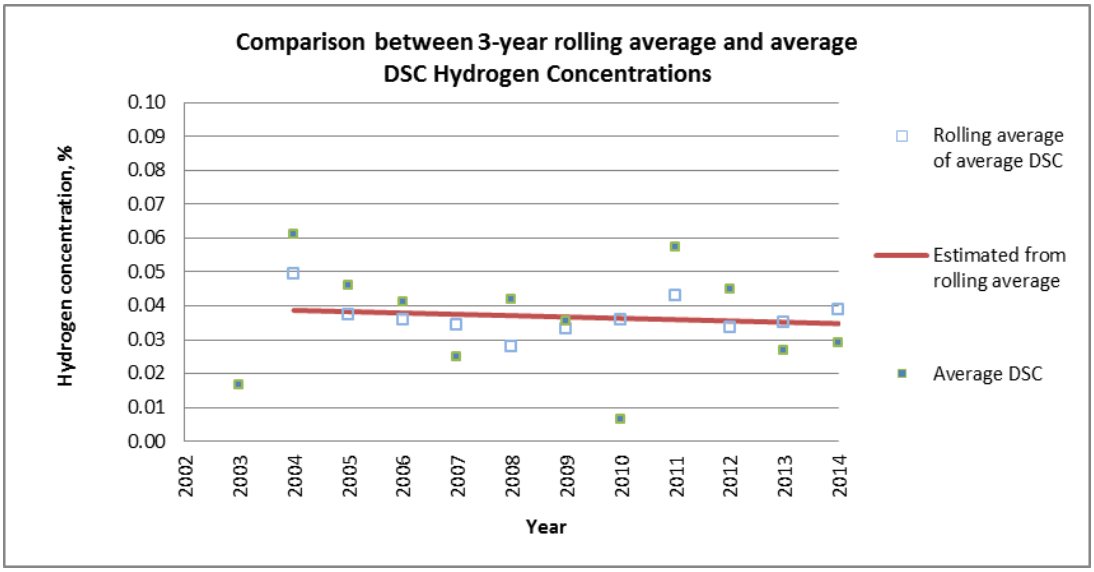

Figure 62. Annual DSC hydrogen concentrations, 2003–2014.

SAR values were based on hydrogen transport modelled in stored configuration. The analysis assumed hydrogen generation rates included 7 cm^3/hr due to radiolysis in each canister plus 33 cm^3/hr due to corrosion in DSC, for a total of 40 cm^3/hr. Release of the produced hydrogen was assumed to be driven by diffusion, seasonal and diurnal temperature and pressure fluctuations, and wind fluctuations. The resulting analysis concluded that hydrogen concentrations would reach 1.5 vol% in the DSC, and individual canisters would be as high as 4.5% (SAR Section 2, Radiolysis).

In the interest of time, hydrogen-gas concentrations were determined using a flammable gas detection instrument of the type used in industrial hygiene personnel-access monitoring. During the first few years of operation, monitoring was performed using a Cannonball unit that was not temperature compensated. This type of instrument measures the temperature change in a catalyst bed as an indication of the presence of flammable gas. For precise measurements, calibration needs to be performed at the same temperature as the measured environment. As a means of getting more-consistent results, in recent years, a photo-ionization detector system has been implemented. At the present time, canisters are only monitored annually, rather than monthly.

Part of the 2019 NRC relicensing involved development of a comprehensive aging-management plan. Per the aging-management plan, the HSMs will be monitored for concrete cracking and potential for absorption of water that would lead to cracking in freeze-thaw cycles. This monitoring includes use of water-absorption testing using a Rilem tube. Other proposed inspections involve insertion of miniature

borescope cameras into the accessible openings to view the external surface of the DSC and the structural support rail that supports the DSC. Figure 63 shows photographs of example cracking of the HSMs.

Figure 63. Examples of cracking of HSM concrete.

The storage-facility safety basis includes full analysis of seismic, tornado, flood, and canister-leakage scenarios. Due to its robust construction and the arid remote location, no significant release is expected that would affect offsite population.

7.6 Disposition

In accordance with the terms of the 1995 agreement to settle a lawsuit between the state of Idaho and the U.S. DOE (sometimes known as either the Settlement or Batt Agreement), the TMI-2 debris are to be removed from Idaho by January 1, 2035. To achieve this goal, it will be necessary to specify a package that will be compatible with proposed disposal approaches. The most developed of the disposal plans was the Yucca Mountain Project design, which was suspended for 8 years starting in 2008 and has not yet been authorized for full construction.

The likely approach for disposal is that the TMI-2 canisters would be removed from the DSC and placed into a unit that has been identified as the DOE standardized canister. This component would function as an overpack and be either selectively placed in a large disposal canister along with high-level waste-glass canisters or loaded as a group into specific disposal canisters.

The DOE standardized canister was developed with the intent of accommodating a variety of fuels and debris in a consistent package that was qualified as a component of the overall final disposal package. It was designed to be constructed of Type 304 stainless-steel, available in 457 or 610 mm diameters in either 3.048 or 4.572 m lengths. Packaging of the TMI-2 debris canisters is assumed to use the 610-mm-diameter by 4.572-m long variant.

Once disposal design commitments have been made, it will be necessary to have a facility that is capable of receiving the retrieved DSCs. Once received, the DSCs would be cut open, and the TMI-2 canisters removed and placed into DOE standardized canisters. Independent of the availability of the final repository, the settlement agreement mandates that the fuel be removed from Idaho.

8. SUMMARY

A total of 268 debris (fuel) canisters, containing relatively large fuel debris, 12 knockout canisters containing pieces between 140 microns and 10 millimeters in diameter, and 62 filter-canisters containing drilling fines, the diameters of which are greater than 140 microns were ultimately shipped from Pennsylvania to the INEL for research purposes, with ultimate disposition to be dependent on availability of a permanent repository. Upon receipt at the TAN-607 hot shop, the canisters were fitted with a standpipe to isolate canister water from pool water, filled with deionized water and transferred to the TAN-607 pool where they were stored in steel racks containing six canisters. The canisters remained in wet storage until 1999 when they were dried at up to 600°C and a target pressure of 2 torr using an HVDS. The elevated temperature drying was presumed to be necessary to adequately dry the LICON in the fuel canisters. Drying was necessary to eliminate moderator that would affect criticality potential, promote corrosion, and provide a medium that would produce free hydrogen resulting from radiolysis that could pressurize a sealed canister.

Drying was certified complete by the falling-rate method, in which the temperature underwent a rapid increase due to evaporation of the bulk pore water in the debris, and the remaining surface water evaporated with little change in the vacuum reading.

The dried canisters were placed in VECTRA NUHOMS DSC, 12 debris canisters per DSC, which were then welded shut and transferred to INTEC using the OS-197 onsite transfer package. The DSC was placed in the concrete HSM that provides shielding against the canister gamma-ray and neutron dose. Due to uncertainty in the effectiveness of drying, the DSC/HSM design was modified to incorporate a stainless-steel sintered-metal filter into the vent path on the lid. This filter provides a vent path and sample and purge connection to the headspace of the DSC, preventing accumulation of potential radiolytic hydrogen in the canister.

Following the first year of monthly sampling which saw gas sample data indicating up to 3 vol% hydrogen, the measured hydrogen concentration was 0.03 vol%, suggesting that the debris was fully dry. The hydrogen values detected show a gradually declining trend and do not depart significantly from that expected from radiolysis of moisture in ambient air.

9. REFERENCES

Akers, D.W., McCardell, R.K., Russell, M.L., and Worku, G., “TMI-2 Core Materials and Fission Product Inventory”, *Nucl. Eng. Design* 118 (1990) 451-461

Argyle, M.D., Aging Management Review of the TMI-2 ISFSI Dry Shielded Canister, Overpack, and TMI-2 Canisters Stored Within, Engineering Design File EDF-10807, March 30, 2016.

Calhoun, Gregory., Fuel Removal Equipment for Three Mile Island Unit 2, Nuclear Technology Vol 87, Nov. 1989.

Christian, J. D., Analysis of TMI-2 Canister Water, JDC-08-97/ WM-100-1074, December 5, 1997.

General Public Utility (GPU) 1993-08-05 Accident-Generated Water Disposal Completion Report.

Henrie, J., et al., “Hydrogen Control in the Handling, Shipping, and Storage of Wet Radioactive Waste”, GEND-052, 1986.

Hofmann, Peter, et al. “Reactor Core Materials Interactions at Very High Temperatures,” Nuclear Technology, Vol 87, Aug 1989, p: 146-–186.

Jensen, S.M., D.W. Akers, R. W. Garner, and G.S. Roybal, GEND-INF-082 Examination of the TMI-2 Core Distinct Components, September 1987.

McConnell, J. W. Jr., D. A. Johnson, and R. D. Sanders, Sr. Radiation degradation in EPICOR-2 ion exchange resins. INEL, Idaho Falls, ID, NUREG CR-5594 https://www.osti.gov/servlets/purl/6571510

Miller, C.J., Review of Destructive Assay Methods for Nuclear Materials Characterization from the Three Mile Island Fuel Debris, INL/EXT-13-30078, Idaho National Laboratory, September 2013.

Nagin, C.A., The Cleanup of Three Mile Island Unit 2: Technical History 1979 to 1990. EPRI NP-6931 September 1990.

Osetek, D.J., J. M. Broughton, and R. R. Hobbins, TMI-2 Accident Evaluation Program, EGG-M-89109, CONF-89-0546, May 1989.

Palmer, A. Joseph, et al., "Drying Tests Conducted on Three Mile Island Fuel Canisters Containing Simulated Debris", CONF-9606116-18, 1996.

Pincock, L.F., Three-Mile Island Core Debris Packaging, Transportation, and Storage Summary LTD-11-22779. Idaho National Laboratory Limited Release Report, February 2012.

Pincock, Layne and Wendell Hintze, Stability of Molten Core Materials, INL/EXT-12-27136, January 2013.

PLN-3660, "Three Mile Island Unit 2 Independent Spent fuel Storage Installation License Renewal Project Plan," PLN-3660, Idaho Cleanup Project, May 3, 2011.

Russell, Malcolm L., Richard K. McCardell, James M. Broughton, and Douglas W. Akers, TMI-2 Accident Evaluation Program Sample Acquisition and Examination Plan for FY-1988 and Beyond, EGG-TMI-7992, February 1988.

Settlement Agreement: Public Service Co. of Colorado v. Batt, No. CV 91-0035-S-EJL (D. Id.) and United States v. Batt, No. CV-91-0065-S-EJL (D. Id.), October 17, 1995.

Standerfer, F.R., (GPU Director, TMI-2) Letter to US Nuclear Regulatory Commission Defueling "Canister Gas Sampling", October21, 1987.

TMI-2 SAR-II-8.4, "Three-Mile Island Unit 2 Debris Independent Spent Fuel Storage Installation (ISFSI) Safety Analysis Report," Rev. 6, September 27, 2018. TMI-2 SAR-II-8.4 Section 2.

TMI-2 SAR-II-8.4, "Three-Mile Island Unit 2 Debris Independent Spent Fuel Storage Installation (ISFSI) Safety Analysis Report," Rev. 6, September 27, 2018. TMI-2 SAR-II-8.4—Section 3.

Tolman, E. L., R. P. Smith, M. R. Martin, R. K. McCardell, and J. M. Broughton, TMI-2 Core Bore Acquisition Summary Report, EGG-TMI-7385, February 1987.

Trotobas, M., et al, TMI-2 Core Materials Examination at (CEA), December 1989. SEMCI-89-DT-667.

Zirker, L. R., R. A. Rankin, and L. J. Ferrell, "Processes, Techniques, and Successes in Welding the Dry Shielded Canisters of the TMI-2 Reactor Core Debris." WM'02 Conference, February 24-–28, 2002, Tucson, AZ

Appendix A Canister-Specific Requirements

Debris canister design criteria included:

1. Maximum dewatered loaded weight 1270 kg, based on floor-loading limits in the TAN-607 water pit with a maximum loaded weight of 1453 kg
2. 3.81 m overall length, 356 mm outer diameter, 3.46 m cavity length
3. Chemical compatibility with TMI-2 and INEL pools
4. Compatibility with fuel-handling tooling and equipment, both at the reactor and the storage sites
5. Having a lid that could be removed and placed remotely,
6. Having provisions for venting, dewatering, inerting and leak testing,
7. Non-buoyant when empty,
8. Neutron poison completely encased in stainless-steel.
9. Sized to be compatible with shipping casks.
10. Providing containment during transport
11. 20-micron particle-size limit in effluent when dewatering
12. Incorporating hydrogen oxygen recombiner catalyst (control of radiolysis?)
13. Equipped with a removable pressure-relief valve to limit internal pressure to less than 103.4 kPa after loading.

Structural requirements

1. Structural integrity for criticality control maintained for all loadings under normal handling and cask loading operations
2. Able to meet ASME Section VIII Subsection UW
3. Internal design pressure: 1034 kPa at 82°C
4. Hydrostatic test pressure 1551 kPa at 20°C
5. External Pressure 206.8 kPa at 82°C
6. Sustain design-drop accident 3.5 m in air or 1.87 m in air followed by 5.9 m in water, with impact at any orientation, maintaining criticality control with allowable deformation
7. Cask packaging interface parameters:
   - Maximum impact acceleration 40 g axial
   - 100 g lateral with continuous support <12.7-mm gap between canister and support cylinder.

Performance requirements

Fuel Canister

Canister will be able

1. To be handled without top closure installed
2. To accept partial-length full cross-section fuel assembly.

Filter Canister

The filter canister will be able to remove particulates ranging from 800 to 0.5 micron with a flow rate of 473 l/min.

Knockout Canister

The knockout canister will contain neutron-absorbing material fully encapsulated in stainless-steel.

Criticality Criteria

The criticality criteria include:

1. Analyses per 10 Code of Federal Regulations 72.73 and ANSI 8.1, 8.17, 16.5 and 16.9
2. Using optimal fuel size, volume fraction and enrichment
3. Criticality limit $k_{eff} \leq 0.95$; single or array, faulted or normal
4. Criticality limit without poison $k_{eff} \leq 0.95$; single canister normal configuration.